Staphylococcus lugdunensis and its influence on the nasal microbiome

Dissertation

der Mathematisch-Naturwissenschaftlichen Fakultät

der Eberhard Karls Universität Tübingen

zur Erlangung des Grades eines

Doktors der Naturwissenschaften

(Dr. rer. nat.)

vorgelegt von

Claudia Sauer

aus Würzburg

Tübingen

2019

Gedruckt mit Genehmigung der Mathematisch-Naturwissenschaftlichen Fakultät der Eberhard Karls Universität Tübingen.

Tag der mündlichen Qualifikation:	02.12.2019
Dekan:	Prof. Dr. Wolfgang Rosenstiel
1. Berichterstatter:	Prof. Dr. Andreas Peschel
2. Berichterstatter:	Prof. Dr. Christiane Wolz

Table of contents

Abstract

Staphylococcus aureus is a frequently multi-resistant pathogen whose preferred habitat is the nose. Infections caused by *S. aureus* are often endogenous and range from soft skin and tissue infections to life-threatening invasive infections. Application of nasal ointments with the antibiotic mupirocin for decolonisation has established itself as an effective preventive measure in high-risk patients. However, the prevalence of resistance to mupirocin and most other antibiotics has increased significantly in recent decades. Therefore, the search for new strategies for decolonisation and for new therapeutics against *S. aureus* infections is more important than ever.

In a screening for new antimicrobial compounds a nasal *Staphylococcus lugdunensis* strain could be identified, which produced a novel non-ribosomally synthesized peptide antibiotic with efficacy against *S. aureus*. This antibiotic, called lugdunin, has bactericidal activity against *S. aureus* and other Gram-positive bacteria.

The nasal colonization frequency of *S. lugdunensis* and its influence on the colonization rate of *S. aureus* as well as on the nasal microbiome was analysed. Based on two independent studies with either risk patients or healthy volunteers it was found that nasal carriage of *S. lugdunensis* is associated with a significantly reduced *S. aureus* colonization rate. In addition, an almost two-year long-term study of healthy *S. lugdunensis* carriers showed that nasal colonization by *S. lugdunensis* is rather stable but may vary to some degree over time.

In addition, nasal metagenome analyses showed that at the genus level two different types of metagenomic profiles can be observed in permanent *S. lugdunensis* carriers. Furthermore, one of these profiles showed at the species level that *S. lugdunensis* has an influence on the composition of the nasal microbiome.

A better understanding of the interactions of nasal bacterial species is important for developing new *S. aureus* decolonization approaches. To this end, lugdunin or lugdunin producing strains are a promising new candidate agent for the control of *S. aureus*.

Zusammenfassung

Staphylococcus aureus ist ein häufig multiresistenter Krankheitserreger, dessen bevorzugtes Habitat die Nase ist. Infektionen mit *S. aureus* sind oftmals endogenen Ursprungs und reichen von leichten Hautentzündungen bis hin zu lebensbedrohlichen, invasiven Infektionen. Eine Dekolonisation in Form von Nasensalben mit dem Antibiotikum Mupirocin hat sich bei Risikopatienten als effektive Präventionsmaßnahme etabliert. Allerdings nahm in den letzten Jahrzehnten die Zahl an Resistenzen sowohl gegenüber Mupirocin als auch vor allem gegen systemisch angewandte Antibiotika stark zu. Somit ist die Suche nach neuen Strategien zur Dekolonisation von *S. aureus* sowie neuen Therapeutika bei entsprechenden Infektionen wichtiger denn je.

Bei der Suche nach neuen Wirkstoffproduzenten konnte ein nasaler *Staphylococcus lugdunensis* Stamm identifiziert werden, welcher durch die Produktion eines nichtribosomal synthetisierten Peptidantibiotikums mit Wirksamkeit gegenüber *S. aureus* aufgefallen war. Dieses neuartige Antibiotikum, Lugdunin genannt, wirkt bakterizid gegen *S. aureus* sowie gegen weitere Gram-positive Bakterien.

Die nasale Kolonisationshäufigkeit von *S. lugdunensis* sowie dessen Einfluss auf die Kolonisationsrate von *S. aureus* und auf das nasale Mikrobiom wurden näher bestimmt. So konnte anhand zweier unabhängiger Studien sowohl in einer Gruppe von Risikopatienten als auch in einer Gruppe gesunder Probanden gezeigt werden, dass eine nasale *S. lugdunensis* Trägerschaft mit einer signifikant reduzierten *S. aureus* Kolonisationsrate assoziiert ist. Darüber hinaus deutete eine fast zweijährige Untersuchung gesunder *S. lugdunensis* Träger darauf hin, dass eine nasale Kolonisation mit *S. lugdunensis* weitestgehend stabil ist, welche jedoch im Laufe der Zeit bis zu einem gewissen Grad variieren kann.

Außerdem zeigte eine nasale Metagenomanalyse, dass bei permanenten *S. lugdunensis* Trägern zwei unterschiedliche Typen metagenomischer Profile auf Gattungsebene beobachtet werden können. Des Weiteren konnte bei einem dieser Profile auf Artebene gezeigt werden, dass *S. lugdunensis* einen Einfluss auf die Zusammensetzung des nasalen Mikrobioms ausübt.

Ein besseres Verständnis der Interaktionen nasaler Bakterienspezies ist wichtig, um neue Ansätze zur Dekolonisation von *S. aureus* zu entwickeln. Lugdunin bzw. Lugdunin produzierende Stämme stellen hierbei eine vielversprechende Alternative bei der Bekämpfung von *S. aureus* dar.

Chapter 1 - General introduction

Staphylococcus aureus colonization of the human nose and interaction with other microbiome members

Claudia Laux, Andreas Peschel, Bernhard Krismer

University of Tübingen, Interfaculty Institute for Microbiology and Infection Medicine Tübingen, Infection Biology Unit, Auf der Morgenstelle 28, 72076 Tübingen, Germany

***Microbiol Spectr* 7, doi:10.1128/microbiolspec.GPP3-0029-2018 (2019)**

Abstract

Staphylococcus aureus is usually regarded as a bacterial pathogen due to its ability to cause multiple types of invasive infections. Nevertheless, *S. aureus* colonizes about 30% of the human population asymptomatically in the nares, either transiently or persistently, and can therefore be regarded a human commensal as well, although carriage increases the risk of infection. Whereas many facets of the infection processes have been studied intensively, little is known about the commensal lifestyle of *S. aureus*. Recent studies highlight the major role of the composition of the highly variable nasal microbiota in promoting or inhibiting *S. aureus* colonization. Competition for limited nutrients, trace elements, and epithelial attachment sites, different susceptibilities to host defense molecules and the production of antimicrobial molecules by bacterial competitors may determine whether nasal bacteria outcompete each other. This chapter summarizes our knowledge about mechanisms that are used by *S. aureus* for efficient nasal colonization and strategies used by other nasal bacteria to interfere with its colonization. An improved understanding of naturally evolved mechanisms might enable us to develop new strategies for pathogen eradication.

Introduction

The human body offers several distinct niches for specific microbiomes, variable consortia of bacterial communities. The skin, for instance, is primarily colonized by members of the genera *Propionibacterium*, *Corynebacterium* and *Staphylococcus* (1). A similar pattern of genera is found in the human nose, which is regarded as a transition zone from the dry skin to the moist, mucoid airways (2). This rather confined area, more specifically, the region from the anterior nasal vestibule to the posterior nasopharyngeal cavity is the favored colonization site of *Staphylococcus aureus*. While *S. aureus* is a member of the normal nasal microbiome in ca. 30% of the human population, it can also become an aggressive, life-threatening pathogen (3). Nasal carriage is a major risk factor for *S. aureus* infections. Accordingly*, S. aureus* is eradicated from the nose in patients at risk by treatment with the antibiotic mupirocin. Interestingly, a significant percentage of humans seem never to be colonized by *S. aureus,* for reasons that are currently unknown. Increasing evidence suggests that the composition of the nasal microbiome is an important factor for the exclusion of *S. aureus* from the nose (2).

This chapter summarizes knowledge on *S. aureus* nasal colonization and its interaction with other bacterial species that share the same habitat. Understanding naturally occurring *S. aureus* elimination strategies might enable the development of new eradication approaches in the future.

S. aureus as a human commensal and pathogen

The preferred habitat of *S. aureus* is the anterior nares. Approximately 20% of the human population is permanently colonized by *S. aureus*, whereas another 20 are considered to be non-carriers. The remaining 60% of the population belong to the group of intermittent carriers (4). Although several factors that affect the *S. aureus* carrier status were described, it remains elusive why only certain people are colonized. In general, *S. aureus* occurs particularly frequently in men (5) and in women using hormonal contraception (6). Moreover, diabetic (7), hospitalized, and dialysis patients (4) are more often colonized than healthy humans and there is a higher carriage rate during childhood compared to adulthood (8). A negative correlation exists between smoking and *S. aureus* carriage (9). Seasonal differences, such as the transition from winter to spring and temperature and pollen or dust levels, could also affect the nasal microbiome composition (10). Host genetics appear to have only a moderate impact on the shape of the microbiome (11).

S. aureus possesses an extensive arsenal of virulence factors and, therefore, the clinical manifestations of *S. aureus* diseases are diverse and range from rather mild soft skin and tissue infections to severe and life-threatening infections, such as pneumonia, osteomyelitis, endocarditis, and sepsis (12). Although nasal colonization by *S. aureus* is asymptomatic, it increases the risk of invasive infections, especially in immunocompromised and hospitalized patients (4, 13). Analysis of infecting strains revealed that it is usually the nasal strain of a patient that is responsible for subsequent infections (13, 14). Therefore, decolonization of nasal *S. aureus* serves as a very efficacious measure for prevention of invasive infections (13). Since the *S. aureus* transmission from the nose to other parts of the body occurs mainly via hand contact, *S. aureus* usually disappears also from other body sites when it is eliminated from the nose (15, 16).

The high risk of *S. aureus* carriers to suffer infections justifies the widely applied mupirocin treatment to eradicate *S. aureus* from the nares of patients. Mupirocin interferes with the synthesis of bacterial proteins by reversibly binding to bacterial isoleucyl-tRNA (17). Application of a mupirocin ointment twice a day over five consecutive days typically leads to eradication of *S. aureus* from the nose and to a reduced risk of invasive *S. aureus* infections (14, 17). The success rate of mupirocin treatment reaches approximately 90%, yet resistance is increasing, reaching up to 30% in some parts of the USA. Hence, new antimicrobial compounds for *S. aureus* decolonization are urgently needed (17, 18). Re-colonization by *S. aureus* after the end of mupirocin treatment frequently occurs after a few weeks, probably as a result of *S. aureus* cells using the posterior vestibula as a hidden reservoir, which can hardly be reached by mupirocin treatment (19-21).

Resistance to several common antibiotics has increased in *S. aureus* in the last decades. Resistance to the entire class of ß-lactam antibiotics, including methicillin, characterizes the epidemic methicillin-resistant *S. aureus* (MRSA) strains. However, multi-drug resistant MRSA strains, which have acquired resistance to additional antibiotics, such as erythromycin, clindamycin, ciprofloxacin, tetracycline, or mupirocin, have also been observed (22). MRSA infections used to be acquired in hospitals by patients and are called hospital-associated (HA-) MRSA infections. However, in the last decade, increasing numbers of MRSA infections are acquired outside the healthcare system by emerging MRSA clones referred to as community-associated (CA-) MRSA. Many CA-MRSA clones are much more virulent and transmissible than HA-MRSA clones (23).

Diversity of the human nasal microbiome

In addition to the genus *Staphylococcus*, which belongs to the phylum Firmicutes, the nasal microbiome also contains members of other phyla in particular Actinobacteria and Proteobacteria. Within these phyla, the genera *Corynebacterium*, *Propionibacterium, Staphylococcus*, and *Moraxella* are most common in the human nose (24). Other genera are less frequently found (11). Interestingly, the nasal cavities are also colonized by various anaerobic species (19).

To classify different microbiome compositions, seven community state types (CST) were defined according to the dominance of specific nasal species, genera, or families. CST1 is dominated by *S. aureus* and CST2 is defined by the major occurrence of *Enterobacteriaceae*, such as *Escherichia* spp., *Proteus*. spp. and *Klebsiella* spp.. *S. epidermidis* dominates CST3, whereas *Propionibacterium* spp. are major colonizers in CST4. *Corynebacterium* is the dominating genus of CST5, and *Moraxella* spp. are most prevalent in CST6, whereas CST7 is defined by the predominance of *Dolosigranulum pigrum*. The most common nasal CST is CST4, followed by CST3 and CST1, whereas CST6 is the least prevalent (Table 1). Although the conspicuous presence of various species or genera defines the CST, these species can also be identified at lower abundances in other CSTs (11). Comparing the microbiome compositions at various body sites, it is obvious that the nasal bacterial composition overlaps with those of the oral cavity and skin and can therefore be regarded as a bridge between the microbiomes of these two body sites (24, 25).

Table 1: Community state types of the human nose. Seven major community state types (CST) were defined according to the abundance of dominant nasal bacterial species, genera, or families (11).

Community state type	Dominated by	Prevalence (%)
CST1	*S. aureus*	12.4
CST2	Enterobacteriaceae (e.g. *Escherichia* spp. (11); *Proteus* spp. (11); *Klebsiella* spp. (11))	9.0
CST3	*S. epidermidis*	22.5
CST4	*Propionibacterium* spp. (e.g. *P. acnes* (88))	28.7
CST5	*Corynebacterium* spp. (e.g. *C. accolens (88); C. pseudodiptheriticum (88); C. propinquum* (88))	11.2
CST6	*Moraxella* spp. (e.g. *M. lacunata (88); M. nonliquefaciens* (88))	5.6
CST7	*Dolosigranulum pigrum*	10.7

Human skin areas with mostly dry, sebaceous, or moist properties differ in the abundance of bacterial microbiome members while the core species are largely the same (1). It remains unclear if the individual differences in the skin microbiomes can also be attributed to specific CSTs. *S. epidermidis, S. capitis, S. hominis, and S. warneri* are the most abundant coagulase-negative staphylococci (CoNS) on skin (1). *S. aureus* also occurs transiently on the skin of healthy humans, especially in skin areas of the axillae and perineum (26, 27). Notably, the skin of atopic dermatitis patients is often permanently colonized by *S. aureus* on inflamed and non-inflamed skin parts (28).

CoNS do not only colonize the human skin, they can also occasionally be detected in the nose (29, 30). Only *S. epidermidis* is a core microbiome member of both, the skin and nose, (29). In general, the nasal microbiome is less dense and less diverse than, for instance, the gut microbiome (31, 32). *S. epidermidis* is particularly prevalent on moist areas of the body, such as the axillae, inguinal and perineal areas, toe tissue, and conjunctiva, and is also a common resident of the anterior nares (29). In addition, a variety of other CoNS occupy specific regions of the skin. *S. hominis* and *S. haemolyticus* are often found in the axillae and pubic areas (29). *S. capitis* can be preferentially isolated from the sebaceous glands on the forehead and scalp (29) and is

also found on the skin and in the nares (33). Whereas *S. auricularis* is part of the external ear microbiome, *S. saprophyticus* often colonizes the rectum and genitourinary tract (29). *S. lugdunensis* is also part of the human skin flora and is particularly prevalent in the pelvic and perineal regions, the groin, axillae, and in the nail bed of the first toe. *S. lugdunensis* has been isolated from the nose of humans at an incidence between 10% to 26% (19, 29, 34, 35). *S. warneri* is typically found at a lower percentage than other CoNS in the nares and on the skin, preferably on the head, arms, and legs (33). Compared to the other CoNS, *S. lugdunensis* and *S. saprophyticus* are considered species with slightly higher pathogenicity (29).

Compared to species such as *S. epidermidis*, which can be present in the nose with multiple different strains simultaneously, nasal *S. aureus* isolates typically belong only to one specific clone (36, 37). Notably, the number *S. aureus* cells, which can be cultivated from carriers by nasal swabbing, varies from only a few to more than 10^7 per swab (38). Attempts to distinguish persistent from intermediate carriers by a single nasal swab indicated that the detection of more than 10^3 *S. aureus* cfu/swab corresponds to persistent carriage with a high probability (39).

The anterior nares are regarded as the primary habitat of *S. aureus* (4), but a recent study showed that this species can be isolated with an even higher incidence from deeper (posterior) areas of the nasal cavity, suggesting that the posterior vestibule or the entire nasal vestibule may be the principle habitat of *S. aureus* (19). Further studies indicated that *S. aureus* can penetrate into the nasal tissue of healthy humans, and individual cells could be visualized even at the *stratum basale* of the nasal epithelium, which differs in structure between the anterior and posterior areas (40, 41). While the anterior nares are characterized by a keratinized, stratified squamous epithelium the posterior nares are defined by a pseudostratified, columnar ciliated epithelial cells (2, 41). In the anterior vestibule, the moist squamous epithelium on the septum adjacent to the nasal ostium harbors the highest number of *S. aureus* cells. By contrast, CoNS prefer the skin of the nasal septum and the anterior, hair-covered epidermal portion of the lateral wall (5).

Metabolism in the human nose

The nose is an environment with very low nutrient supply, which might be the reason for the low species diversity of this habitat. Human nasal secretions contain sodium chloride at concentrations found also in other body fluids, and small amounts of

potassium, magnesium, and phosphate but they are low in potential nutrients such as sugars, amino acids, or other major building blocks (30). Based on the composition of nasal secretions, a synthetic nasal medium (SNM3) was established that enabled the efficient growth of *S. aureus*, whereas CoNS did not steadily grow in SNM3 (30). This finding indicates that *S. aureus* is better adapted to life in the human nose than many CoNS, which may use the human nose only as a temporary, but not preferred habitat. *S. aureus* and many other nasal bacteria, such as *S. epidermidis*, *Finegoldia magna*, *Propionibacterium acnes,* and *Streptococcus pyogenes*, secrete proteases that degrade human proteins, such as albumin, lactoferrin, mucin, cytokeratin 10, and hemoglobin. These proteins are present at considerable amounts in human nasal secretions and might serve as nutrient sources for various bacteria (42-44). It is likely that secretory proteases produced by a specific bacterial strain will generate peptides and amino acids that can be utilized by many other microbiome members and may have a broad impact on microbiome metabolism.

Mechanisms of nasal epithelial attachment

Efficient attachment mechanisms are a prerequisite for bacterial nasal colonizers to remain in tight contact with epithelial cells and resist clearance by mucociliar movement. *S. aureus* binds to fully keratinized, dead desquamated cells of the anterior nasal cavity and adheres also to live ciliated cells in the posterior nasal cavity. Obviously, *S. aureus* uses different adhesion mechanisms, depending on specific epithelial characteristics at different parts of the nares (45-48).

The cell wall glycopolymer wall teichoic acid (WTA) mediates the initial attachment of *S. aureus* to epithelial cells and WTA is crucial for *S. aureus* nasal colonization (41, 47, 49). WTA-deficient *S. aureus* mutants are limited in their ability to bind to nasal epithelial cells. In addition, mutations in the *dltABCD* operon, leading to a loss of D-alanine modification of WTA, also exhibit diminished epithelial binding capacities (47, 49). Similarly, the modification of WTA with N-acetylglucosamine (GlcNAc) in α- or β-configuration is essential for efficient binding to nasal epithelial cells, and a lack of WTA glycosylation significantly abolished the ability of *S. aureus* to colonize cotton rat nares *in vivo* (50).

The scavenger receptor class-F member 1 (SREC1) on nasal epithelia in the posterior nasal cavity is a target for the WTA of *S. aureus* and allows *S. aureus* binding to

epithelial cells (46). The charged zwitterionic properties of the ribitol-phosphate repeating units of WTA are essential in SREC1 binding (51). The loss of the D-alanine modification of the WTA significantly reduces the SREC1 binding.

The adherence of *S. aureus* to the nasal epithelium is also mediated by cell-wall anchored proteins, which are involved in long-term persistence within the anterior nasal cavity. *S. aureus* expresses a variety of cell wall proteins, which belong to the group of MSCRAMMs (microbial surface components recognizing adhesive matrix molecules) (41). MSCRAMMs, such as ClfB, IsdA, and SdrD play an important role in nasal colonization by *S. aureus*.

Clumping factor B (ClfB) is a fibrinogen-binding protein produced by *S. aureus* that binds to the matrix proteins cytokeratin 10 and loricrin. These proteins are exposed on human squamous epithelial cells (48, 52, 53). The iron-regulated surface determinant A (IsdA), which is involved in heme uptake and iron acquisition (54), is expressed during human infections and is responsible for nasal colonization and survival of *S. aureus* on the skin. Similar to ClfB, IsdA interacts with cytokeratin 10 and loricrin as well as with the extracellular matrix protein involucrin (48, 55). Serine-aspartate repeat-containing protein D (SdrD) mediates adhesion to human squamous epithelium by binding to desmoglein 1, a desmosomal cadherin that is mainly expressed by the epidermis and mucosa (56, 57) (Fig. 1). The connective function of desmoglein 1 is required for the epidermis to maintain its integrity and structure (57). In addition, the surface proteins SdrC and SasG promote adhesion to squamous epithelium cells, but their binding partners are still unknown (45, 58). Interfering with glycopolymer-receptor interaction might become a new strategy for controlling *S. aureus* colonization in the nose (46). Furthermore, ClfB could represent an ideal target molecule for new decolonization strategies (53). In this context, ClfB can be considered a promising component for the development of a vaccine that would also reduce nasal colonization by *S. aureus* (59).

S. epidermidis colonizes the human nose at a higher frequency than *S. aureus*. In contrast to *S. aureus*, *S. epidermidis* has a different WTA structure and adhesion proteins related to ClfB, IsdA, SdrD, and SdrC, are absent. Therefore, it remains unclear how *S. epidermidis* accomplishes adhesion in the nose (2, 60).

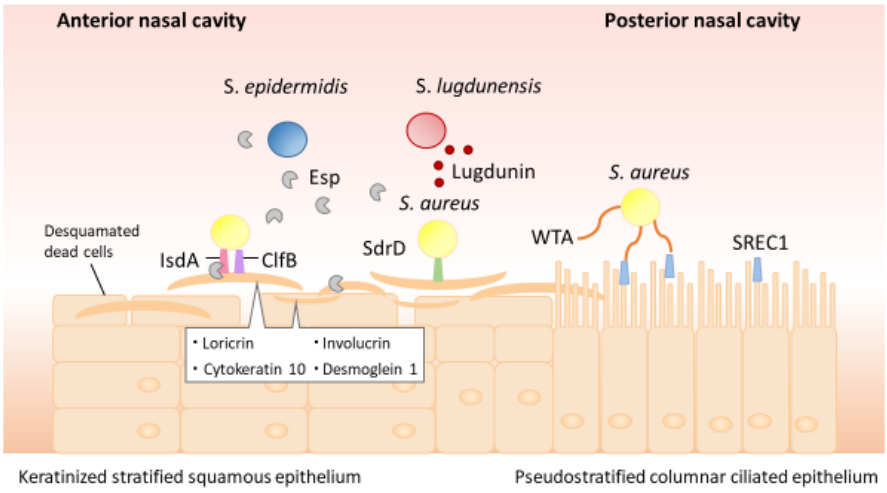

Figure 1: Attachment mechanisms of *S. aureus* in the human nasal cavity. The anterior and posterior parts of the human nose are lined by different types of epithelial cell, which require alternative bacterial adhesion mechanisms. For the keratinized stratified squamous epithelium in the anterior nasal cavity, *S. aureus* predominantly uses cell wall-attached surface proteins (MSCRAMMs) (2, 41). In contrast, the primary attachment in the posterior area, composed of a pseudostratified columnar ciliated epithelium, is mediated by specific interaction of the cell-wall linked wall teichoic acid (WTA) with the scavenger receptor class F member 1 (SREC1) (41, 46).

The corneocytes (desquamated epithelial cells) in the anterior nasal cavity contain high levels of the proteins loricrin, cytokeratin 10, and involucrin (55). *S. aureus* can express a variety of cell wall proteins, which bind to these matrix proteins. The *S. aureus* adhesin clumping factor B (ClfB) binds to cytokeratin 10 and loricrin (48, 52), whereas the iron-regulated surface determinant A (IsdA) can also interact with involucrin (55). In addition, the *S. aureus* serine-aspartate repeat-containing protein D (SdrD) mediates adhesion to human squamous epithelial cells by binding to desmoglein 1 (56). Some *S. epidermidis* isolates secrete an extracellular serine protease (Esp), which inhibits *S. aureus* colonization by degradation of the surface proteins IsdA and SdrD, and of host receptors (77, 78). In addition, *S. lugdunensis* can prevent nasal colonization of *S. aureus* by producing the cyclic thiazolidine-containing peptide antibiotic lugdunin (35).

Bacterial competition

Bacteria from habitats with limited nutrient supply such as the skin and nose have developed mechanisms to increase their fitness in competition with other microbiome members. Competition between bacterial species can be direct or indirect. Direct inhibition can be achieved for instance through production of antimicrobials, whereas indirect inhibition may occur via competition for nutrients or modification of living conditions (61).

Many nasal *Staphylococcus* isolates produce antimicrobial substances against bacterial competitors at an unexpectedly high frequency (84%) with *S. epidermidis* as the most frequent producer of antimicrobial activity (62). Importantly, production of many of the antibacterial activities is strongly enhanced or exclusively detectable under specific environmental stress conditions, which are present in the human nose, such as hydrogen peroxide release or iron limitation (62). Antimicrobial substances, also called bacteriocins, are categorized into various groups and subgroups (63). Many *Staphylococcus* isolates are producers of lantibiotics, ribosomally synthesized antimicrobial peptides characterized by the presence of the thioether amino acids lanthionine and methyllanthionine. A variety of lantibiotics have been described for *Staphylococcus* strains (64). Epidermin (*S. epidermidis* (65)), Pep5 (*S. epidermidis* (66)), epilancin K7 and 15X (*S. epidermidis* (67, 68)), epicidin 280 (*S. epidermidis* (69)), staphylococcin C55 (*S. aureus* (70)), various nukacins (*S. warneri* (71), *S. epidermidis* (62) and *S. hominis* (72)), as well as lantibiotics-α and -β (*S. hominis* (73)) were documented. In addition, putative lantibiotic-biosynthetic gene clusters were found in the genome of *S. capitis*, which share homology with the biosynthetic systems of epidermin/gallidermin and the non-lantibiotic bacteriocin epidermicin (74). Lantibiotics are usually exclusively active against Gram-positive bacteria but often show no activity against *S. aureus* (62, 71). It is rather uncommon that nasal *S. aureus* are severely affected by lantibiotic-producing CoNS. Interestingly, a systematic analysis of *P. acnes* isolates revealed a frequent capacity to inhibit *S. epidermidis* (75). No compound was yet identified that could explain this inhibitory activity; however, the genomes of various *P. acnes* strains encode a putative thiopeptide-biosynthetic gene cluster that is similar to those for antimicrobially active siomycin and berninamycin, which might explain the inhibitory effect (76).

A recent study showed that secretion of the extracellular serine protease Esp by *S. epidermidis* can efficiently inhibit *S. aureus* colonization. Artificial inoculation of Esp-secreting *S. epidermidis* to the nasal cavities of human volunteers was sufficient to eradicate *S. aureus* (77). Nasal colonization of *S. aureus* is probably abolished by Esp via the degradation of both, bacterial adhesive surface proteins IsdA and SdrD, and host receptor proteins (78). Although most *S. epidermidis* isolates produce Esp and some are producers of lantibiotics, there is no clear correlation of the absence of *S. aureus* with the presence of *S. epidermidis* (20, 64, 77).

Nasal *S. lugdunensis* can prevent colonization by *S. aureus* by producing an unusual antimicrobial compound termed lugdunin, which is a novel, cyclic thiazolidine-

containing peptide antibiotic (35). The lugdunin gene cluster is encoded on the *S. lugdunensis* chromosome and present in almost all *S. lugdunensis* strains. Lugdunin is generated by non-ribosomal peptide synthetases (NRPS). It has bactericidal activity against *S. aureus* and other Gram-positive bacteria and it was shown to be active *in vivo* in animal models. Analysis of nasal microbiomes of hospitalized patients revealed that *S. lugdunensis* colonization is associated with a six-fold reduced risk of *S. aureus* carriage in the nose suggesting that lugdunin or lugdunin-producing commensals could become useful for the prevention of *S. aureus* colonization and infection.

Streptococcus spp*.* mainly occur in the oropharynx, but can also be found at low frequency in the nostrils (79). Importantly, *S. pneumoniae* can modify the nasal habitat by releasing hydrogen peroxide, which induces the SOS response in *S. aureus* and activates DNA repair mechanisms as well as resident prophages. Subsequently, phage-produced lytic enzymes destroy *S. aureus* cells (80, 81). Hence, *S. pneumonia* is negatively correlated with nasal *S. aureus* carriage (82, 83).

An ambivalent correlation between *Corynebacterium* spp. and *S. aureus* was reported. While *C. accolens* often occurs together with *S. aureus, C. pseudodiptheriticum* is associated with the absence of *S. aure*us. A mutualistic relationship between *C. accolens* and *S. aureus* might rely on the joint mobilization of nutrients promoting the growth of these strains. In contrast, the competitive interaction between *C. pseudodiptheriticum* and *S. aureus* interferes with *S. aureus* colonization. Thus, the presence of *C. accolens* or *C. pseudodiptheriticum* might become a useful predictor of the propensity of nasal *S. aureus* carriage (20). A bacterial strain replacement study highlighted that nasal inoculation of persistent *S. aureus* carriers with *Corynebacterium* sp. can lead to complete eradication of the pathogen in more than 70% of the probands (84).

Nostril- and skin-associated *Propionibacterium* spp. release coproporphyrin III, a porphyrin metabolite that promotes the aggregation and nasal colonization of *S. aureus* (85) (Fig. 2). A negative association with *S. aureus* carriage was reported for *Simonsiella* spp., *Dolosigranulum pigrum,* and *Finegoldia magna*, which are also regular members of the nasal microbiome (11, 31). The particular sensitivity of *D. pigrum* to a multitude of *Staphylococcus* isolates suggests that *D. pigrum* can only be present when no bacteriocin-producing *Staphylococcus* is in the same habitat (62).

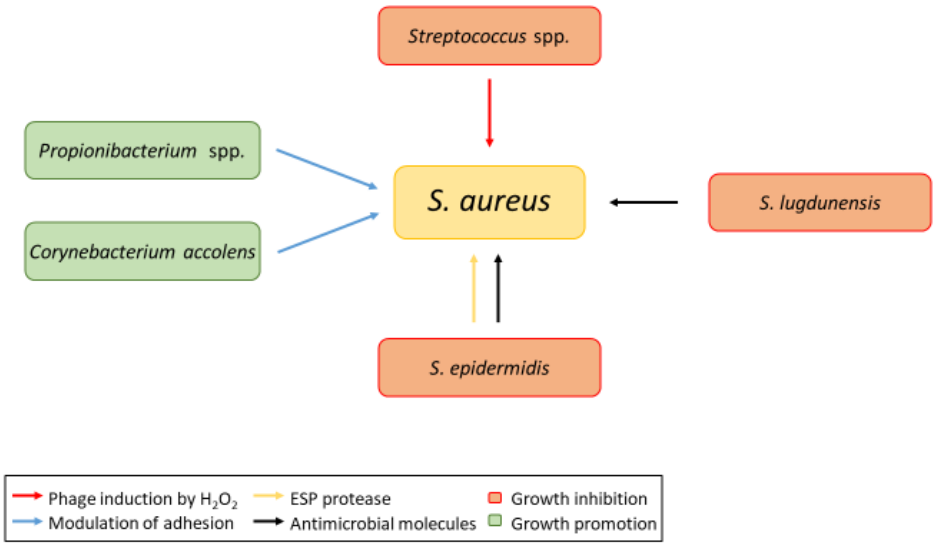

Figure 2: Established interactions between nasal bacteria. *Corynebacterium accolens* and *Propionibacterium* spp. can promote the colonization by *S. aureus* (green box) by modulation of its adhesive capacities (20, 85) (blue arrows), while specific clones of *S. epidermidis*, *S. lugdunensis*, and *Streptococcus spp*. can lead to *S. aureus* growth inhibition (orange box). Some *S. epidermidis* isolates secrete high levels of extracellular serine protease (Esp), which inhibits *S. aureus* nasal colonization (77) (yellow arrow). In addition, *S. epidermidis* and *S. lugdunensis* can impede *S. aureus* colonization by producing antimicrobial molecules (35, 64) (black arrows). *S. pneumoniae* can release hydrogen peroxide, which leads to prophage activation in *S. aureus* along with phage-mediated lysis of *S. aureus* cells (80, 81) (red arrow).

Competition by induction of host defense

In addition to the above-described competition scenarios, the human host can also impact the composition of the nasal microbiome. *S. aureus* expresses surfactant-like phenol-soluble modulin peptides, which mobilize pro-inflammatory lipoproteins from the staphylococcal cytoplasmic membrane. These lipoproteins activate the Toll-like receptor 2 (TLR2) and, consequently, lead to inflammation (86). The resulting inflammatory response in the nasal epithelium provokes the production of antimicrobial peptides. Although these hardly affect *S. aureus* with its intrinsic immune evasion factors, they impair growth of other nasal commensal bacteria (5, 87).

Conclusion and outlook

The mechanisms of microbiome-mediated exclusion of *S. aureus* from the human nose are probably multifactorial. It is likely that in addition to the processes described above further factors are involved. It will be important to further investigate which other antimicrobial substances are produced by nasal commensals and which further strategies are used in their competition with *S. aureus* for nutrients and adhesion sites. New findings on nasal colonization may clarify why 20% of the human population is permanently colonized by *S. aureus* while a similar percentage is never colonized. A better understanding could become helpful for developing new *S. aureus* eradication approaches that protect against recurrent *S. aureus* nasal colonization.

Acknowledgments

Our research is supported by grants from the Deutsche Forschungsgemeinschaft (TRR34, TRR156, SFB766, SFB685, GRK1708, PE805/5-1), the Deutsches Zentrum für Infektionsforschung (TTU HAARBI), and the European Innovative Medicines Initiative (COMBACTE).

References

1. Byrd AL, Belkaid Y, Segre JA. 2018. The human skin microbiome. Nat Rev Microbiol 16:143- 155.
2. Krismer B, Weidenmaier C, Zipperer A, Peschel A. 2017. The commensal lifestyle of Staphylococcus aureus and its interactions with the nasal microbiota. Nat Rev Microbiol 15:675-687.
3. Tong SY, Davis JS, Eichenberger E, Holland TL, Fowler VG, Jr. 2015. Staphylococcus aureus infections: epidemiology, pathophysiology, clinical manifestations, and management. Clin Microbiol Rev 28:603-61.
4. Kluytmans J, van Belkum A, Verbrugh H. 1997. Nasal carriage of Staphylococcus aureus: epidemiology, underlying mechanisms, and associated risks. Clin Microbiol Rev 10:505-20.
5. Cole AM, Tahk S, Oren A, Yoshioka D, Kim YH, Park A, Ganz T. 2001. Determinants of Staphylococcus aureus nasal carriage. Clin Diagn Lab Immunol 8:1064-9.
6. Zanger P, Nurjadi D, Gaile M, Gabrysch S, Kremsner PG. 2012. Hormonal contraceptive use and persistent Staphylococcus aureus nasal carriage. Clin Infect Dis 55:1625-32.
7. Lipsky BA, Pecoraro RE, Chen MS, Koepsell TD. 1987. Factors affecting staphylococcal colonization among NIDDM outpatients. Diabetes Care 10:483-6.
8. Armstrong-Esther CA. 1976. Carriage patterns of Staphylococcus aureus in a healthy non-hospital population of adults and children. Ann Hum Biol 3:221-7.
9. Olsen K, Falch BM, Danielsen K, Johannessen M, Ericson Sollid JU, Thune I, Grimnes G, Jorde R, Simonsen GS, Furberg AS. 2012. Staphylococcus aureus nasal carriage is associated with serum 25-hydroxyvitamin D levels, gender and smoking status. The Tromso Staph and Skin Study. Eur J Clin Microbiol Infect Dis 31:465-73.
10. Camarinha-Silva A, Jauregui R, Pieper DH, Wos-Oxley ML. 2012. The temporal dynamics of bacterial communities across human anterior nares. Environ Microbiol Rep 4:126-32.
11. Liu CM, Price LB, Hungate BA, Abraham AG, Larsen LA, Christensen K, Stegger M, Skov R, Andersen PS. 2015. Staphylococcus aureus and the ecology of the nasal microbiome. Sci Adv 1:e1400216.
12. Lowy FD. 1998. Staphylococcus aureus infections. N Engl J Med 339:520-32.
13. von Eiff C, Becker K, Machka K, Stammer H, Peters G. 2001. Nasal carriage as a source of Staphylococcus aureus bacteremia. Study Group. N Engl J Med 344:11-6.
14. Bode LG, Kluytmans JA, Wertheim HF, Bogaers D, Vandenbroucke-Grauls CM, Roosendaal R, Troelstra A, Box AT, Voss A, van der Tweel I, van Belkum A, Verbrugh HA, Vos MC. 2010. Preventing surgical-site infections in nasal carriers of Staphylococcus aureus. N Engl J Med 362:9-17.
15. Reagan DR, Doebbeling BN, Pfaller MA, Sheetz CT, Houston AK, Hollis RJ, Wenzel RP. 1991. Elimination of Coincident Staphylococcus-Aureus Nasal and Hand Carriage with Intranasal Application of Mupirocin Calcium Ointment. Annals of Internal Medicine 114:101-106.
16. Parras F, Guerrero MC, Bouza E, Blazquez MJ, Moreno S, Menarguez MC, Cercenado E. 1995. Comparative study of mupirocin and oral co-trimoxazole plus topical fusidic acid in eradication of nasal carriage of methicillin-resistant Staphylococcus aureus. Antimicrob Agents Chemother 39:175-9.

17. Septimus EJ, Schweizer ML. 2016. Decolonization in Prevention of Health Care-Associated Infections. Clin Microbiol Rev 29:201-22.

18. Antonov NK, Garzon MC, Morel KD, Whittier S, Planet PJ, Lauren CT. 2015. High prevalence of mupirocin resistance in Staphylococcus aureus isolates from a pediatric population. Antimicrob Agents Chemother 59:3350-6.

19. Kaspar U, Kriegeskorte A, Schubert T, Peters G, Rudack C, Pieper DH, Wos-Oxley M, Becker K. 2016. The culturome of the human nose habitats reveals individual bacterial fingerprint patterns. Environ Microbiol 18:2130-42.

20. Yan M, Pamp SJ, Fukuyama J, Hwang PH, Cho DY, Holmes S, Relman DA. 2013. Nasal microenvironments and interspecific interactions influence nasal microbiota complexity and S. aureus carriage. Cell Host Microbe 14:631-40.

21. Wertheim HFL, Verveer J, Boelens HAM, van Belkum A, Verbrugh HA, Vos MC. 2005. Effect of mupirocin treatment on nasal, pharyngeal, and perineal carriage of Staphylococcus aureus in healthy adults. Antimicrobial Agents and Chemotherapy 49:1465-1467.

22. Otto M. 2012. MRSA virulence and spread. Cell Microbiol 14:1513-21.

23. DeLeo FR, Otto M, Kreiswirth BN, Chambers HF. 2010. Community-associated meticillin- resistant Staphylococcus aureus. Lancet 375:1557-68.

24. Human Microbiome Project C. 2012. Structure, function and diversity of the healthy human microbiome. Nature 486:207-14.

25. Faust K, Sathirapongsasuti JF, Izard J, Segata N, Gevers D, Raes J, Huttenhower C. 2012. Microbial co-occurrence relationships in the human microbiome. PLoS Comput Biol 8:e1002606.

26. Casewell MW, Hill RL. 1986. The carrier state: methicillin-resistant Staphylococcus aureus. J Antimicrob Chemother 18 Suppl A:1-12.

27. Peacock SJ, de Silva I, Lowy FD. 2001. What determines nasal carriage of Staphylococcus aureus? Trends Microbiol 9:605-10.

28. Geoghegan JA, Irvine AD, Foster TJ. 2017. Staphylococcus aureus and Atopic Dermatitis: A Complex and Evolving Relationship. Trends Microbiol S0966-842X(17)30257-3.

29. Becker K, Heilmann C, Peters G. 2014. Coagulase-negative staphylococci. Clin Microbiol Rev 27:870-926.

30. Krismer B, Liebeke M, Janek D, Nega M, Rautenberg M, Hornig G, Unger C, Weidenmaier C, Lalk M, Peschel A. 2014. Nutrient limitation governs Staphylococcus aureus metabolism and niche adaptation in the human nose. PLoS Pathog 10:e1003862.

31. Wos-Oxley ML, Plumeier I, von Eiff C, Taudien S, Platzer M, Vilchez-Vargas R, Becker K, Pieper DH. 2010. A poke into the diversity and associations within human anterior nare microbial communities. Isme j 4:839-51.

32. Quercia S, Candela M, Giuliani C, Turroni S, Luiselli D, Rampelli S, Brigidi P, Franceschi C, Bacalini MG, Garagnani P, Pirazzini C. 2014. From lifetime to evolution: escales of human gut microbiota adaptation. Frontiers in Microbiology 5.

33. Kloos WE, Schleifer KH. 1975. Isolation and Characterization of Staphylococci from Human Skin . II. Descriptions of Four New Species – Staphylococcus warneri, Staphylococcus capitis, Staphylococcus hominis, and Staphylococcus simulans. International Journal of Systematic Bacteriology 25:62-79.

34. Bieber L, Kahlmeter G. 2010. Staphylococcus lugdunensis in several niches of the normal skin flora. Clin Microbiol Infect 16:385-8.

35. Zipperer A, Konnerth MC, Laux C, Berscheid A, Janek D, Weidenmaier C, Burian M, Schilling NA, Slavetinsky C, Marschal M, Willmann M, Kalbacher H, Schittek B, Brotz-Oesterhelt H, Grond S, Peschel A, Krismer B. 2016. Human commensals producing a novel antibiotic impair pathogen colonization. Nature 535:511-6.

36. Hu L, Umeda A, Kondo S, Amako K. 1995. Typing of Staphylococcus aureus colonising human nasal carriers by pulsed-field gel electrophoresis. J Med Microbiol 42:127-32.

37. Hu L, Umeda A, Amako K. 1995. Typing of Staphylococcus epidermidis colonizing in human nares by pulsed-field gel electrophoresis. Microbiol Immunol 39:315-9.

38. Warnke P, Devide A, Weise M, Frickmann H, Schwarz NG, Schaffler H, Ottl P, Podbielski A. 2016. Utilizing Moist or Dry Swabs for the Sampling of Nasal MRSA Carriers? An In Vivo and In Vitro Study. Plos One 11:e0163073.

39. Verhoeven PO, Grattard F, Carricajo A, Lucht F, Cazorla C, Garraud O, Pozzetto B, Berthelot P. 2012. An algorithm based on one or two nasal samples is accurate to identify persistent nasal carriers of Staphylococcus aureus. Clin Microbiol Infect 18:551-7.

40. Hanssen AM, Kindlund B, Stenklev NC, Furberg AS, Fismen S, Olsen RS, Johannessen M, Sollid JUE. 2017. Localization of Staphylococcus aureus in tissue from the nasal vestibule in healthy carriers. BMC Microbiology 17:89.

41. Weidenmaier C, Goerke C, Wolz C. 2012. Staphylococcus aureus determinants for nasal colonization. Trends Microbiol 20:243-50.

42. Casado B, Pannell LK, Iadarola P, Baraniuk JN. 2005. Identification of human nasal mucous proteins using proteomics. Proteomics 5:2949-59.

43. Tomazic PV, Birner-Gruenberger R, Leitner A, Obrist B, Spoerk S, Lang-Loidolt D. 2014. Nasal mucus proteomic changes reflect altered immune responses and epithelial permeability in patients with allergic rhinitis. J Allergy Clin Immunol 133:741-50.

44. Koziel J, Potempa J. 2013. Protease-armed bacteria in the skin. Cell Tissue Res 351:325-37.

45. Corrigan RM, Miajlovic H, Foster TJ. 2009. Surface proteins that promote adherence of Staphylococcus aureus to human desquamated nasal epithelial cells. BMC Microbiology 9:22.

46. Baur S, Rautenberg M, Faulstich M, Grau T, Severin Y, Unger C, Hoffmann WH, Rudel T, Autenrieth IB, Weidenmaier C. 2014. A nasal epithelial receptor for Staphylococcus aureus WTA governs adhesion to epithelial cells and modulates nasal colonization. PLoS Pathog 10:e1004089.

47. Weidenmaier C, Kokai-Kun JF, Kristian SA, Chanturiya T, Kalbacher H, Gross M, Nicholson G, Neumeister B, Mond JJ, Peschel A. 2004. Role of teichoic acids in Staphylococcus aureus nasal colonization, a major risk factor in nosocomial infections. Nat Med 10:243-5.

48. Mulcahy ME, Geoghegan JA, Monk IR, O'Keeffe KM, Walsh EJ, Foster TJ, McLoughlin RM. 2012. Nasal Colonisation by Staphylococcus aureus Depends upon Clumping Factor B Binding to the Squamous Epithelial Cell Envelope Protein Loricrin. PLoS Pathog 8:e1003092.

49. Weidenmaier C, Peschel A. 2008. Teichoic acids and related cell-wall glycopolymers in Gram-positive physiology and host interactions. Nat Rev Microbiol 6:276-87.

50. Winstel V, Kuhner P, Salomon F, Larsen J, Skov R, Hoffmann W, Peschel A, Weidenmaier C. 2015. Wall Teichoic Acid Glycosylation Governs Staphylococcus aureus Nasal Colonization. MBio 6:e00632-15.

51. Schade J, Weidenmaier C. 2016. Cell wall glycopolymers of Firmicutes and their role as nonprotein adhesins. FEBS Lett 590:3758-3771.

52. O'Brien LM, Walsh EJ, Massey RC, Peacock SJ, Foster TJ. 2002. Staphylococcus aureus clumping factor B (ClfB) promotes adherence to human type I cytokeratin 10: implications for nasal colonization. Cell Microbiol 4:759-70.

53. Wertheim HF, Walsh E, Choudhurry R, Melles DC, Boelens HA, Miajlovic H, Verbrugh HA, Foster T, van Belkum A. 2008. Key role for clumping factor B in Staphylococcus aureus nasal colonization of humans. PLoS Med 5:e17.

54. Foster TJ, Geoghegan JA, Ganesh VK, Hook M. 2014. Adhesion, invasion and evasion: the many functions of the surface proteins of Staphylococcus aureus. Nat Rev Microbiol 12:49-62.

55. Clarke SR, Andre G, Walsh EJ, Dufrene YF, Foster TJ, Foster SJ. 2009. Iron-regulated surface determinant protein A mediates adhesion of Staphylococcus aureus to human corneocyte envelope proteins. Infect Immun 77:2408-16.

56. Askarian F, Ajayi C, Hanssen AM, van Sorge NM, Pettersen I, Diep DB, Sollid JU, Johannessen M. 2016. The interaction between Staphylococcus aureus SdrD and desmoglein 1 is important for adhesion to host cells. Sci Rep 6:22134.

57. Hammers CM, Stanley JR. 2013. Desmoglein-1, differentiation, and disease. J Clin Invest 123:1419-22.

58. Roche FM, Meehan M, Foster TJ. 2003. The Staphylococcus aureus surface protein SasG and its homologues promote bacterial adherence to human desquamated nasal epithelial cells. Microbiology 149:2759-67.

59. Schaffer AC, Solinga RM, Cocchiaro J, Portoles M, Kiser KB, Risley A, Randall SM, Valtulina V, Speziale P, Walsh E, Foster T, Lee JC. 2006. Immunization with Staphylococcus aureus clumping factor B, a major determinant in nasal carriage, reduces nasal colonization in a murine model. Infect Immun 74:2145-53.

60. Winstel V, Liang C, Sanchez-Carballo P, Steglich M, Munar M, Broker BM, Penades JR, Nubel U, Holst O, Dandekar T, Peschel A, Xia G. 2013. Wall teichoic acid structure governs horizontal gene transfer between major bacterial pathogens. Nat Commun 4:2345.

61. Brugger SD, Bomar L, Lemon KP. 2016. Commensal-Pathogen Interactions along the Human Nasal Passages. PLoS Pathog 12:e1005633.

62. Janek D, Zipperer A, Kulik A, Krismer B, Peschel A. 2016. High Frequency and Diversity of Antimicrobial Activities Produced by Nasal Staphylococcus Strains against Bacterial Competitors. PLoS Pathog 12:e1005812.

63. Lee H, Kim HY. 2011. Lantibiotics, class I bacteriocins from the genus Bacillus. J Microbiol Biotechnol 21:229-35.

64. Bierbaum G, Sahl HG. 2009. Lantibiotics: mode of action, biosynthesis and bioengineering. Curr Pharm Biotechnol 10:2-18.

65. Allgaier H, Jung G, Werner RG, Schneider U, Zahner H. 1986. Epidermin: sequencing of a heterodetic tetracyclic 21-peptide amide antibiotic. Eur J Biochem 160:9-22.

66. Kaletta C, Entian KD, Kellner R, Jung G, Reis M, Sahl HG. 1989. Pep5, a new lantibiotic: structural gene isolation and prepeptide sequence. Arch Microbiol 152:16-9.

67. van de Kamp M, van den Hooven HW, Konings RN, Bierbaum G, Sahl HG, Kuipers OP, Siezen RJ, de Vos WM, Hilbers CW, van de Ven FJ. 1995. Elucidation of the primary structure of the lantibiotic epilancin K7 from Staphylococcus epidermidis K7. Cloning and characterisation of the epilancin-K7-encoding gene and NMR analysis of mature epilancin K7. Eur J Biochem 230:587-600.

68. Ekkelenkamp MB, Hanssen M, Danny Hsu ST, de Jong A, Milatovic D, Verhoef J, van Nuland NA. 2005. Isolation and structural characterization of epilancin 15X, a novel lantibiotic from a clinical strain of Staphylococcus epidermidis. FEBS Lett 579:1917-22.

69. Heidrich C, Pag U, Josten M, Metzger J, Jack RW, Bierbaum G, Jung G, Sahl HG. 1998. Isolation, characterization, and heterologous expression of the novel lantibiotic epicidin 280 and analysis of its biosynthetic gene cluster. Appl Environ Microbiol 64:3140-6.

70. Navaratna MA, Sahl HG, Tagg JR. 1998. Two-component anti-Staphylococcus aureus lantibiotic activity produced by Staphylococcus aureus C55. Appl Environ Microbiol 64:4803-8.

71. Sashihara T, Kimura H, Higuchi T, Adachi A, Matsusaki H, Sonomoto K, Ishizaki A. 2000. A novel lantibiotic, nukacin ISK-1, of Staphylococcus warneri ISK-1: cloning of the structural gene and identification of the structure. Biosci Biotechnol Biochem 64:2420-8.

72. Wilaipun P, Zendo T, Okuda K, Nakayama J, Sonomoto K. 2008. Identification of the nukacin KQU-131, a new type-A(II) lantibiotic produced by Staphylococcus hominis KQU-131 isolated from Thai fermented fish product (Pla-ra). Biosci Biotechnol Biochem 72:2232-5.

73. Nakatsuji T, Chen TH, Narala S, Chun KA, Two AM, Yun T, Shafiq F, Kotol PF, Bouslimani A, Melnik AV, Latif H, Kim JN, Lockhart A, Artis K, David G, Taylor P, Streib J, Dorrestein PC, Grier A, Gill SR, Zengler K, Hata TR, Leung DY, Gallo RL. 2017. Antimicrobials from human skin commensal bacteria protect against Staphylococcus aureus and are deficient in atopic dermatitis. Sci Transl Med 9.

74. Kumar R, Jangir PK, Das J, Taneja B, Sharma R. 2017. Genome Analysis of Staphylococcus capitis TE8 Reveals Repertoire of Antimicrobial Peptides and Adaptation Strategies for Growth on Human Skin. Scientific Reports 7.

75. Christensen GJM, Scholz CFP, Enghild J, Rohde H, Kilian M, Thurmer A, Brzuszkiewicz E, Lomholt HB, Bruggemann H. 2016. Antagonism between Staphylococcus epidermidis and Propionibacterium acnes and its genomic basis. BMC Genomics 17.

76. Brzuszkiewicz E, Weiner J, Wollherr A, Thurmer A, Hupeden J, Lomholt HB, Kilian M, Gottschalk G, Daniel R, Mollenkopf HJ, Meyer TF, Bruggemann H. 2011. Comparative genomics and transcriptomics of Propionibacterium acnes. PLoS One 6:e21581.

77. Iwase T, Uehara Y, Shinji H, Tajima A, Seo H, Takada K, Agata T, Mizunoe Y. 2010. Staphylococcus epidermidis Esp inhibits Staphylococcus aureus biofilm formation and nasal colonization. Nature 465:346-9.

78. Sugimoto S, Iwamoto T, Takada K, Okuda K, Tajima A, Iwase T, Mizunoe Y. 2013. Staphylococcus epidermidis Esp degrades specific proteins associated with Staphylococcus aureus biofilm formation and host-pathogen interaction. J Bacteriol 195:1645-55.

79. Lemon KP, Klepac-Ceraj V, Schiffer HK, Brodie EL, Lynch SV, Kolter R. 2010. Comparative analyses of the bacterial microbiota of the human nostril and oropharynx. MBio 1:e00129-10.

80. Selva L, Viana D, Regev-Yochay G, Trzcinski K, Corpa JM, Lasa I, Novick RP, Penades JR. 2009. Killing niche competitors by remote-control bacteriophage induction. Proc Natl Acad Sci U S A 106:1234-8.

81. Uehara Y, Kikuchi K, Nakamura T, Nakama H, Agematsu K, Kawakami Y, Maruchi N, Totsuka K. 2001. H(2)O(2) produced by viridans group streptococci may contribute to inhibition of methicillin-resistant Staphylococcus aureus colonization of oral cavities in newborns. Clin Infect Dis 32:1408-13.

82. Bogaert D, van Belkum A, Sluijter M, Luijendijk A, de Groot R, Rumke HC, Verbrugh HA, Hermans PW. 2004. Colonisation by Streptococcus pneumoniae and Staphylococcus aureus in healthy children. Lancet 363:1871-2.

83. Regev-Yochay G, Dagan R, Raz M, Carmeli Y, Shainberg B, Derazne E, Rahav G, Rubinstein E. 2004. Association between carriage of Streptococcus pneumoniae and Staphylococcus aureus in Children. JAMA 292:716-20.

84. Uehara Y, Nakama H, Agematsu K, Uchida M, Kawakami Y, Abdul Fattah AS, Maruchi N. 2000. Bacterial interference among nasal inhabitants: eradication of Staphylococcus aureus from nasal cavities by artificial implantation of Corynebacterium sp. J Hosp Infect 44:127-33.

85. Wollenberg MS, Claesen J, Escapa IF, Aldridge KL, Fischbach MA, Lemon KP. 2014. Propionibacterium-produced coproporphyrin III induces Staphylococcus aureus aggregation and biofilm formation. MBio 5:e01286-14.

86. Hanzelmann D, Joo HS, Franz-Wachtel M, Hertlein T, Stevanovic S, Macek B, Wolz C, Gotz F, Otto M, Kretschmer D, Peschel A. 2016. Toll-like receptor 2 activation depends on lipopeptide shedding by bacterial surfactants. Nat Commun 7:12304.

87. Riechelmann H, Essig A, Deutschle T, Rau A, Rothermel B, Weschta M. 2005. Nasal carriage of Staphylococcus aureus in house dust mite allergic patients and healthy controls. Allergy 60:1418-23.

88. Wos-Oxley ML, Chaves-Moreno D, Jauregui R, Oxley AP, Kaspar U, Plumeier I, Kahl S, Rudack C, Becker K, Pieper DH. 2016. Exploring the bacterial assemblages along the human nasal passage. Environ Microbiol 18:2259-71. 558

Chapter 2

Human commensals producing a novel antibiotic impair pathogen colonisation

Alexander Zipperer[1,2]*, Martin C. Konnerth[3]*, Claudia Laux[1,2], Anne Berscheid[4], Daniela Janek[1,2,†], Christopher Weidenmaier[5,2], Marc Burian[6], Nadine A. Schilling[3,7], Christoph Slavetinsky[1,2], Matthias Marschal[5], Matthias Willmann[5,2], Hubert Kalbacher[7], Birgit Schittek[6], Heike Brötz-Oesterhelt[4,2], Stephanie Grond[3], Andreas Peschel[1,2] & Bernhard Krismer[1,2]

[1] Interfaculty Institute of Microbiology and Infection Medicine, Infection Biology, University of Tübingen, 72076 Tübingen, Germany

[2] German Centre for Infection Research (DZIF), Partner Site Tübingen, 72076 Tübingen, Germany

[3] Institute of Organic Chemistry, University of Tübingen, 72076 Tübingen, Germany

[4] Interfaculty Institute of Microbiology and Infection Medicine, Microbial Bioactive Compounds, University of Tübingen, 72076 Tübingen, Germany

[5] Interfaculty Institute of Microbiology and Infection Medicine, Medical Microbiology, University of Tübingen, 72076 Tübingen, Germany

[6] Department of Dermatology, Division of Dermatooncology, University of Tübingen, 72076 Tübingen, Germany

[7] Interfaculty Institute of Biochemistry, University of Tübingen, 72076 Tübingen, Germany

[†]present address: Boehringer Ingelheim, 88400 Biberach, Germany

*These authors contributed equally to this work

***Nature* Vol 535, 511-516 (28 July 2016)**

Summary

The vast majority of systemic bacterial infections is caused by facultative, often antibiotic-resistant pathogens colonising human body surfaces. Nasal carriage of *Staphylococcus aureus* predisposes to invasive infection, but the mechanisms permitting or interfering with pathogen colonisation have remained largely unknown. Whereas soil microbes are known to compete by production of antibiotics, such processes have rarely been reported for human microbiomes. We show that nasal *Staphylococcus lugdunensis* strains produce lugdunin, a novel thiazolidine-containing cyclic peptide antibiotic prohibiting colonisation by *S. aureus,* and a rare example of a non-ribosomally synthesized bioactive compound from human-associated bacteria. Lugdunin is bactericidal against major pathogens, effective in animal models, and not prone to resistance development. Importantly, human nasal colonisation by *S. lugdunensis* was associated with a significantly reduced *S. aureus* carriage rate suggesting that lugdunin or lugdunin-producing commensals could be valuable for preventing staphylococcal infections. Moreover, human microbiota should be considered as a source for new antibiotics.

Introduction

Infections caused by highly antibiotic–resistant bacteria have strongly increased in recent years and represent a major cause of morbidity and mortality world-wide, including the developed countries[1,2]. Multi-drug resistant organisms (MDRO), such as methicillin-resistant *S. aureus* (MRSA)[3], vancomycin-resistant enterococci (VRE)[4], and third-generation cephalosporin-resistant Gram-negative bacteria (3GCRGB)[5], are expected to become a more frequent cause of death than cancer within the next decades[6]. Despite the urgent need for new resistance-breaking antibiotics, very few compounds are in developmental pipelines, the majority of which are congeners of currently used antibiotic classes[7,8]. Nevertheless, innovative approaches for cultivation of so far uncultured potential antibiotic producers or activation of silent biosynthetic gene clusters have recently led to the discovery of entirely new antimicrobial compounds with interesting properties[9-12]. Moreover, new compound sources, such as the large inventory of antimicrobial host defence peptides from higher organisms, open new avenues for the development of new antiinfectives[13,14]. As the available antibiotics lose their efficacy, it is of increasing importance to limit the ongoing spread of resistant bacteria[15]. Unfortunately, most of the major MDROs are increasingly disseminating in the community and cannot be effectively targeted by standard infection control measures[2]. The strong antibiotic selection pressure in humans and in farm animals and the increasing fitness of MRSA, VRE, and 3GCRGB in competition with commensals leads to the symptomless and usually unrecognized presence of MDRO in the microbiota of many humans[16-18]. Notably, the vast majority of systemic bacterial infections is caused by endogenous pathogens from human microbiomes, and MDRO-colonised individuals are exposed to a substantially higher risk of invasive, difficult-to-treat infections when they undergo surgery or suffer from trauma or immunosuppression[1,19,20]. *S. aureus* is found in the anterior nares of approximately 30% of the human population. Its eradication by the antibiotic mupirocin strongly reduces the predisposition to invasive infection[19]. However, mupirocin has to be applied repeatedly over five days, requiring strict compliance and costly extension of patient hospitalization; additionally, mupirocin resistance rates are steadily increasing[21]. Moreover, current decolonisation strategies targeting MDRO at other body surfaces, such as the intestine, depend on broad-spectrum antibiotics and are highly controversial[22]. Thus, there is not only an urgent need for new therapeutic antibiotics but also for new effective MDRO decolonisation strategies.

While many ongoing research efforts address major virulence and resistance mechanisms, the processes governing bacterial fitness, competition, and dissemination in microbiomes remain poorly understood. Recent studies have shown how diverse and dynamic human microbiomes are, especially those of the environment-exposed microbiomes of the skin[23] and upper airways[24]. These ecological niches are particularly poor in nutrients[25], suggesting that colonising bacteria are probably in fierce competition and may use a variety of strategies to overcome competitors[25,26]. Bacteria from human microbiomes have occasionally been found to produce bacteriocins, antimicrobial substances acting against closely related bacteria[27,28]. Genes related to antibiotic biosynthesis have been identified in human metagenomes[29] leading to the discovery of lactocillin, a ribosomally synthesised thiopeptide antibiotic produced by a human vaginal commensal[30]. However, the potential roles of such complex bioactive compounds in shaping human microbiomes are still unknown.

Results

Anti-*S. aureus* activity of a nasal commensal

A previously described collection of nasal *Staphylococcus* isolates[25] was screened for antimicrobial activity against *S. aureus*. Whereas most isolates did not affect *S. aureus*, the strain *Staphylococcus lugdunensis* IVK28 was found to have a particularly strong capacity to prevent the growth of *S. aureus* (Fig. 1a). IVK28 produced its antibacterial substance only under iron-limiting conditions and only on solid agar surfaces, not in liquid culture.

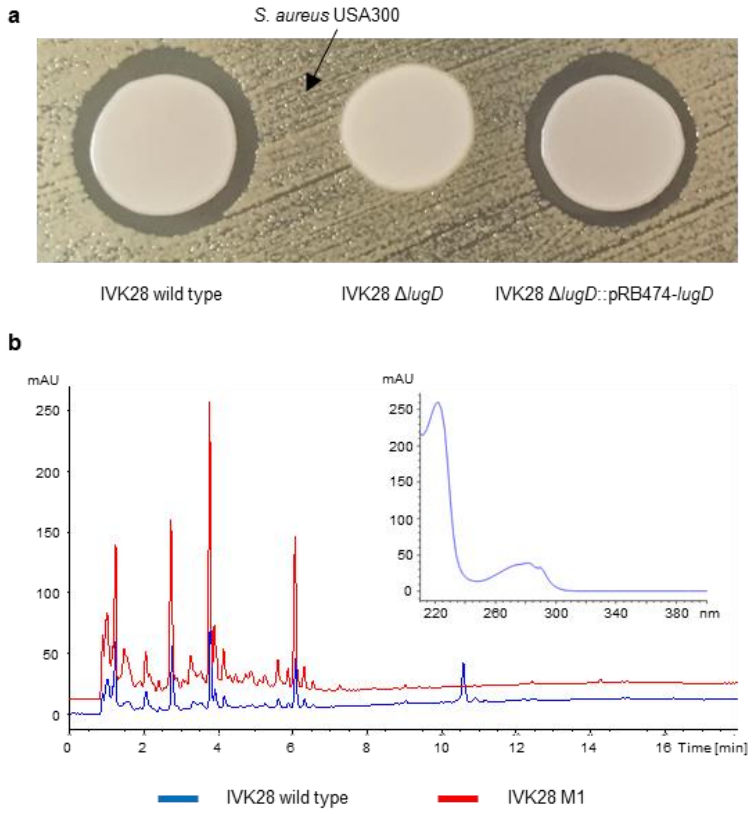

Figure 1 | Lugdunin production by *S. lugdunensis* wild type and isogenic mutants. a, Bioactivity assay with the *S. lugdunensis* IVK28 wild type, the Δ*lugD* mutant and the complemented mutant against *S. aureus* USA300. BM plates were inoculated with a lawn of *S. aureus* USA300. Thereon *S. lugdunensis* IVK28 cells from overnight cultures of the wild type, the mutant Δ*lugD* and the complemented mutant Δ*lugD*::pRB474-*lugD* were spotted. **b,** HPLC-UV-chromatogram shows comparison of *S. lugdunensis* IVK28 wild type and transposon mutant M1. Cell extracts of the IVK28 wild type (blue) and the transposon mutant M1 (red) were compared by RP-HPLC-UV. The inlay depicts the absorption spectrum of lugdunin with the prominent absorption at 280 nm, indicating the presence of tryptophan.

Transposon mutagenesis of IVK28 led to isolation of mutant M1, which did not inhibit *S. aureus*. Analysis of the transposon insertion site revealed the disruption of an uncharacterized gene encoding a putative non-ribosomal peptide synthetase (NRPS; position 860375/76 of SLUG_RS03940 in the annotated genome sequence of *S. lugdunensis* N920143[31]; Acc.no: NC_017353.1). This gene is encoded in an operon of approximately 30 kbp with several other NRPS and antibiotic biosynthesis-related genes (Fig. 2a and Extended Data Fig. 1a), suggesting that the inhibitory molecule of IVK28 may be a complex, non-ribosomally synthesized peptide compound. The NRPS operon was found in all *S. lugdunensis* genomes in the databases, and it was identified by PCR in each of the *S. lugdunensis* strains from our strain collection, indicating that it represents a species characteristic rather than a strain-specific feature. Nevertheless, the GC-content of the operon of 26.9% is clearly distinct from that of the whole genome (33.8%) indicating that the gene cluster may have been transferred to *S. lugdunensis* by horizontal gene transfer from another bacterial species. The operon consists of four NRPS genes (named *lugA, B, C, D*) encoding adenylation domains for five amino acids (Fig. 2b). The *lug* operon further includes all genes whose products are required for the synthesis and transport of a non-ribosomally synthesized peptide compound (Extended Data Fig. 1a). Gene clusters for secondary metabolite production are frequently found in streptomycetes and other soil bacteria but are exceptional in human-associated bacteria[29]. The *lug* operon was exclusively found in *S. lugdunensis* and encodes a unique combination of antibiotic biosynthesis enzymes, all with less than 35% identity to any other described enzyme, suggesting that it may be responsible for biosynthesis of a novel compound. To confirm that the *lug* operon is responsible for the antimicrobial activity of IVK28, the smallest NRPS gene, *lugD*, was deleted by gene replacement. The mutant Δ*lugD* showed no detectable antimicrobial activity, but the phenotype was restored by complementation with a plasmid-encoded copy of *lugD* (Fig. 1a).

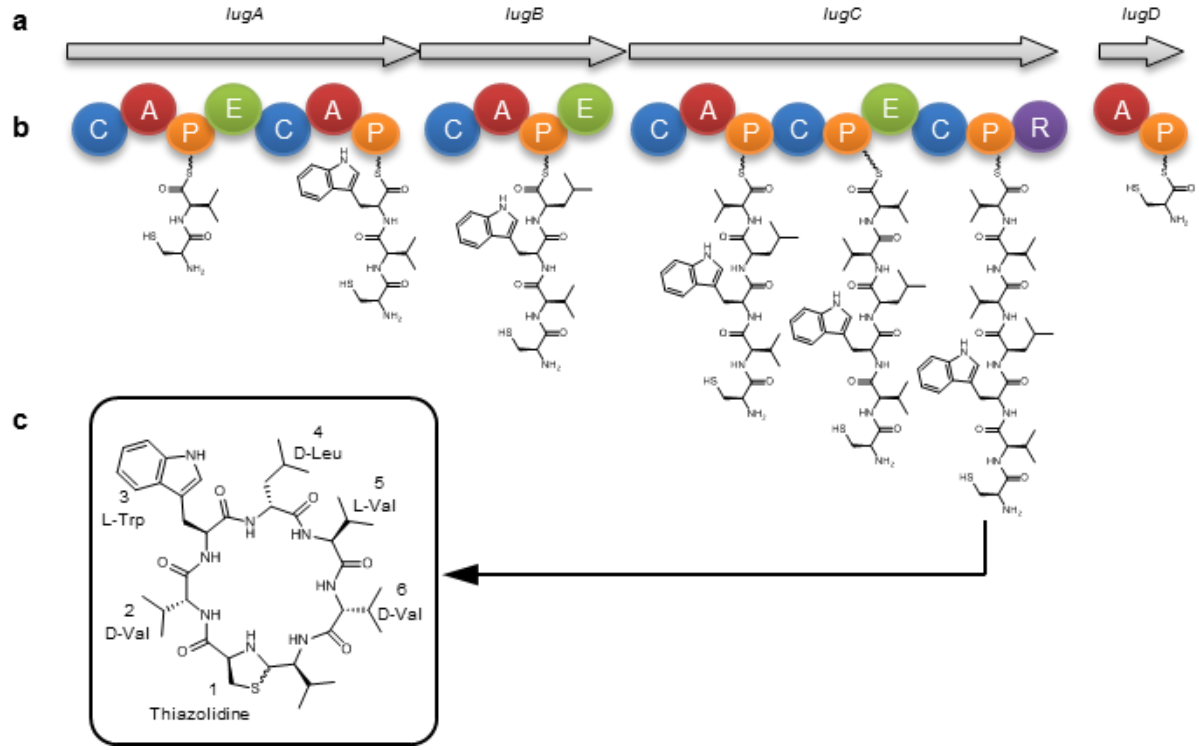

Figure 2 | Gene cluster, proposed biosynthesis pathway, and chemical structure of lugdunin. a, NRPS genes *lugABCD.* **b,** Modular organization of gene products. Functional domains: A, adenylation; P, peptidyl carrier protein; C, condensation; E, epimerization; R, reductase. The sequential biosynthesis of lugdunin starts presumably at the characteristic initiation module of LugD and continues with LugA-C. The C-terminal reductase domain of LugC catalyses aldehyde formation at the thioester of the terminal valine and enables subsequent ring closure of the thiazolidine, leading to the cyclopeptide. **c,** Chemical structure of lugdunin. Cyclization of the reactive C-terminal aldehyde and N-terminal cysteine is assumed to occur via thiohemiacetal to the thiazolidine building block (Extended Data Fig. 4d).

Lugdunin, a novel peptide antibiotic

The antimicrobial activity of IVK28 was enriched by ethanol extraction of agar-grown cells. Reversed-phase high-pressure liquid chromatography coupled with UV and mass spectrometry (RP-HPLC-UV-MS) revealed obvious differences between extracts from IVK28 wild type and mutant M1 in only one signal (Fig. 1b). The molecular formula, $C_{40}H_{62}N_8O_6S$, deduced from electrospray ionization high-resolution mass spectrometry (ESI-HR MS, Extended Data Figs. 2a, b; $[M+H]^+$ $C_{40}H_{63}N_8O_6S^+$, calculated 783.45858, found 783.45850, Δ0.1 ppm, relative molecular mass M_r = 783.03) did not correspond to

any known molecule. Spectral UV absorbance at 280 nm indicated the presence of a tryptophan moiety (Fig. 1b). To circumvent the problem that the compound was not produced in liquid culture, which impeded isolation of sufficient amounts for chemical characterisation and biological profiling, expression of the biosynthetic genes was uncoupled from the native *lug* operon promoter and its regulation. This strategy has recently been successfully applied to other antimicrobial gene clusters[10,32,33]. The putative *tetR*-like regulator gene of the *lug* operon (*lugR*) was deleted, and the strong *xylAB* promoter was inserted upstream of the NRPS genes, along with the gene for its corresponding xylose-sensitive repressor XylR. Cultivation of the resulting strain *S. lugdunensis* IVK28-Xyl (Extended Data Fig. 1b) in liquid culture with xylose led to strong production of inhibitory activity, which could be purified by consecutive steps of 1-butanol extraction, gel filtration, and reversed-phase HPLC. The pure compound exhibited exactly the same mass as determined for the compound from the wild type strain IVK28 and was named lugdunin.

NMR, ESI-HR-MS, and an advanced Marfey's analysis of lugdunin revealed a cyclic peptide (Fig. 2c, Extended Data Figs. 3a, b, c, and Extended Data Table 1) comprising an unusual thiazolidine heterocycle and five amino acids (D-valine, L-tryptophan, D-leucine, L-valine, and D-valine) (Fig. 2c). The thiazolidine building block occurs in certain linear NRPS products, like watasemycins[34] and yersiniabactin[35], but is yet unprecedented in macrocyclic peptides (Extended Data Fig. 4). Lugdunin's thiazolidine ring is most likely formed by condensation of an N-terminal L-cysteine with a C-terminal L-valine residue (position one and seven, respectively, of the precursor peptide) upon reductive release of a linear heptapeptide aldehyde from the NRPS mega-enzyme by the terminal reductase of LugC (Fig. 2b and Extended Data Fig. 4d). Total chemical synthesis of lugdunin yielded a product with identical chemical properties and antimicrobial activity compared to the natural product from strain IVK28, which confirmed the assigned lugdunin structure.

The origin of lugdunin from a heptapeptide was unexpected because the NRPS proteins from the *lug* operon encompass only five adenylation domains, central enzymatic domains whose number usually determines the number of incorporated amino acids (Fig. 2b). The predicted specificities of NRPS adenylation domains[36] were in agreement with the identified amino acids, except for position three (tryptophan instead of threonine), indicating a new specificity for the second adenylation domain of LugA. Moreover, LugC exhibited an exceptional modular organization[37] with one adenylation

domain (valine) but two downstream peptide-bond forming condensation and three peptidyl carrier protein domains required for amino acid transfer. This organisation suggested that the single adenylation domain of LugC is responsible for activation of three consecutive valine units, which are subsequently incorporated in alternating L- and D-configurations. An in part similar mechanism has been described for yersiniabactin biosynthesis[38] (see also Supplementary discussion). Thus, the LugC domains represent a very unusual assembly line compared to characterized NRPS machineries.

Activity against major human pathogens

Lugdunin has potent antimicrobial activity against a wide range of Gram-positive bacteria, including opportunistic pathogens such as difficult-to-treat MRSA, glycopeptide-intermediate resistant *S. aureus* (GISA) and VRE isolates. Minimal inhibitory concentration (MIC) values in the micromolar range (1.5-12 µg/mL; 1.9-15.3 µM) demonstrated high potency, and this activity was not impaired in the presence of human serum (Table 1).

Table 1 | Lugdunin spectrum of activity

Species and strain	Resistance	Lugdunin MIC (µg/ml)
Staphylococcus aureus USA300 (LAC)	MRSA	1.5
+ 50% human serum		1.5
Staphylococcus aureus USA300 (NRS384)	MRSA	1.5
Staphylococcus aureus Mu50	GISA	3
Staphylococcus aureus SA113		3
Staphylococcus aureus RN4220		3
Enterococcus faecium BK463	VRE	3
Enterococcus faecalis VRE366	VRE	12
Listeria monocytogenes ATCC19118		6
Streptococcus pneumoniae ATCC49619		1.5
Bacillus subtilis 168 (*trpC2*)		4
Pseudominas aeruginosa PAO1		>50
Escherichia coli DH5α		>50

MRSA, methicillin-resistant *S. aureus*; GISA, glycopeptide-resistant *S. aureus*; VRE, vancomycin-resistant *Enterococcus*

Lugdunin was bactericidal against MRSA with complete killing at 10 x MIC (Fig. 3a). Lugdunin did not cause lysis of primary human neutrophils or erythrocytes, and even high amounts of lugdunin showed no substantial inhibition of the metabolic activity of the human monocytic cell line HL60 (IC_{50}> 50 µg/mL) (Extended Data Fig 5). Bacterial cells exposed to lugdunin stopped incorporating radioactive DNA, RNA, protein or cell wall precursors almost simultaneously even at concentrations below the MIC (Extended Data Fig. 6), suggesting that lugdunin may lead to rapid breakdown of bacterial energy resources. In this respect lugdunin resembles daptomycin, where parallel cessation of all four metabolic pathways has also been observed[39] and whose exact mode of action is still unknown. During lugdunin purification a 2-D-*allo*-isoleucine variant (instead of 2-D-valine) was isolated. This derivative with additional methyl group and stereogenic centre is produced by *S. lugdunensis* in small amounts and is inactive. No resistance development was observed in *S. aureus* during continuous serial passaging in the presence of subinhibitory concentrations of lugdunin over 30 days (Fig. 3b). In contrast, *S. aureus* developed rapidly resistance to rifampicin within a few days of exposure (Fig. 3b).

The capacity of lugdunin to cure infections *in vivo* was analysed in a mouse skin infection model reflecting a typical human *S. aureus* infection and a common indication for antibiotic treatment[40,41]. The back skin of shaved black-6 mice (C57BL/6) was superficially damaged by multiple stripping with adhesive tape and was infected with *S. aureus*. Then, 24, 30, and 42 hours after infection mice were treated with 1.5 µg lugdunin per time point and infection site, and six hours later mice were sacrificed. Lugdunin treatment led to a strong reduction or even complete eradication of viable *S. aureus* on the surface and in the deeper layers of the skin (Figs. 3c, d), demonstrating that lugdunin eradicates *S. aureus* and penetrates tissues *in vivo*. Note that infection was not affected by lugdunin in two samples, most probably because some animals removed the lugdunin ointment by intensive licking. Bacteria obtained from these skin samples exhibited unchanged susceptibility to lugdunin, indicating that they had not developed resistance.

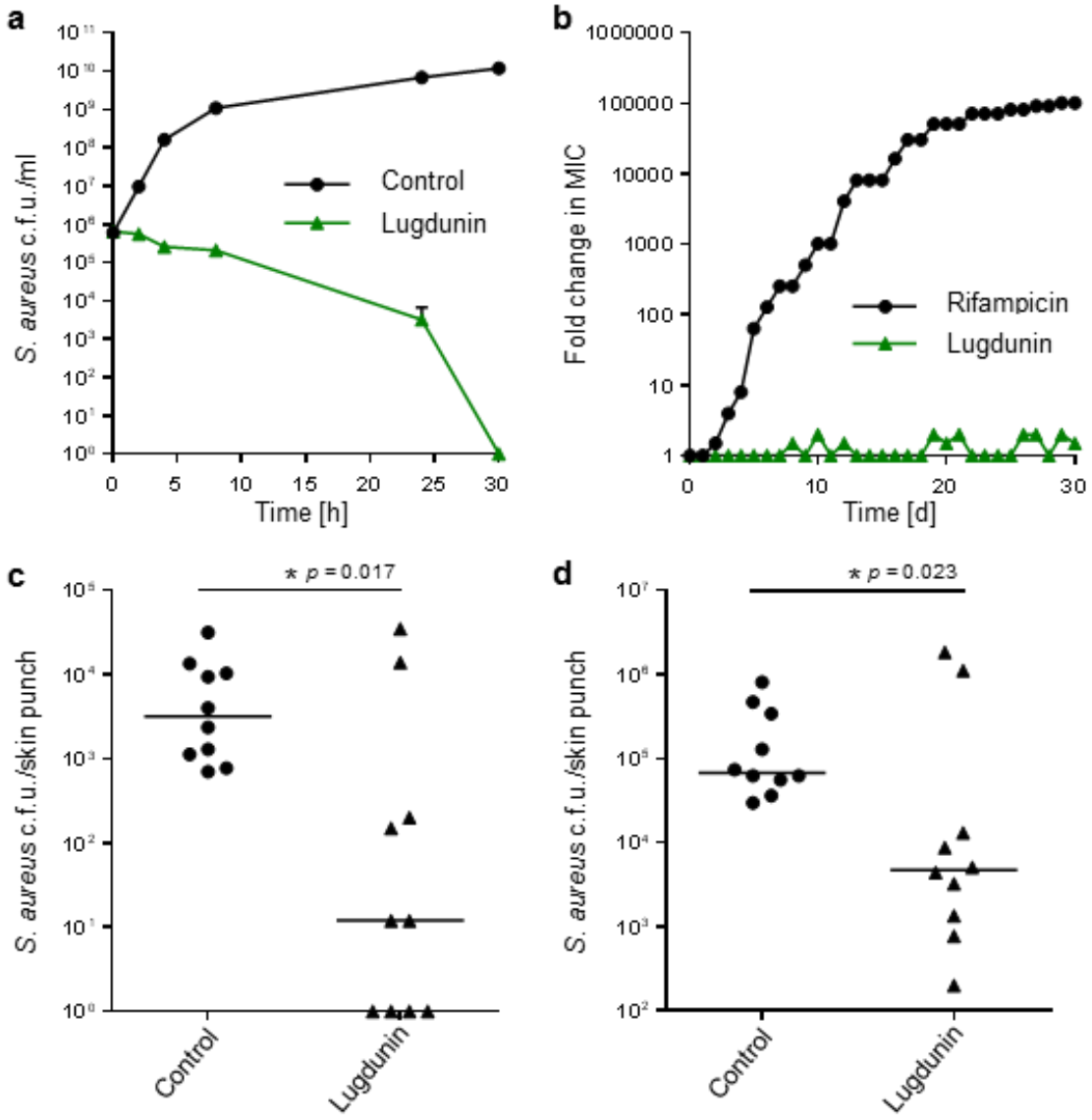

Figure 3 | Lugdunin has bactericidal activity, a low risk for resistance development and efficacy in a mouse skin infection model. a, Killing curve. Incubation of *S. aureus* with a 10 x MIC of lugdunin leads to complete killing of the inoculum after 30 h (detection limit is 10^0 CFU/mL). Data represent medians ± S.D. of three independent experiments. **b,** Serial passaging of *S. aureus* with sub-inhibitory concentrations of rifampicin leads to high resistance against rifampicin. However, such resistance development is not observed with lugdunin. A representative of two independent experiments is shown. **c, d,** Mouse skin infection. Lugdunin treatment (3 times, 1.5 µg/skin area) of *S. aureus* skin infections (5 mice ≙ 10 skin punches per group) leads to strongly reduced numbers of viable bacteria after two days. CFUs for surface-attached bacteria (**c**) or bacteria located in the deeper skin tissue (**d**) per skin punch are shown. Horizontal lines represent the median of each group. Significant differences between groups were analysed by the Mann Whitney test (*, $p< 0.05$).

Lugdunin production outcompetes *S. aureus*

The production of antimicrobials, mostly plasmid-encoded ribosomally synthesized bacteriocins, has been sporadically documented in individual bacterial strains from human microbiomes[27]. However, the roles of such compounds in microbial fitness and in microbiota dynamics have remained largely unknown. To determine whether lugdunin contributes to the capacity of *S. lugdunensis* IVK28 to prevail in competition with *S. aureus*, the two species were co-cultivated on solid agar surface, promoting lugdunin production, and bacterial numbers were monitored for three days.

As shown in Fig. 4a, the lugdunin-producing IVK28 wild type overgrew *S. aureus* efficiently, even when the inoculum contained 10-times higher numbers of *S. aureus* than *S. lugdunensis* cells. No viable *S. aureus* cells were recovered after three days indicating complete killing by *S. lugdunensis*. In contrast, IVK28 Δ*lugD* could not outcompete *S. aureus* (Fig. 4b) and was even overgrown when inoculated at 10-times higher numbers than *S. aureus* (Fig. 4d). The *S. aureus*-eradicating capacity of Δ*lugD* could be largely restored by complementation with *lugD* on a plasmid (Fig. 4c). These data demonstrate that *S. lugdunensis* IVK28 wild type can effectively eradicate *S. aureus* and that lugdunin production is responsible for this trait.

Nasal carriage is known to be a major risk factor for invasive *S. aureus* infections[19,42]. To explore whether *S. lugdunensis* can interfere with nasal *S. aureus* colonisation *in vivo* in vertebrates, the noses of cotton rats, a well-established animal model for investigating *S. aureus* nasal colonisation[43], were instilled with mixtures of *S. lugdunensis* IVK28 wild type or Δ*lugD* plus *S. aureus*. The three test strains colonised cotton rat noses stably over the 5-day test period when instilled individually (Extended Data Fig. 7). However, when the two species were co-inoculated, significantly less *S. aureus* cells were retrieved from animals co-colonised by IVK28 wild type compared to those co-colonised with Δ*lugD* (Fig. 4e). This finding indicates that lugdunin production can effectively interfere with *S. aureus* colonisation *in vivo*.

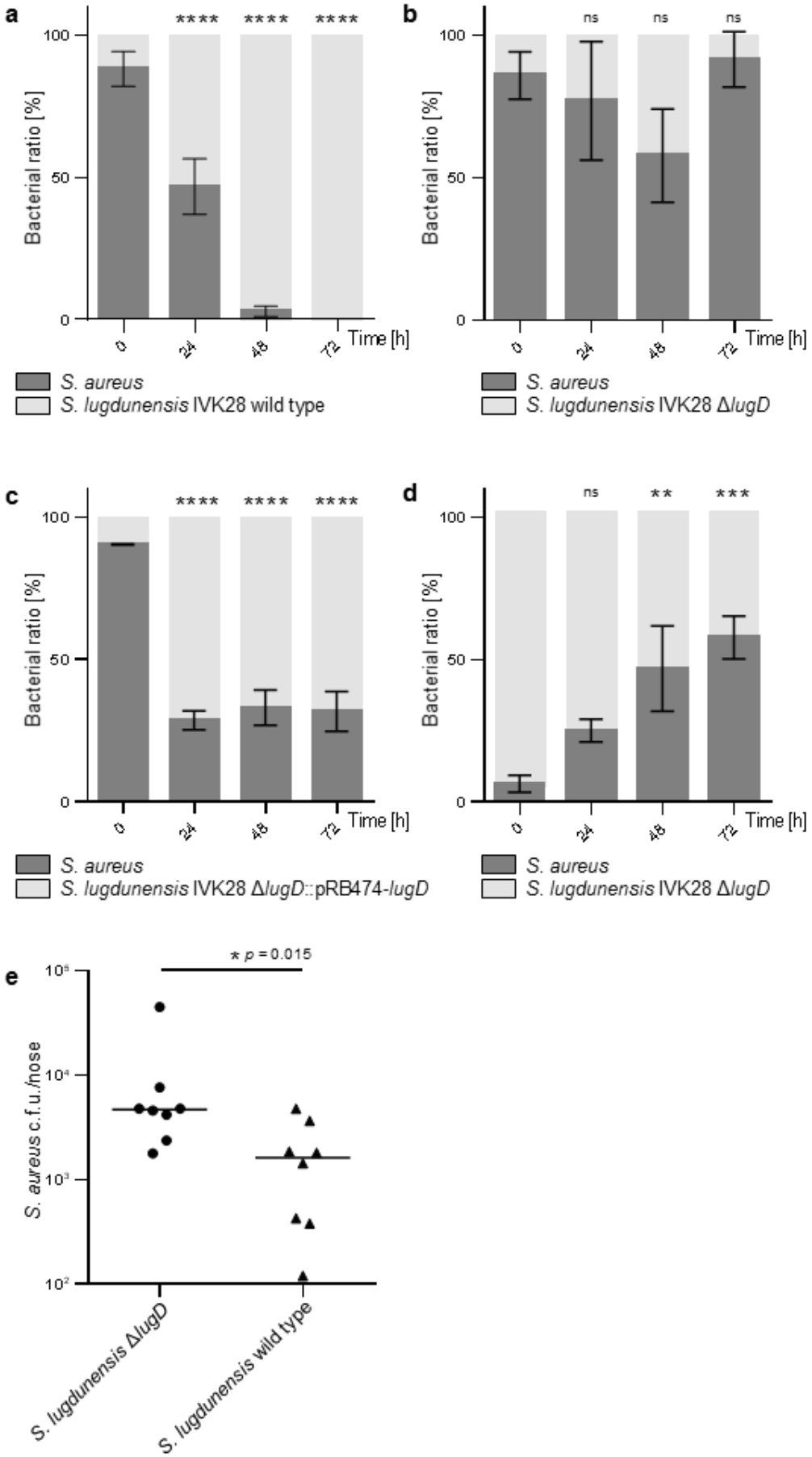
a
b
c
d
e
Bacterial ratio [%]
Time [h]
****
ns
**
***
S. aureus
S. lugdunensis IVK28 wild type
S. lugdunensis IVK28 ΔlugD
S. lugdunensis IVK28 ΔlugD::pRB474-lugD
* p = 0.015
S. aureus c.f.u./nose
S. lugdunensis ΔlugD
S. lugdunensis wild type

Figure 4 | Lugdunin-producing *S. lugdunensis* IVK28 wild type restricts the growth of *S. aureus* *in vitro* and *in vivo* in cotton rats. a, *S. aureus* is overgrown by *S. lugdunensis* IVK28 (dark or light grey columns, respectively) wild type on agar plates inoculated at ratios of ~ 90:10. In contrast, the ratio between IVK28 Δ*lugD* and *S. aureus*, inoculated at a ratio of ~ 90:10, does not change significantly over time (**b**). **c,** The capacity of *S. lugdunensis* Δ*lugD* to overgrow *S. aureus* is largely restored by plasmid-encoded *lugD*. **d,** *S. aureus* displaces IVK28 Δ*lugD* even when inoculated in ratios of ~ 10:90. Data represent mean values ± S.D. of three independent experiments. Significant differences between starting conditions and indicated time points were analysed by one-way ANOVA (*, $p< 0.05$; **, $p< 0.01$; ***, $p< 0.001$; ****, $p<0.0001$; n.s, not significant). **e,** Cotton rat noses (8 animals per group) co-colonised by *S. aureus* and *S. lugdunensis* IVK28 wild type show significantly less *S. aureus* CFUs after five days compared to *S. lugdunensis* IVK28 Δ*lugD*. Horizontal lines represent the median of each group. Significant differences, calculated by the Mann Whitney test, are indicated (*, $p< 0.05$).

Interference with *S. aureus* carriage

Factors governing the human nasal *S. aureus* carrier status have remained largely unknown[42,44]. To investigate whether the presence of *S. lugdunensis* in the human nose can prevent co-colonisation by *S. aureus*, we examined nasal swabs from 187 hospitalized patients for colonisation by *S. lugdunensis, S. aureus,* or both. The overall colonisation rates of *S. aureus* and *S. lugdunensis* were 32.1% and 9.1%, respectively (Table 2), which corresponds to published data[20,45]. Of note, the percentage of *S. aureus* colonisation in *S. lugdunensis*-positive individuals was 5.9-fold lower than in *S. lugdunensis*-negative individuals (5.9% vs. 34.7%, respectively). Chi^2 statistical analysis showed that the reduced *S. aureus* detection rate in the presence of *S. lugdunensis* for the entire study population was significant (risk ratio 0.169; 95%-confidence interval 0.025 - 1.147; $p = 0.015$; Table 2) indicating that a strong interference precludes the simultaneous presence of *S. aureus* and *S. lugdunensis* in the human nose. In accord with this finding, PCR analysis demonstrated that all nasal *S. lugdunensis* isolates contained the *lug* operon and all tested *S. aureus* (30 nasal as well as seven laboratory strains) were found to be highly susceptible to lugdunin. Together with the ability of the lugdunin producer IVK28 to reduce *S. aureus* numbers in cotton rat noses, these data provide strong evidence for the potent capacity of *S. lugdunensis* to prevent human nasal colonisation by *S. aureus*.

Table 2 | *S. aureus* and *S. lugdunensis* distribution in hospitalized patients

	S. lugdunensis-positive	*S. lugdunensis*-negative	Total
***S. aureus*-positive**	**1**	**59**	**60**
***S. aureus*-negative**	**16**	**111**	**127**
Total	**17**	**170**	**187**
Risk§	**0.059***	**0.347***	**0.321**

Significant differences between *S. lugdunensis*-positive and *S. lugdunensis* negative patients were analyzed by the Chi^2 test

§ 0.059 vs. 0.347: Risk ratio 0.169; 95%-confidence interval 0.025 - 1.147; *$p = 0.015$

Conclusions

The human predisposition to *S. aureus* nasal carriage is governed by several host genetic or microbiota-related factors, which may affect the capacity of *S. aureus* to adhere to and multiply on nasal epithelia[43,44,46]. Here, we provide evidence for a crucial role of *S. lugdunensis* and its antimicrobial product, lugdunin, in preventing *S. aureus* colonisation of the human nose. *S. aureus* can only rarely be isolated from the axillae or groin, further habitats of *S. lugdunensis* in addition to nares[45], which may also be related to the production of lugdunin. Accordingly, lugdunin or lugdunin-producing commensal staphylococci could become a valuable strategy for preventing *S. aureus* colonisation and invasive infections in high-risk patients facing for instance elective surgery, immuno-suppression, or regular haemodialysis. The concept of probiotic bacteria interfering with the predisposition to infection has been pursued mostly for enteric pathogens[47]. Our study suggests that the probiotics concept should be extended to body sites other than the gut, such as the nasal mucous membranes, and to additional major pathogens such as *S. aureus*. *S. lugdunensis* is known as a rare cause of opportunistic infections[48], but a mutant lacking all potential virulence factors or introduction of the *lug* genes into an exclusively commensal species might enable the development of a safe probiotic strain.

Lugdunin represents the first example of a new class of compounds we suggest to name macrocyclic thiazolidine peptide antibiotics, combining bactericidal activity against many major pathogens with a particularly high barrier to resistance by mutation even under prolonged selective pressure. The fact that all tested nasal and clinical *S. aureus* isolates maintained pronounced susceptibility to lugdunin supports the notion that it may be particularly difficult for bacteria to develop resistance to lugdunin. This indicates that lugdunin has apparently evolved for the purpose of bacterial elimination in the human organism, implying that it is optimized for efficacy and tolerance at its physiological site of action. Thus, lugdunin is a promising drug lead for inhibiting growth of *S. aureus* in the nares and potentially other body sites.

The genetic inventory of human-associated microbiomes is of utmost importance for many critical human body functions e.g. degradation of ingested polymers, detoxification of xenobiotics, or release of immunomodulatory molecules[49]. Our discovery of commensal bacteria producing a potent antibiotic is in accord with recent reports on the presence of gene clusters for complex secondary metabolites in human-associated metagenomes[30] and suggests that many humans are constantly exposed to potent bioactive compounds from microbiomes. The impact of such compounds on human body

functions may vary substantially with the dynamic changes in microbiota structure. Whereas it has become increasingly difficult to identify novel compound structures from soil microbes such as actinomycetes, bacteria from human microbiomes may become a valuable source for new types of antibiotics. It will be a challenge for future research to elucidate the identity, variability, activity, and ecological roles of such compounds and to exploit them for the development of new drugs.

Acknowledgments

We thank Verena Winstel for technical assistance and Ana Bobic, Simon Heilbronner, Wolfgang Hoffmann, Ana Jorge, Dorothee Kretschmer, Andreas Kulik, Mulugeta Nega, Evi Stegmann, Volker Winstel, Tillmann Weber, and Wolfgang Wohlleben for assistance and helpful discussions. Thanks to Bruker Daltonics, Bremen for selected initial HR-MS analysis and to Thomas Paululat for NMR experiments. This work was financed by German Research Council grants GRK1708 to S.G. and A.P.; TRR156 to B.S. and A.P (Schi510/8-1 and PE805/5-1, respectively); TRR34 to C.W. and A.P; and SFB766 to C.W., H.B.-O., S.G., and A.P.; and by the German Center for Infection Research (DZIF) to C.W., A.P., B.K, M.W, and H.B.-O.

Contributions

A.Z. isolated lugdunin, designed experiments and investigated the biological activities of lugdunin. M.C.K. purified lugdunin, designed experiments and determined the structure of lugdunin. D.J. identified IVK28 and performed transposon mutagenesis. A.B. designed and performed precursor incorporation studies. C.L. designed the human colonisation study and analysed data. M.B., A.Z., C.S.and C.W. performed animal experiments and M.W. and C.W. analysed data and performed statistical analysis. M.M. provided patient samples and supported MALDI-TOF analysis. N.A.S. and H.K. established total chemical synthesis of lugdunin. B.K. isolated lugdunin, analysed operon structure and performed bioinformatic analyses, A.Z., M.C.K., B.S., H. B.-O., S.G., A.P. and B.K. designed the study, analysed results, and wrote the paper.

Author information

The authors declare no competing financial interests. Correspondence and requests for materials should be addressed to A.P. (andreas.peschel@uni-tuebingen.de).

References

1 Arias, C. A. & Murray, B. E. Antibiotic-resistant bugs in the 21st century--a clinical super-challenge. *N Engl J Med* **360**, 439-443 (2009).

2 Laxminarayan, R. *et al.* Antibiotic resistance-the need for global solutions. *Lancet Infect Dis* **13**, 1057-1098 (2013).

3 DeLeo, F. R., Otto, M., Kreiswirth, B. N. & Chambers, H. F. Community-associated meticillin-resistant Staphylococcus aureus. *Lancet* **375**, 1557-1568 (2010).

4 Arias, C. A. & Murray, B. E. The rise of the Enterococcus: beyond vancomycin resistance. *Nat Rev Microbiol* **10**, 266-278 (2012).

5 Boucher, H. W. *et al.* Bad bugs, no drugs: no ESKAPE! An update from the Infectious Diseases Society of America. *Clin Infect Dis* **48**, 1-12 (2009).

6 WHO. Antimicrobial resistance: global report on surveillance (2014).

7 Cooper, M. A. & Shlaes, D. Fix the antibiotics pipeline. *Nature* **472**, 32 (2011).

8 Bierbaum, G. & Sahl, H. G. The search for new anti-infective drugs: untapped resources and strategies. *Int J Med Microbiol* **304**, 1-2 (2014).

9 Ling, L. L. *et al.* A new antibiotic kills pathogens without detectable resistance. *Nature* **517**, 455-459 (2015).

10 Laureti, L. *et al.* Identification of a bioactive 51-membered macrolide complex by activation of a silent polyketide synthase in Streptomyces ambofaciens. *P Natl Acad Sci USA* **108**, 6258-6263 (2011).

11 Hosaka, T. *et al.* Antibacterial discovery in actinomycetes strains with mutations in RNA polymerase or ribosomal protein S12. *Nat Biotechnol* **27**, 462-464 (2009).

12 Lincke, T., Behnken, S., Ishida, K., Roth, M. & Hertweck, C. Closthioamide: An Unprecedented Polythioamide Antibiotic from the Strictly Anaerobic Bacterium Clostridium cellulolyticum. *Angew Chem Int Edit* **49**, 2011-2013 (2010).

13 Schroeder, B. O. *et al.* Reduction of disulphide bonds unmasks potent antimicrobial activity of human beta-defensin 1. *Nature* **469**, 419-423 (2011).

14 Zasloff, M. Inducing endogenous antimicrobial peptides to battle infections. *Proc Natl Acad Sci U S A* **103**, 8913-8914 (2006).

15 Bush, K. *et al.* Tackling antibiotic resistance. *Nat Rev Microbiol* **9**, 894-896 (2011).

16 Marshall, B. M. & Levy, S. B. Food animals and antimicrobials: impacts on human health. *Clin Microbiol Rev* **24**, 718-733 (2011).

17 Penders, J., Stobberingh, E. E., Savelkoul, P. H. & Wolffs, P. F. The human microbiome as a reservoir of antimicrobial resistance. *Front Microbiol* **4**, 87 (2013).

18 Davis, M. F., Price, L. B., Liu, C. M. & Silbergeld, E. K. An ecological perspective on U.S. industrial poultry production: the role of anthropogenic ecosystems on the emergence of drug-resistant bacteria from agricultural environments. *Curr Opin Microbiol* **14**, 244-250 (2011).

19 Bode, L. G. *et al.* Preventing surgical-site infections in nasal carriers of Staphylococcus aureus. *N Engl J Med* **362**, 9-17 (2010).

20 Wertheim, H. F. *et al.* The role of nasal carriage in Staphylococcus aureus infections. *Lancet Infect Dis* **5**, 751-762 (2005).

21 Thomas, C. M., Hothersall, J., Willis, C. L. & Simpson, T. J. Resistance to and synthesis of the antibiotic mupirocin. *Nat Rev Microbiol* **8**, 281-289 (2010).

22 van der Meer, J. W. & Vandenbroucke-Grauls, C. M. Resistance to selective decontamination: the jury is still out. *Lancet Infect Dis* **13**, 282-283 (2013).

23 Schloss, P. D. Microbiology: An integrated view of the skin microbiome. *Nature* **514**, 44-45 (2014).

24 Laufer, A. S. *et al.* Microbial communities of the upper respiratory tract and otitis media in children. *MBio* **2** (2011).

25 Krismer, B. *et al.* Nutrient limitation governs Staphylococcus aureus metabolism and niche adaptation in the human nose. *PLoS pathogens* **10** (2014).

26 Hibbing, M. E., Fuqua, C., Parsek, M. R. & Peterson, S. B. Bacterial competition: surviving and thriving in the microbial jungle. *Nat Rev Microbiol* **8**, 15-25 (2010).

27 Dobson, A., Cotter, P. D., Ross, R. P. & Hill, C. Bacteriocin production: a probiotic trait? *Appl Environ Microbiol* **78**, 1-6 (2012).

28 Kommineni, S. *et al.* Bacteriocin production augments niche competition by enterococci in the mammalian gastrointestinal tract. *Nature* **526**, 719-722 (2015).

29 Challinor, V. L. & Bode, H. B. Bioactive natural products from novel microbial sources. *Ann N Y Acad Sci* **1354**, 82-97 (2015).

30 Donia, M. S. *et al.* A systematic analysis of biosynthetic gene clusters in the human microbiome reveals a common family of antibiotics. *Cell* **158**, 1402-1414 (2014).

31 Heilbronner, S. *et al.* Genome sequence of Staphylococcus lugdunensis N920143 allows identification of putative colonization and virulence factors. *FEMS Microbiol Lett* **322**, 60-67 (2011).

32 Sidda, J. D. *et al.* Discovery of a family of gamma-aminobutyrate ureas via rational derepression of a silent bacterial gene cluster. *Chem Sci* **5**, 86-89 (2014).

33 Rutledge, P. J. & Challis, G. L. Discovery of microbial natural products by activation of silent biosynthetic gene clusters. *Nature Reviews Microbiology* **13**, 509-523 (2015).

34 Sasaki, T., Igarashi, Y., Saito, N. & Furumai, T. Watasemycins A and B, new antibiotics produced by Streptomyces sp TP-A0597. *J Antibiot* **55**, 249-255 (2002).

35 Miller, D. A., Luo, L., Hillson, N., Keating, T. A. & Walsh, C. T. Yersiniabactin synthetase: a four-protein assembly line producing the nonribosomal peptide/polyketide hybrid siderophore of Yersinia pestis. *Chem Biol* **9**, 333-344 (2002).

36 Weber, T. *et al.* antiSMASH 3.0-a comprehensive resource for the genome mining of biosynthetic gene clusters. *Nucleic Acids Res* **43**, W237-243 (2015).

37 Walsh, C. T. Insights into the chemical logic and enzymatic machinery of NRPS assembly lines. *Nat Prod Rep* (2015).

38 Mootz, H. D., Schwarzer, D. & Marahiel, M. A. Ways of assembling complex natural products on modular nonribosomal peptide synthetases. *Chembiochem* **3**, 490-504 (2002).

39 Hobbs, J. K., Miller, K., O'Neill, A. J. & Chopra, I. Consequences of daptomycin-mediated membrane damage in Staphylococcus aureus. *J Antimicrob Chemother* **62** (2008).

40 Tacconelli, E. & Kern, W. V. New antibiotics for skin and skin-structure infections. *Lancet Infect Dis* **14**, 659-661 (2014).

41 Zervos, M. J. *et al.* Epidemiology and outcomes of complicated skin and soft tissue infections in hospitalized patients. *J Clin Microbiol* **50**, 238-245 (2012).

42 Weidenmaier, C., Goerke, C. & Wolz, C. Staphylococcus aureus determinants for nasal colonization. *Trends Microbiol* **20**, 243-250 (2012).

43 Baur, S. *et al.* A nasal epithelial receptor for Staphylococcus aureus WTA governs adhesion to epithelial cells and modulates nasal colonization. *PLoS pathogens* **10** (2014).

44 Andersen, P. S. *et al.* Influence of host genetics and environment on nasal carriage of staphylococcus aureus in danish middle-aged and elderly twins. *J Infect Dis* **206**, 1178-1184 (2012).

45 Bieber, L. & Kahlmeter, G. Staphylococcus lugdunensis in several niches of the normal skin flora. *Clin Microbiol Infect* **16**, 385-388 (2010).

46 Iwase, T. *et al.* Staphylococcus epidermidis Esp inhibits Staphylococcus aureus biofilm formation and nasal colonization. *Nature* **465**, 346-349 (2010).

47 Sanders, M. E. Impact of probiotics on colonizing microbiota of the gut. *J Clin Gastroenterol* **45 Suppl**, S115-119 (2011).

48 Becker, K., Heilmann, C. & Peters, G. Coagulase-negative staphylococci. *Clin Microbiol Rev* **27**, 870-926 (2014).

49 Clemente, J. C., Ursell, L. K., Parfrey, L. W. & Knight, R. The impact of the gut microbiota on human health: an integrative view. *Cell* **148**, 1258-1270 (2012).

Methods

Strains and growth conditions. The *Staphylococcus* strains used in this study were *S. aureus* USA300 LAC, *S. aureus* USA300 NRS384, *S. aureus* Mu50, *S. aureus* RN4220, *S. aureus* SA113, *S. aureus* Newman, *S. aureus* PS187, *S. lugdunensis* IVK28, *S. lugdunensis* IVK28 Δ*lugD*, and *S. lugdunensis* IVK28-Xyl. Further strains used for MIC determination were *Enterococcus faecium* BK463, *E. faecalis* VRE366, *Listeria monocytogenes* ATCC19118, *Streptococcus pneumoniae* ATCC49619, *Pseudomonas aeruginosa* PAO1, and *Escherichia coli* DH5α. *E. coli* DC10B was used as the cloning host and *B. subtilis* 168 (*trpC2*) was used for precursor incorporation studies. In addition, a set of 60 *S. aureus* and 17 *S. lugdunensis* strains were isolated from diagnostic samples in the course of the colonisation study described below.

Basic medium (BM: 1% soy peptone, 0.5% yeast extract, 0.5% NaCl, 0.1% glucose and 0.1% K_2HPO_4, pH 7.2) was used as the standard growth medium. MIC determinations and killing assays were performed in Mueller Hinton Broth (MHB; Roth, Karlsruhe, Germany). For the identification of *S. lugdunensis*, selective *S. lugdunensis* medium (SSL) was used as previously described[50]. When necessary, antibiotics were used at concentrations of 250 µg/mL for streptomycin, 10 µg/mL for chloramphenicol, 2.5 µg/mL for erythromycin and 100 µg/mL for ampicillin.

Bioactivity test. The anti-*S. aureus* activity of *S. lugdunensis* IVK28 was identified by screening 90 nasal staphylococcal isolates for the capacity to inhibit growth of *S. aureus.* For this purpose, BM agar was inoculated 1:10,000 with an overnight culture of *S. aureus* USA300 LAC. The test strains were inoculated on the resulting bacterial lawn, and the plates were incubated for 24-48 h at 37°C. To investigate the production of antimicrobial activity by IVK28 under iron-limiting conditions, BM agar was supplemented with 200 µM 2, 2'-bipyridine[25].

Transposon mutagenesis and elucidation of the lugdunin gene cluster. The temperature-sensitive plasmid pTV1ts, which contains the 5.3-kb transposon *Tn*917 (*erm*^{R}) from *E. faecalis*, was transferred into *S. lugdunensis* IVK28 by electroporation. Transposition mutants were screened for loss of antimicrobial activity against *S. aureus*. Chromosomal DNA was isolated by standard procedures from non-inhibitory clones, and the primers Tn917 up and Tn917 down (Extended Table 2) were used to directly

sequence the flanking regions of the transposon insertion site. Sequence analysis was performed with DNASTAR Lasergene software (DNASTAR Inc., Madison, WI, USA). Bioinformatic analysis was performed by BLAST® (http://blast.ncbi.nlm.nih.gov/Blast.cgi) and antiSMASH 3.0[36].

Generation of *S. lugdunensis* IVK28-Xyl. The flanking regions of *lugR* were amplified by PCR with the primer pairs SIPr1–up/SIPr1–down and SIPr2–up/SIPr2–down (Extended Data Table 2). The plasmid pBASE6-erm/lox 1, a derivative of pBASE6[51], already containing an erythromycin resistance cassette in the singular SmaI site, was linearized with Acc65I. The identically digested SIPr1 PCR product, containing one natural Acc65I restriction site and one introduced by the primer, was ligated into pBASE6-erm/lox1. The resulting vector with the correctly oriented SIPr1 PCR product and the SIPr2 PCR product were ligated after digestion with EcoRV and BglII. The resulting pBASE6-erm/lox 1 construct with both flanking regions inserted was linearized with BssHII, treated with Klenow enzyme and digested with BglI. The required *xylR* fragment with the downstream-located *xylAB*-promoter was excised from pTX15 by HindIII restriction, treated with Klenow enzyme and subsequently digested with BamHI. The ligation of the *xylR* fragment into the appropriate vector generated pBASE6-erm/lox1-*xylR*, which was transferred into *E.coli* DC10B and subsequently into *S. aureus* PS187. The resulting plasmid pBASE6-erm/lox1-*xylR* was transduced into *S. lugdunensis* IVK28 via the bacteriophage Φ187 according to Winstel et al.[52]. Homologous recombination for replacement of *lugR* by *erm/xylR* was performed as previously described, generating the xylose-inducible lugdunin producer strain *S. lugdunensis* IVK28-Xyl.

Production and purification of lugdunin. A fresh overnight culture of *S. lugdunensis* IVK28-Xyl was inoculated 1:1,000 in BM without glucose and was supplemented with 0.5% xylose. After incubation at 37°C under continuous shaking (160 rpm) for 24 h, whole cultures were extracted with 1-butanol at a ratio of 5:1. The aqueous phase was discarded, and the organic phase was evaporated at 37°C under reduced pressure and finally dissolved in methanol. The methanol extract was applied to a gel filtration column (Sephadex LH20, 1.6 x 80 cm, flow rate 1 mL/min methanol). The active fractions containing lugdunin were pooled, evaporated at 37°C under reduced pressure and

dissolved in dimethyl sulfoxide (DMSO). This solution was then subjected to a preparative reverse-phase HPLC column (Kromasil C18, 7 µm, 250 x 20 mm; Dr. Maisch, Ammerbuch, Germany) with an isocratic elution at 79% methanol in water for 20 min. The fractions containing lugdunin were baseline-separated from the remaining compounds. Methanol was evaporated at 37°C under reduced pressure to yield lugdunin as a white powder.

Chemical synthesis of lugdunin. Total chemical synthesis was achieved by a Fmoc (9-fluorenylmethoxycarbonyl) strategy-based manual solid-phase peptide synthesis and was established on an H-Val-H NovaSyn® TG resin (Novabiochem, Switzerland). Amino acids were coupled in a four-fold excess using HATU (1-[Bis(dimethylamino)methylene]-1*H*-1,2,3-triazolo[4,5-*b*]pyridinium 3-oxid hexafluorophosphate). Valine positions were coupled twice by use of PyOxim (**[Ethyl cyano(hydroxyimino)acetato-O^2]tri-1-pyrrolidinylphosphonium hexafluorophosphate)** for the second coupling instead of HATU. Deprotection was performed in trifluoroacetic acid for 30 min. Peptides were cleaved from the resin with acetonitrile/water/trifluoroacetic acid (79.95/20/0.05) for 30 min. Lyophilisation yielded the crude product. Crude synthetic lugdunin products was purified by RP-HPLC and compared with the natural product by HR-LC-ESI-MS, additional chiral-HPLC methods (column: Dr. Maisch Reprosil Chiral NR, Ammerbuch, Germany; elution with 80% premixed methanol in H_2O at 1.5 mL/min flow rate), bioactivity assay and advanced Marfey's analysis.

MIC assay, serum stability and spectrum of activity. *S. aureus* RN4220, *S. aureus* USA300 (LAC), *S. aureus* USA300 (NRS384), *S. aureus* SA113, *S. aureus* Mu50, *E. coli* DH5α and *P. aeruginosa* PAO1 were grown overnight in MHB. *E. faecalis* VRE366, *E. faecium* BK463, *S. pneumoniae*, and *L. monocytogenes* were grown in tryptic soy broth (TSB: Difco Laboratories, Augsburg, Germany). Serum stability of lugdunin was determined in 50% MHB with 50% human serum, which was obtained by standard Histopaque/Ficoll centrifugation of freshly isolated blood. All strains were incubated at 37°C under continuous shaking. Early log-phase grown bacteria were adjusted in MHB to 1 x 10^6 CFU/mL in microtiter plates (MTP), mixed with varying concentrations of the antibiotic and incubated at 37°C for 24 h under continuous shaking. The OD_{600} of each well was measured with a microplate reader, and the lowest peptide concentrations,

which displayed no bacterial growth, were defined as the MIC. The assays were performed in 96-well microtiter plates. MIC values for *B. subtilis* 168 to be used as points of reference in precursor incorporation studies were determined in Belitzky minimal medium[53], using a final inoculum of 5 x 10^5 CFU/mL.

Killing assay. Fresh MHB was inoculated 1:10,000 with an overnight culture of *S. aureus* USA300 LAC and was incubated at 37°C under continuous shaking (160 rpm) until bacteria were grown to 1x10^6 CFU/mL. Then, 10 x MIC lugdunin was added. At the time points 0 h, 2 h, 4 h, 8 h, 24 h and 30 h, samples were taken and centrifuged. The pellet was resuspended in 1 x PBS and serially diluted. The dilutions were spotted on tryptic soy agar, and colony counts were determined after overnight incubation at 37°C. To determine cell numbers <10^2 CFU/mL, whole cultures were centrifuged and plated on TSA.

Precursor incorporation studies. *B. subtilis* 168 (trpC2) is a widely used model organism for mode of action investigations and was also used for orienting studies on the mechanism of lugdunin[54-56]. To measure incorporation of radioactive precursors into acid-precipitable macromolecules, *B. subtilis* 168 (*trpC2*), exponentially growing in Belitzky minimal medium (OD_{600} of 0.04), was labeled with 0.02 MBq/mL of [methyl-H3]-thymidine (DNA synthesis), [5,6-H3]-uridine (RNA synthesis), [4,5-H3]-L-leucine (protein synthesis) or [1-3H]-glucosamine D-hydrochloride (cell wall synthesis). After 5 min culture aliquots were treated with lugdunin at concentrations of 2, 1, 0.67 or 0.5 µg/mL, corresponding to 1/2 x, 1/4 x, 1/6 x or 1/8 x the MIC, respectively. Ciprofloxacin (2 µg/mL, 4x MIC), rifampicin (1 µg/mL, 4 x MIC), chloramphenicol (16 µg/mL, 4 x MIC) or vancomycin (2 µg/mL, 4 x MIC) served as reference antibiotics for inhibition of DNA, RNA, protein or cell wall biosynthesis, respectively. Samples (0.1 mL) were taken in regular time intervals and precipitated with 6% perchloric acid in a multiscreen filter plate (Millipore, 0.45 µm). After washing the precipitates with 0.15 mL of ethanol, plates were dried and radioactivity was determined with scintillation fluid (Ultima Gold, Perkin Elmer) in a 1450 MicroBeta TriLux counter (Wallac).

Cytotoxicity against eukaryotic cells. Human neutrophil granulocytes were freshly isolated from the blood of healthy volunteers by standard Histopaque/Ficoll

centrifugation. Lysis of neutrophil granulocytes was monitored by the release of the enzyme lactate dehydrogenase (LDH), as is described by Wang, R. et al[57]. Lugdunin was added at final concentrations of 50, 25 and 12.5 µg/mL in 0.5% DMSO to wells of a 96-well tissue culturing plate containing 1 x 10^6 neutrophil granulocytes per well in 200 µL RPMI-1640 medium (2 g/l $NaHCO_3$, 10% foetal calf serum, 1% L-glutamine and 1% penicillin-streptomycin, PAN Biotech) without phenol red. The plates were incubated at 37°C and 5% CO_2 for 3 h and the lysis was determined with the LDH Cytotoxicity Detection Kit (Roche Applied Sciences, Mannheim, Germany).

Haemolytic activity was determined with human erythrocytes, freshly isolated from the blood of healthy volunteers by standard Histopaque/Ficoll centrifugation. Lugdunin was added at final concentrations of 50, 25 and 12.5 µg/mL in 0.5% DMSO to 2% erythrocytes in 1 x PBS. The cells were incubated for 1 h and afterwards centrifuged for 10 min at 1,000 rpm. The supernatant was diluted 1:10 in 1 x PBS, and the absorbance was measured at a wavelength of 540 nm. As a positive control for neutrophil granulocyte or erythrocyte lysis, 2% Triton X-100 was added to the samples.

HL60 cells were cultured in RPMI-1640 medium. Their metabolic activity was monitored using the cell health indicator alamarBlue (Invitrogen) as described by Bara, R. et al.[58]. Lugdunin was added at final concentrations of 50, 25 and 12.5 µg/mL in 0.5% DMSO to wells of a 96-well tissue culturing plate containing 1 x 10^4 HL60 cells per well. The plates were incubated at 37°C and 5% CO_2 for 24 h. As a positive control for high cytotoxicity, staurosporine was added to the samples.

Resistance development study. MIC assays for the antibiotics used in this study were performed as described above. We determined 1 x MICs of 0.01 µg/mL rifampicin and 1.5 µg/mL lugdunin against *S. aureus* USA300. Fresh MHB was inoculated 1:10,000 with an overnight culture of *S. aureus* USA300 LAC and was incubated at 37°C under continuous shaking. Cells were grown to early log phase, adjusted to 1 x 10^6 cells/mL, and dispensed into 96-well MTPs with 100 µL per well. Lugdunin and rifampicin were added at concentrations of 0.25 x MIC, 0.5 x MIC, 1 x MIC, 1.5 x MIC, 2 x MIC and 4 x MIC. After 24 h incubation at 37°C under continuous shaking, growth was determined with a microplate reader at an OD_{600}, and cells from the second highest concentration showing visible growth were used to inoculate the subsequent culture.

Statistical analyses. Statistical analysis was performed by using GraphPad Prism (GraphPad Software, Inc., La Jolla, USA; version 5.04). Statistically significant differences were calculated by using appropriate statistical methods as indicated. For the human study, risk of nasal colonisation with *S. aureus* in the presence or absence of *S. lugdunensis*, as well as the respective point estimates of the risk ratio and confidence intervals, were determined using Stata version 12.1 (Stat Corp., College Station, TX, USA). *P* values of ≤0.05 were considered significant.

Animal models and ethics statement. All animal experiments were conducted in strict accordance with the German regulations of the Gesellschaft für Versuchstierkunde/Society for Laboratory Animal Science (GV-SOLAS) and the European Health Law of the Federation of Laboratory Animal Science Associations (FELASA) in accordance with German laws after approval (protocol HT1/12 for mouse skin infection and T1/10 for cotton rat colonisation) by the local authorities (Regierungspraesidium Tuebingen). All, animal and human studies were carried out at the University Hospital Tuebingen and conformed to institutional animal care and use policies. No randomization or blinding was necessary for the animal infection/colonisation models, and no samples were excluded. Animal studies were performed with female C57BL/6 mice, 6–8 weeks old, or cotton rats of both genders, 8-10 weeks old, respectively. The human nasal colonization study was approved by the ethics committee of the medical faculty of the University Hospital Tuebingen (project number 577/2015A).

Skin infection of C57BL/6 mice. A streptomycin-resistant *S. aureus* Newman strain was used to infect C57BL/6 mice epicutaneously by the tape-stripping technique according to Wanke, I. et al.[59]. TSB with 500 µg/mL streptomycin was inoculated 1:10,000 with a fresh overnight culture of the test strain and was incubated at 37°C under continuous shaking until an OD_{600} = 0.5 was reached. Cells were harvested, washed twice with 1 x PBS, and adjusted to $1x10^8$ cells/mL. The integrity of the shaved skin of the mice was affected by repeated (seven times) vigorous tape stripping to enable *S. aureus* Newman infection. An inoculum of 15 µL from the bacterial suspension was added to 7-mm filter paper discs, placed onto the prepared skin with two discs per animal, and covered with Finn chambers on Scanpor tape (Smart Practise, Phoenix, AZ, USA). Finn chamber fixation occurred via Fixomull stretch plasters (BSN medical GmbH,

Hamburg, Germany). After incubation for 24 h, the Finn chambers were removed and 1.5 µg of lugdunin per colonised area was applied, followed by a second and third treatment with the same amount of lugdunin after 30 h and 42 h. Six hours after the final application, mice were euthanized, the skin was large-scale detached and 4-mm punches of the originally colonised areas were vortexed in 1 x PBS for 30 seconds to remove the attached bacteria from the skin (wash fraction). The skin was dissected with a scalpel to expose bacteria from deeper areas of the skin (tissue fraction), which was homogenized by vortexing in 1 x PBS for 30 seconds. CFUs of both fractions were determined by serial dilutions in 1 x PBS, which were spotted onto TSA, supplemented with streptomycin, for *S. aureus* Newman^{strep}-specific selection. The plates were incubated overnight at 37°C.

Generation of *S. lugdunensis* Δ*lugD* and complementation. For the construction of a marker-less knock-out strain, 1-kb flanking regions of *lugD* were amplified by PCR with the primer pairs *lugD* upstream-SacI/*lugD* upstream-Acc65I and *lugD* downstream-Acc65I/*lugD* downstream-BglII (Extended Data Table 2). The fragments were digested according to their introduced restriction sites and were ligated into the plasmid pBASE6 generating pBASE6-Δ*lugD*, which was transferred to *E. coli* DC10B. The correct plasmid was transferred to *S. aureus* PS187 by electroporation, which was then infected with the bacteriophage Φ187 for the transduction of pBASE6-Δ*lugD* into *S. lugdunensis* IVK28 wild type. The knockout was generated by homologous recombination of the flanking regions into the genome, and deletion of *lugD* was confirmed by PCR. For the complementation of the mutant, *lugD* was amplified by the primer pair *lugD* comp. forw-PstI/*lugD* comp. rev-Acc65I (Extended Data Table 2), digested with the appropriate restriction enzymes and ligated into identically digested pRB474. The resulting pRB474-*lugD* was transduced into *S. lugdunensis* IVK28 Δ*lugD* as described for the knock-out mutant.

Competition assay. *S. lugdunensis* IVK28 wild type, *S. lugdunensis* IVK28 Δ*lugD, S. lugdunensis* IVK28 Δ*lugD*::pRB474-lugD, and a streptomycin-resistant *S. aureus* Newman were grown in BM overnight at 37°C under continuous shaking. These strains were then adjusted to 1 x 10^9 CFU/mL in 1 x PBS and diluted 1:10. For the starting condition of 90% *S. aureus*, equal volumes of 1 x 10^9 *S. aureus* CFU/mL and 1 x 10^8 *S.*

lugdunensis CFU/mL were mixed. Co-cultures with only 10% *S. aureus* were also performed, and 20 µL of these mixtures were spotted in triplicate on BM agar and incubated at 37°C. Samples were taken at 0 h, 24 h, 48 h and 72 h by scraping cells from the agar plates and suspending them in 1 x PBS. Serial dilutions of these samples were plated on BM and BM containing streptomycin for selection of *S. aureus*. After overnight incubation at 37°C, colony counts were determined, and the bacterial ratios of *S. aureus* and *S. lugdunensis* were calculated.

Co-colonisation of cotton rat noses. For the colonisation of cotton rat noses, spontaneous streptomycin-resistant mutants of *S. lugdunensis* IVK28 wild type and *S. lugdunensis* IVK28 Δ*lugD* were selected on BM agar plates containing 250 µg/mL streptomycin. Co-colonisation was conducted with *S. aureus* Newman^{strep}. The cotton rat model was described earlier[43]. Since the capacity of *S. lugdunensis* to colonize cotton rat nares has not been studied before, we determined the inoculum required for stable colonization by IVK28 wild type and its mutant Δ*lugD* over 5 days. Our previous studies have shown that for *S. aureus* an inoculum of 10^7 bacteria per nose results in a stable colonization of about 10^3 CFUs per nose (Extended Data Fig. 7a). To achieve a comparable colonization level with *S. lugdunensis*, an inoculum of 10^8 bacteria per nose was required, and there was no detectable difference in colonization efficiency between wild type and Δ*lugD* (Extended Data Fig. 7b, c). Therefore, co-colonization experiments in cotton rat noses were performed with 10-fold more *S. lugdunensis* than *S. aureus* to obtain a 1:1 colonization ratio.

Cotton rats were anesthetized and instilled intranasally with mixtures of either 1 x 10^8 *S. lugdunensis* wild type/1 x 10^7 *S. aureus* Newman or 1 x 10^8 *S. lugdunensis* Δ*lugD*/1 x 10^7 *S. aureus* Newman. Five days after bacterial instillation, the animals were euthanized, and noses were surgically removed. The noses were heavily vortexed in 1 mL of 1 x PBS for 30 s. Dilutions of the samples in PBS were plated on SSL agar containing 250 µg/mL streptomycin to select for the used strains and to separate *S. aureus* (yellow) and *S. lugdunensis* (purple) by colour. The plates were incubated for two days under anaerobic conditions (anaerobic jar with Anaerocult ® A, MerckKGaA), for the specific detection of ornithine decarboxylase activity. *S. aureus* Newman CFUs were determined afterwards. All animals received drinking water with 2.5 mg/mL streptomycin continuously, starting three days prior to the experiment, to reduce the natural nasal flora.

Human colonisation study. A total of 187 nasal swab samples from hospitalized patients were received from the diagnostics laboratory of the Institute of Medical Microbiology and Hygiene (University Hospital Tuebingen, Germany). Dilutions from each sample were plated on blood agar and SSL agar for a phenotypic identification of *S. aureus* and *S. lugdunensis*. Identity was confirmed by coagulase test and matrix-assisted laser desorption/ionization-time-of-flight mass spectrometry (Mass spectrometer: AXIMA Assurance, Shimadzu Europa GmbH, Duisburg, Database: SARAMIS™ with 23.980 spectra and 3.380 superspectra, BioMérieux, Nuertingen).

50 Ho, P. L. et al. Novel selective medium for isolation of Staphylococcus lugdunensis from wound specimens. J Clin Microbiol 52, 2633-2636 (2014).

51 Geiger, T. et al. The stringent response of Staphylococcus aureus and its impact on survival after phagocytosis through the induction of intracellular PSMs expression. PLoS pathogens 8 (2012).

52 Winstel, V., Kuhner, P., Krismer, B., Peschel, A. & Rohde, H. Transfer of plasmid DNA to clinical coagulase-negative staphylococcal pathogens by using a unique bacteriophage. *Appl Environ Microbiol* **81**, 2481-2488 (2015).

53 Wenzel, M. *et al.* Small cationic antimicrobial peptides delocalize peripheral membrane proteins. *Proc Natl Acad Sci U S A* **111**, E1409-1418 (2014).

54 Bandow, J. E., Brotz, H., Leichert, L. I., Labischinski, H. & Hecker, M. Proteomic approach to understanding antibiotic action. *Antimicrob Agents Chemother* **47**, 948-955 (2003).

55 Hutter, B. *et al.* Prediction of mechanisms of action of antibacterial compounds by gene expression profiling. *Antimicrob Agents Chemother* **48**, 2838-2844 (2004).

56 Sass, P. *et al.* Antibiotic acyldepsipeptides activate ClpP peptidase to degrade the cell division protein FtsZ. *Proc Natl Acad Sci U S A* **108**, 17474-17479 (2011).

57 Wang, R. *et al.* Identification of novel cytolytic peptides as key virulence determinants for community-associated MRSA. *Nat Med* **13**, 1510-1514 (2007).

58 Bara, R. *et al.* Atropisomeric dihydroanthracenones as inhibitors of multiresistant Staphylococcus aureus. *J Med Chem* **56**, 3257-3272 (2013).

59 Wanke, I. *et al.* Staphylococcus aureus skin colonization is promoted by barrier disruption and leads to local inflammation. *Exp Dermatol* **22**, 153-155 (2013).

Supplementary Discussion

Identification of the transposon insertion site in *S. lugdunensis* IVK28 mutant M1 and revision of the *lug* operon annotation. Direct chromosomal sequencing of the *S. lugdunensis* mutant M1, lacking inhibitory activity against *S. aureus*, revealed the transposon insertion site in an uncharacterized gene encoding a putative non-ribosomal peptide synthetase (NRPS; position 860375/76 of SLUG_RS03945 in the annotated genome sequence of *S. lugdunensis* N920143; Acc.no: NC_017353.1). The available *S. lugdunensis* genomes differed in numbers and lengths of annotated genes in the NRPS operon because of potential sequencing errors. To clarify the operon structure, ambiguous positions were amplified by PCR from strain IVK28 and sequenced. The sequence of IVK28 corresponded to that of strain N920143 and its annotation, except for nucleotide position 863515, which is located at the 3'-end of gene SLUG_RS03945. In contrast to N920143, IVK28 comprises a stretch of eight instead of seven adenosine nucleotides, leading to the fusion of genes SLUG_RS03945 and SLUG_RS03950 to one open reading frame, which we named *lugB*. Amplification by PCR and sequencing of the corresponding region from 10 independent isolates confirmed the presence of only one open reading frame (*lugB*).

The lug operon of IVK28 contains four NRPS genes (*lugABCD*) encoding five adenylation domains. They are preceded upstream by a putative regulator gene (*lugR*), four putative ABC transporter genes (*lugEFGH*) and two open reading frames encoding hypothetical proteins of unknown function (*lugIJ*). A putative type-II thioesterase (*lugT*), required for recycling of misprimed PCP domains, is located between NRPS genes *lugC* and *lugD*. The operon's 3' end encodes a gene (*lugZ*) with similarity to 4'-phosphopantetheinyltransferases, responsible for the transfer of 4'-phosphopantetheine from coenzyme A onto the PCP domain. Further downstream a putative mono-oxygenase is encoded (*lugM*), although the proposed lugdunin biosynthetic pathway does not include a mono-oxygenease reaction (Extended Fig. 5d). Within the interspace of *lugZ* and *lugM* remnants of a transposase were identified, which supports the idea that the *lug* operon may have originated from a mobile genetic element.

Structure determination: Lugduin was found to exist in two interconverting diastereoisomers. Coupled analytical HPLC-UV-HR-MS was applied for chemical analysis of the two isomers using a Macherey-Nagel Nucleoshell® EC RP-C_{18} (150/2

RP18, 2.7 µm) column with a flow rate of 0.3 mL/min. Methanol (system B, containing 0.06% formic acid) and H_2O (system A, containing 0.1% formic acid) acted as eluting solvent for the following gradient: 0 min (10% B), 20 min (100% B), 25 min (100% B), 26 min (10% B), 30 min (10% B). Instrumental setup: Thermo Scientific/DIONEX UltiMate 3000 UHPLC system. For high-resolution mass detection the parameters of a Bruker Maxis-4G High Resolution ESI-TOF (Electro Spray Ionization Time Of Flight) mass spectrometer were set as follows: end plate offset = 500 V, capillary voltage = 3,000 V, nebulizer pressure = 0.4 bar, dry gas flow = 4.0 L/min, dry gas temperature = 200°C. Column, gradient, flow rate, solvent composition and MS detection parameters are refered to as “standard LC-MS conditions” hereafter.

Two separated signals (retention time (Rt) of 17.0 and 17.5 min) showed identical exact masses and UV spectra (see below). Preparative isolation of the separated signals, solvent evaporation, solubilization in methanol and subsequent analysis by HPLC-UV-HR-MS showed the same signals at Rt 17.0 and 17.5 min again. Thus, both species interconvert rapidly within minutes and can not be isolated individually. In conclusion, lugdunin exhibits dynamic diastereomerization at the thiazolidine (C-atom 40, Extended data Fig. 4b). Such a behaviour is well known for non-cyclopeptide thiazolidine-bearing compounds such as pyochelin or yersinibactin[60].

Under the HPLC-UV-HR-MS conditions stated above, a second, minor compound (about 5% of lugdunin according to HPLC-UV) with slightly prolonged retention time (Rt of 17.2 and 17.7 min) was detected. Its mass was 14 Da higher than that of lugdunin (molecular formula $C_{41}H_{64}N_8O_6S$) pointing to a natural derivative of lugdunin. UV spectra and MS/MS fragmentation patterns supported this notion. The minor compound was found to contain a D-*allo*-isoleucin instead of D-valine (position 2 in lugdunin; Fig. 1c). The following discussion refers to both lugdunins, if not stated otherwise.

Sum formulas were deduced from HR-ESI-TOF-MS experiments. The following quasi molecular ions and the salt adducts thereof were detected for lugdunins and their thiazolidine diastereomers.

HR-MS (m/z) lugdunin:

$[M+H]^+$ calcd for $C_{40}H_{63}N_8O_6S$, 783.4585; found, 783.4591 (0.7 ppm err; 5.1 mSigma)

$[M+Na]^+$ calcd for $C_{40}H_{62}N_8NaO_6S$, 805.4405; found, 805.4412 (0.8 ppm err; 4.4 mSigma)

$[M+K]^+$ calcd for $C_{40}H_{62}KN_8O_6S$, 821.4145; found, 821.4134 (1.3 ppm err; 42.5 mSigma)

$[M+2Na]^{2+}$ calcd for $C_{40}H_{62}N_8Na_2O_6S$, 414.2148; found, 414.2157 (0.9 ppm err)

HRMS (m/z) minor lugdunin derivative:

$[M+H]^+$ calcd for $C_{41}H_{65}N_8O_6S$, 797.4742; found, 797.4746 (0.4 ppm err; 7.7 mSigma)

$[M+Na]^+$ calcd for $C_{41}H_{64}N_8NaO_6S$, 819.4562; found, 819.4565 (0.4 ppm err; 5.3 mSigma)

[M+K]+ calcd for $C_{41}H_{64}KN_8O_6S$, 835.4301; found, 835.4326 (2.9 ppm err; 36.8 mSigma)

Amino acid sequential assignment was achieved by multistep tandem MS on a Bruker Esquire 3000 Plus Ion Trap (source parameters: nebulizer pressure = 15 psi, dry gas flow = 4.0 L/min, dry gas temperature = 300°C, sample application via direct infusion) and matching of these data to high-resolution ESI MS/MS experiments (Extended data Fig. 3a, b). Fragmentation of lugdunin follows four fragmentation routes, which generate mainly b-ions of high intensity. Usually, abundant y-ions, which are characteristic for linear peptides but not for cyclic peptides, were not detected for lugdunin. The sites of initial ring cleavage upon collision-induced decay is in good agreement with theoretical explanations. The secondary amine of the thiazolidine moiety is initially protonated and transfers a proton onto peptide bonds in close proximity to where ring cleavage occurs subsequently. Four fragmentation pathways were determined by multistep tandem MS. The fragment ion masses were then matched with corresponding signals generated by a high-resolution MS/MS experiment. Of note, matching of low-resolution multistage tandem MS data with high-resolution data turned out to be vital for the (sequential) discrimination between the corpus masses of tryptophan and thiazolidine, which differ only by 0.003 Da.

Amino acid stereochemistry was determined by an advanced Marfey's analysis for lugdunin. Peptide hydrolysis was performed for 24 hours at 110°C under vacuum. Peptide hydrolysis-grade 6 N HCl was supplemented with 5% thioglycolic acid as antioxidant and 1% phenol as halogen scavenger. Amino acid FDLA (1-fluoro-2-4-dinitrophenyl-5-L-alanine amide) adducts were analysed via HPLC-UV-HR-MS under the standard LC-MS conditions mentioned above.

Small cyclic peptides composed of 6 or 7 amino acids are rare anyway (e.g. baceridin[61]). Moreover, the fully reduced thiazolidine heterocycle in the lugdunin peptide sequence has not been reported before. Therefore, the rare thiazolidine building block

was addressed in more detail. The b2-ion at m/z = 269.1298 Da from fragmentation route I (Extended data Fig. 3a) was selected from an in-source collision-induced decay experiment and further fragmented in a second stage of MS/MS in order to generate high-resolution MS data. This revealed a signal with m/z = 170.0635 Da, which could be annotated to be the missing b1-ion (Extended data Fig. 5a). Generated ions, such as m/z = 86.0095 Da, further supported the presence of a thiazolidine heterocycle. The thiazolidine building block was further addressed by a photometric detection reaction, which was originally developed for bio-orthogonal detection of proline analogs such as thiaprolines (Extended data Fig. 5b, c). Cleavage of the thiazolidine heterocycle by iodine was followed by modification of the released aldehyde with Sawicki's reagent (3-methyl-2-benzothiazolone hydrazone hydrochloride) generating a blue dye with characteristic absorbance at 670 nm. Lugdunin as well as thiazolidine-4-carboxylic acid as positive control exhibited strong absorbance at 670 nm upon modification. 2-methyl-2-thiazoline was chosen as a negative control, which mimics the thiazolidine as closely as possible but lacks the ability to generate a free aldehyde upon modification. Observed colouring during modification are shown in Extended Data Fig. 5c.

Spectroscopic data: IR (600 µg lugdunin, in KBr): 3451, 3287, 3061, 2963, 2932, 2875, 1637, 1547, 1459, 1385, 1370, 1280, 1233, 1157, 1107, 1012, 741 cm-1.

UV/Vis spectroscopy: 32 µM lugdunin in LC/MS-grade methanol. λ_{max} 220 nm (logε = 4.15); 275 nm (logε = 3.29); 282 nm (logε = 3.3); 289 nm (logε = 3.26).

Lugdunin biosynthesis. Bioinformatic analysis of the four NRPS enzymes LugABCD with AntiSMASH 3.0 revealed the presence of five adenylation domains. Biosynthesis of NRPS products usually starts with so-called initiation modules, which enclose an adenylation domain at the N-terminus of the enzyme. Interestingly, the last operon-encoded enzyme, LugD, appears to represent this initiation module with a predicted L-cysteine specificity, which is in perfect agreement with the proposed amino acid order in the linear precursor peptide. Synthesis is most probably extended by the action of LugA, adding valine, which is epimerized to its D-form, and L-tryptophan. Of note, the specificity for the second adenylation domain of LugA was predicted to be most likely L-threonine, although with a low score value of 60%. However, we unambiguously identified L-tryptophan at this position in lugdunin indicating that we discovered a new adenylation domain specificity for the second LugA module with the corresponding Stachelhaus code

DPFSIGMIIK. The modules encoded in LugC exhibit a very uncommon organization. The predicted and found specificity was valine. The single A-domain is succeeded by three PCP domains, two condensation domains, and the terminal reductase. Importantly, the determined structure of lugdunin contains three consecutive valine residues as C-terminal amino acids. Whereas the first of these is in L-conformation, the second valine appears in D-conformation, which can be explained by the presence of an epimerase domain after the second PCP domain of LugC. Subsequently, a third L-valine is incorporated, which is predicted to form a C-terminal reactive aldehyde after release from the NRPS enzyme by the terminal reductase, able to form the stable thiazolidine ring with the N-terminal L-cysteine. This predicted biosynthesis mechanism is based on the assumption that a single A-domain is able to activate three valine residues, which are subsequently incorporated in alternating L- and D-configurations, which, to our knowledge, has not been described before. Therefore, LugC is the prototype of a new NRPS enzyme type with new biosynthesis characteristics. A partially related mechanism has been shown previously for the siderophore yersiniabactin, where a single A-domain is responsible for the incorporation of two consecutive L-cysteines plus a third one *in trans* by a different NRPS enzyme[38].

60 Ino, A. & Murabayashi, A. Synthetic studies of thiazoline and thiazolidine-containing natural products. Part 3: Total synthesis and absolute configuration of the siderophore yersiniabactin. *Tetrahedron* **57**, 1897-1902 (2001).

61 Niggemann, J. *et al.* Baceridin, a cyclic hexapeptide from an epiphytic bacillus strain, inhibits the proteasome. *Chembiochem* **15,** 1021-1029 (2014)

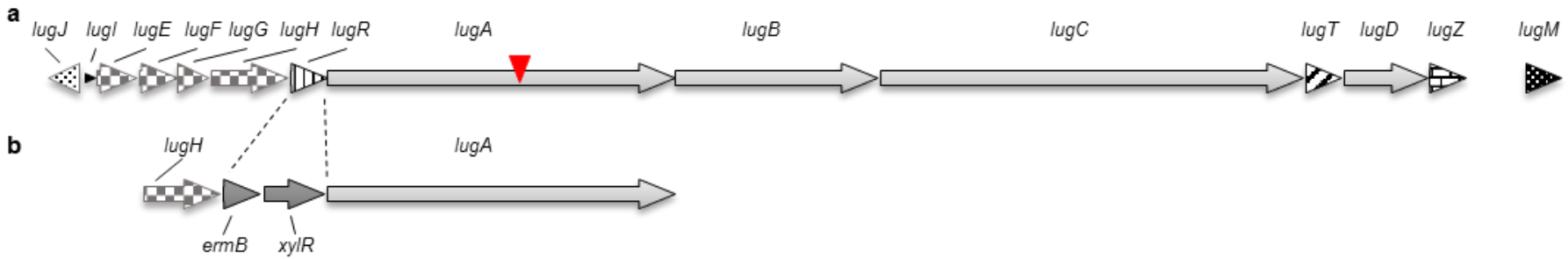

Extended Data Figure 1 | Gene cluster of lugdunin and generation of *S. lugdunensis* IVK28-Xyl. a, The lugdunin genes are located on a 30-kbp operon. *lugA-D* encode the four NRPS, which are preceded by the putative regulator gene *lugR*. Upstream encoded are putative ABC transporter genes (*lugE-H*) and genes for proteins with no described function (*lugI*/*lugJ*). A type-II thioesterase that functions as a repair enzyme for stalled PCP domains, is encoded between *lugC* and *lugD*. The 4'-phosphopantetheinyl transferase LugZ converts inactive PCPs (*apo* PCP) into the active *holo* form by attachment of the 4'-phosphopantetheine cofactor. Downstream encoded is a putative monooxygenase (LugM). The transposon insertion site of Tn917, generating the lugdunin-deficient mutant IVK28 M1, is indicated by a red arrow. **b,** The xylose-inducible lugdunin producer strain *S. lugdunensis* IVK28-xyl was generated by replacement of the regulator gene *lugR* by the *xylAB* promoter along with the *xylR* gene encoding a xylose-sensitive repressor. The erythromycin resistance cassette *ermB* was integrated for selection purposes.

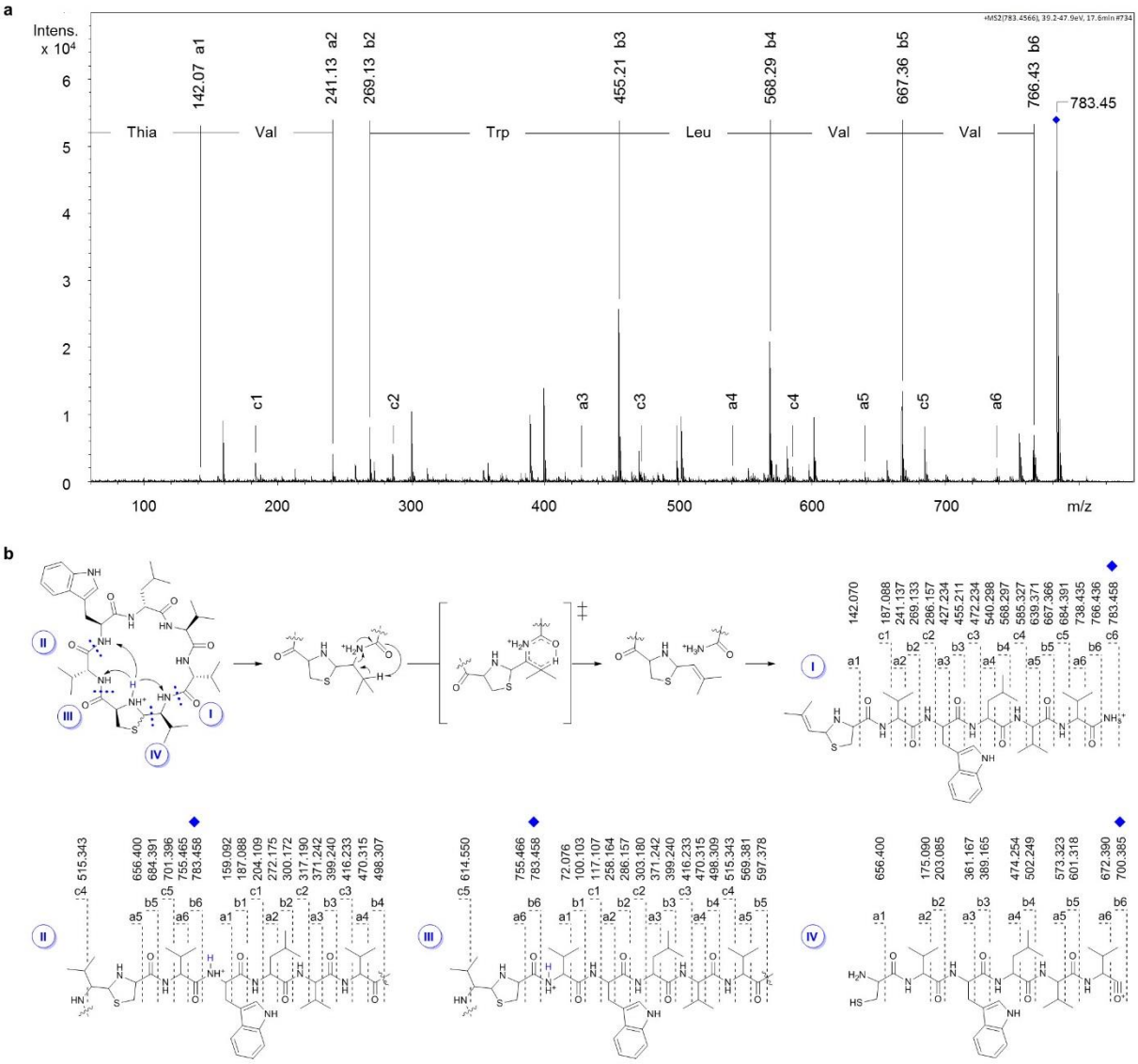

Extended Data Figure 2 | Structure elucidation by multistage tandem and HR-ESI-MS. a, A single-stage high-resolution MS/MS experiment revealed a superposition of fragment ions typically found for cyclic peptides. Quasi molecular ion selected for fragmentation is marked with a blue rhombus (m/z = 783.45). For sequence annotation fragment ions were searched for b-ions of high intensity. One fragmentation route is annotated exemplarily by highlighting respective a-, b- and c-ion series signals ("Thia", Thiazoldine). **b,** Data generated by multistage tandem mass spectrometry show that lugdunin mainly fragmented along four routes (blue digits; (I), (II), (III), (IV)). Initial protonation occurs at the thiazolidine's secondary amine (blue H-atom). Proton transfer to nearby peptide bonds initiated ring cleavage with subsequent fragmentation. Initial loss of ammonia for fragmentation route (I) can be explained by a precedent six-membered transition state. Intensities are in arbitrary units. Blue rhombuses label the position of initial ring cleavage. Fragmentation route molecules are shown in linearized form.

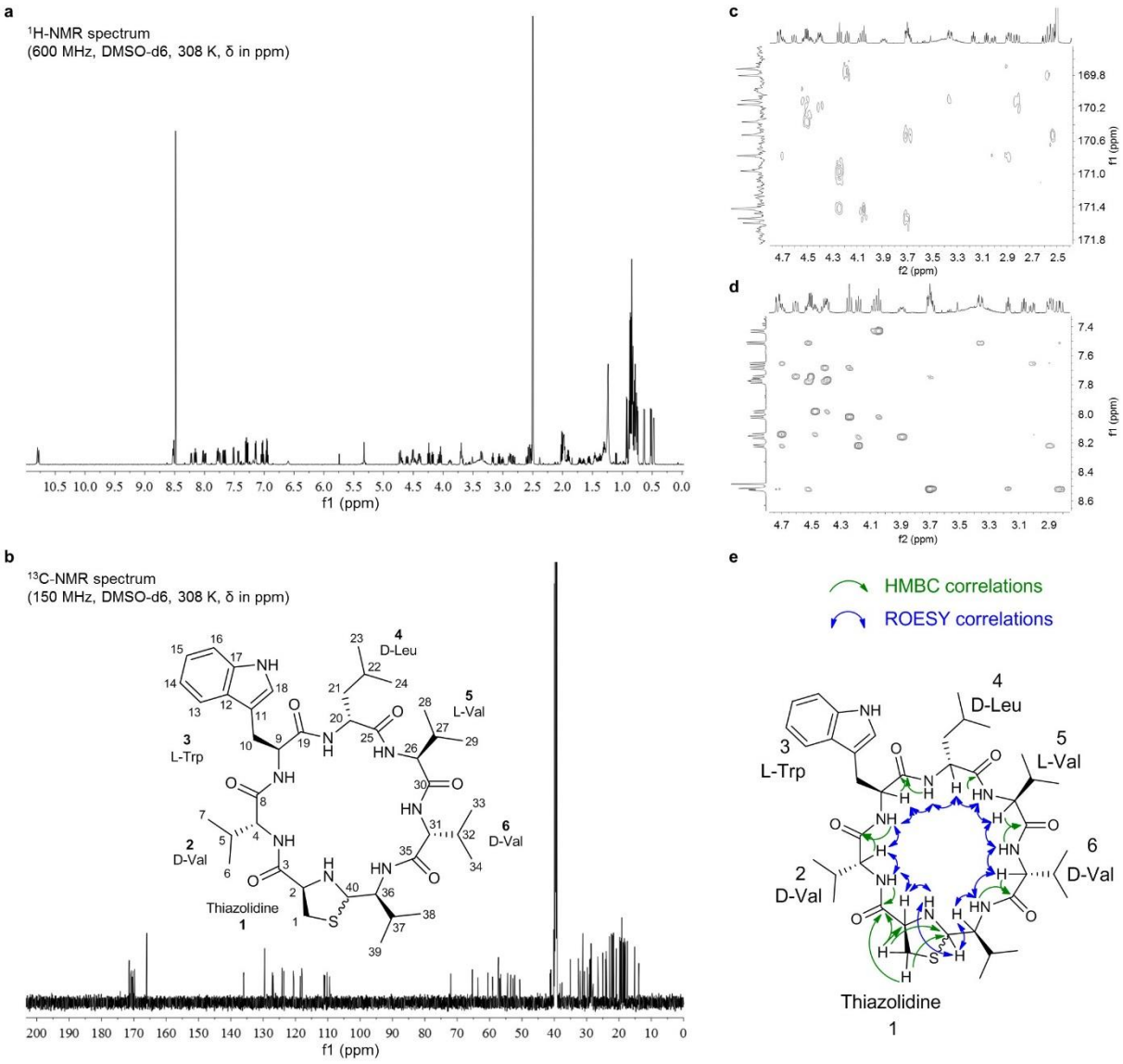

Extended Data Figure 3 | NMR spectra of the natural product lugdunin. The two diastereomeric and interconvertible forms of lugdunin (see imine intermediate, Extended data Fig. 4d) show distinctive sets of NMR signals with consistent patterns, which were assigned by 2D NMR methods (COSY, HMBC, HSQC-DEPT, ROESY and TOCSY) and corroborated the thiazolidine heterocycle as a special feature of lugdunin. Chemical shifts (δ) are shown in ppm. **a,** ^{1}H NMR spectrum (600 MHz) of lugdunin in DMSO-d6 at 308 K. **b,** ^{13}C NMR spectrum (150 MHz) of lugdunin in DMSO-d6 at 308 K. Atom numbering refers to full spectral assignment shown in Extended Data Table 1. **c,** Expansion of HMBC spectrum (heteronuclear multiple bond correlation) shows distinct correlations between the amino acid α-proton and the carbonyl C-atom of the respective amino acid. **d,** Expansion of ROESY spectrum (rotation frame nuclear Overhauser effect spectroscopy) shows short-ranged correlations through space between α-protons and amino acid amide protons. **e,** Taken together, HMBC (green arrows)

and ROESY (double headed blue arrows) correlations allowed for a full sequential walk along the peptide backbone, which readily confirmed the amino acid sequence of both lugdunin diastereomers (The sequential walk is exemplarily shown for one diastereomer).

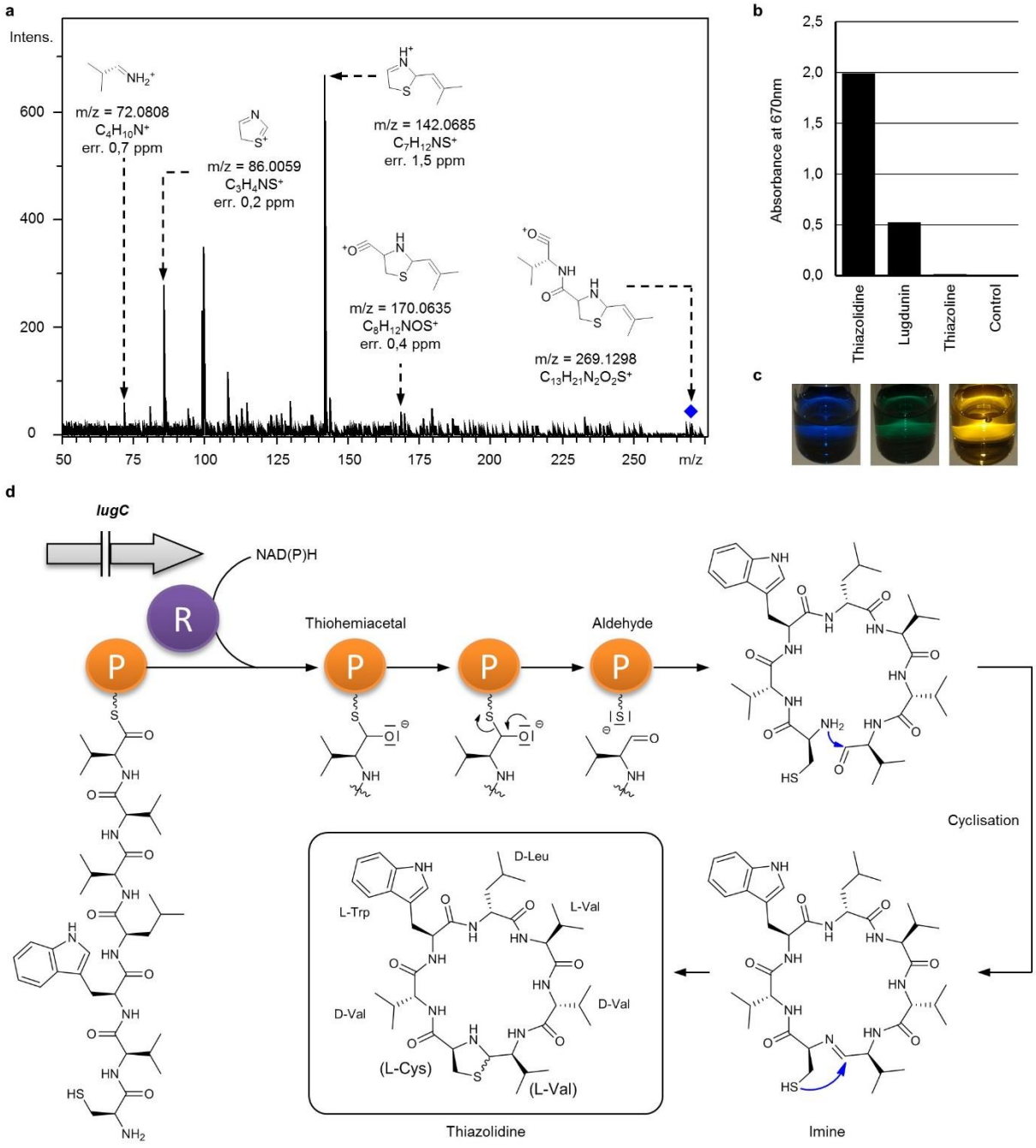

Extended Data Figure 4 | The thiazolidine moiety of lugdunin and its formation by peptide cyclisation. a, Blue rhombus marks the b2-ion from fragmentation route I (Extended Data Fig. 2). The ion was selected from an in-source collision-induced decay (isCID) experiment and was further fragmented in order to find thiazolidine-specific fragment ions. High-resolution MS data are shown with annotated sum formulas and respective deviations from calculated masses (err. in ppm). Shown

fragment ions reveal the b1-ion at m/z = 170.0635 Da. Intensity is shown in arbitrary units. **b,** Photometric detection of thiazolidines at 670 nm. A positive colour reaction with 3-methyl-2-benzothiazolone hydrazone hydrochloride (Sawicki reagent) gives rise to detectable absorbance at 670 nm. Thiazolidine-4-carboxylic acid (thiazolidine) was chosen as positive control, whereas 2-methyl-2-thiazoline (thiazoline) and DMSO acted as negative controls. **c,** Observable colours for the thiazolidine detection reaction. Thiazolidine-4-carboxlic acid (blue), lugdunin (green) and negative controls (yellow). **d**, The terminal reductase of Lug C is proposed to initiate cleavage of the thioester-bound peptide chain with the aid of a NAD(P)H cofactor. The mature heptapeptide is liberated reductively from the NRPS multienzyme complex and cyclises via the N-terminal amine (L-Cys) and C-terminal aldehyde (L-Val) to form a macrocyclic imine/Schiff base. Subsequent nucleophilic attack of the cysteine's thiol group generates the five-membered thiazolidine heterocycle. Nucleophilic attack by the L-cysteine sulfhydryl group may occur either at the imine's *re* or *si* face thus leading to a diastereomeric mixture of two structural populations (depicted with wavy bond). Lug C is shown truncated (||).

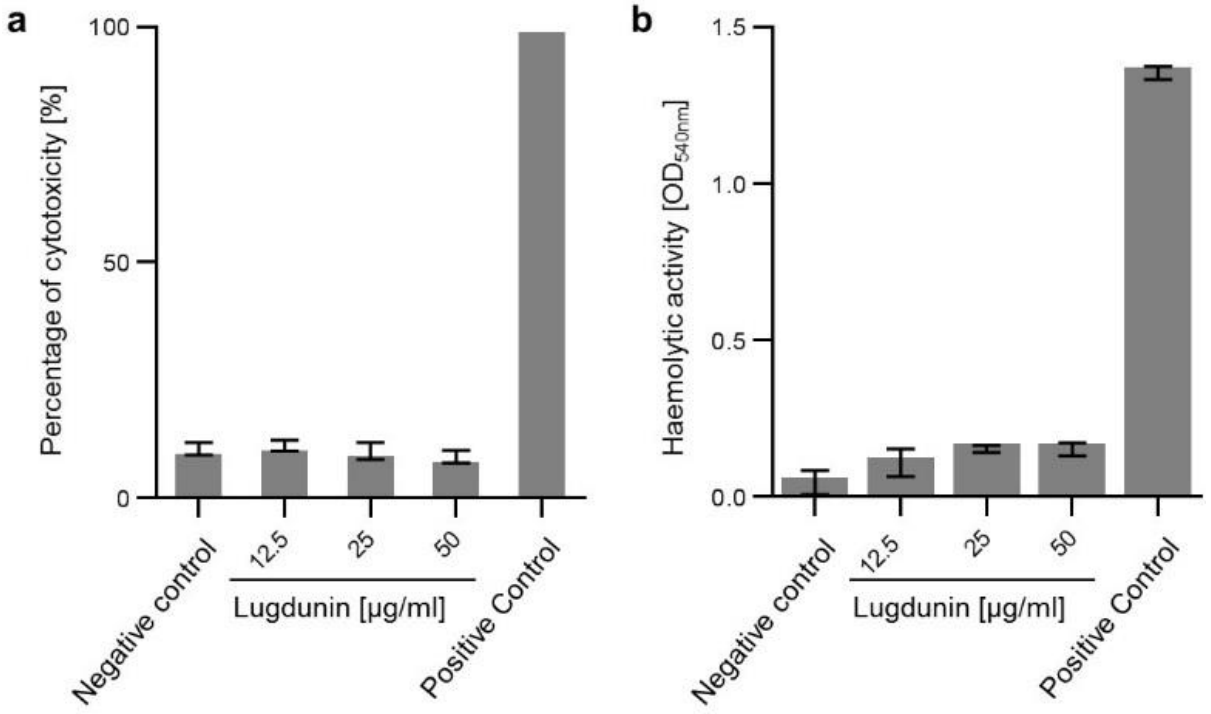

c

	HL60 - promyelocytic leukemia cells
Compound	IC_{50} [µg/ml]
Lugdunin	> 50
Staurosporine	2

IC_{50}, 50 % inhibitory concentration

Extended Data Figure 5 | Lugdunin activity against eukaryotic cells. Human neutrophil granulocytes (**a**) or erythrocytes (**b**) were incubated with high concentrations of lugdunin. Their lysis was monitored by the release of the enzyme lactate dehydrogenase (**a**) or haemoglobin (**b**), respectively. Cells without lugdunin were used as negative control. Incubation of cells in 2% Triton X-100 was used as positive control for high lysis. The data represent three independent experiments ± S.D. **c**, Promyelocytic leukemia (HL60) cells were incubated with high concentrations of lugdunin. In order to determine the 50% inhibitory concentration of lugdunin, the metabolic activity of HL60 cells was measured by the conversion of resazurin into the highly fluorescent resorufin. The apoptosis-inducing staurosporine was used as positive control. IC_{50} values were calculated from the means of three independent experiments.

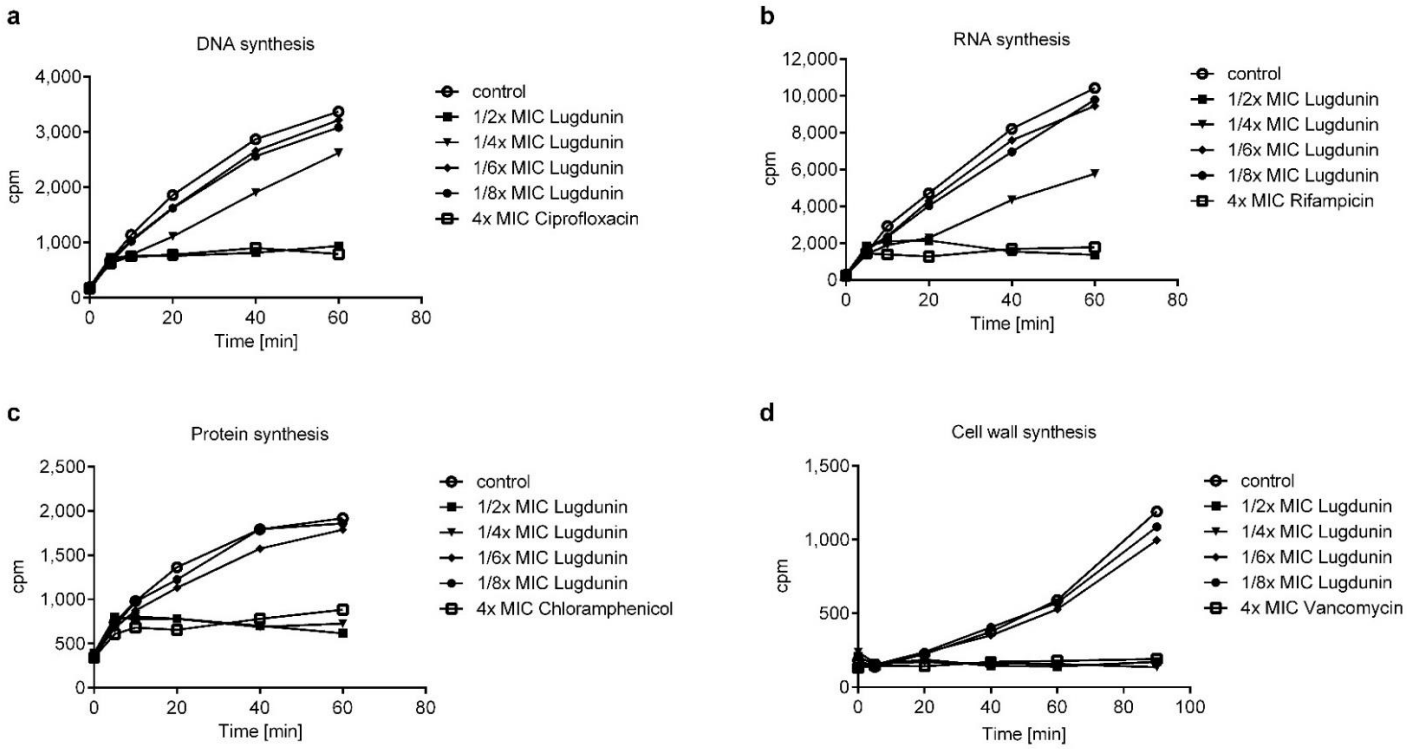

Extended Data Figure 6 | Time course of incorporation of tritium-labelled metabolic precursors into lugdunin-treated *B. subtilis*. *B. subtilis* 168 (trpC2) is a widely used model organism for mode of action investigations and was also used for orienting studies on the mechanism of lugdunin. Susceptibility of *B. subtilis* and *S. aureus* to lugdunin is similar (Table 1), with an MIC for *B. subtilis* of 4 µg/mL in the Belitzky minimal medium used in this assay. Incorporation of **a,** thymidine into DNA, **b,** uridine into RNA, **c,** leucine into protein or **d,** *N*-acetylglucosamine into peptidoglycan ceased within minutes during lugdunin-treatment. The experiment was repeated on three days with three independent bacterial cultures. One representative experiment is shown. At a concentration of half the MIC (1/2 MIC) incorporation of precursors into all pathways ceased reproducibly. At 1/8 MIC incorporation continued repeatedly in parallel with the untreated control. At 1/4 MIC the depicted experiment shows protein and peptidoglycan syntheses slightly more impaired than DNA and RNA syntheses, whereas it was *vice versa* in another experiment. In summary, all four metabolic pathways seem to be equally impaired by lugdunin.

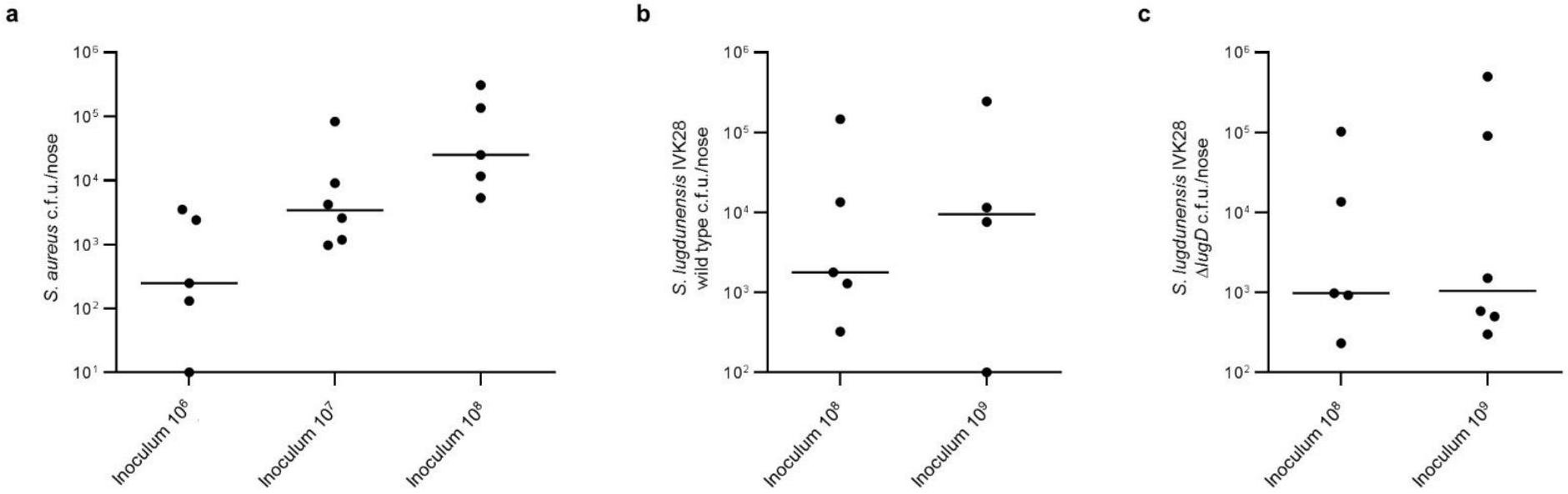

Extended Data Figure 7 | Nasal colonisation rates by *S. aureus* and *S. lugdunensis* in cotton rats. Different inocula of *S. aureus* Newman (**a**), *S. lugdunensis* IVK 28 wild type (**b**) and *S. lugdunensis* IVK 28 Δ*lugD* (**c**) were instilled intranasally to determine their efficiency to colonise the noses of cotton rats (5 or 6 animals per group). CFUs of each strain were determined per nose after 5 days and plotted as individual dots. Lines represent the median of each group.

Extended Data Table 1| NMR spectral assignment of lugdunin diastereomers

Chemical shifts (δ) are given in parts per million (ppm). Multiplicity (mult.). Coupling constants (*J*) are given in Hertz (Hz). Asterisks (*) mark strong signal overlap.

	Diastereomer I		Diastereomer II		
C-Atom	δ_C	δ_H (mult., *J* in Hz)	δ_C	δ_H (mult., *J* in Hz)	C-Atom
		1 L-Cys-Thiazolidine			
2-NH	-	2.88 (1H, m)	-	n.d.	2-NH
1	38.2	2.58 (1H, m)	37.5	2.54 (1H, m)	1
		3.06 (1H, dd, 9.7, 6.4)		3.17 (1H, dd, 9.2, 6.0)	
2	63.3	3.89 (1H, m)	65.3	3.69 (1H, m)	2
3	169.8	-	171.5	-	3
		2 D-Val			
4-NH	-	8.16 (1H, d, 9.8)	-	8.52 (1H, d, 8.6)	4-NH
4	57.2	4.18 (1H, dd, 10.0, 8.4)	60.5	3.70 (1H, m)	4
5		1.65 (1H, m)	28.5	1.71 (1H, m)	5
6, 7	18.6, 18.0	0.47 (3H, d, 6.6), 0.63 (3H, d, 6.6)	18.5, 19.3	0.52 (3H, d, 6.8), 0.84 (3H, m)*	6, 7
8	169.7	-	170.5	-	8
		3 L-Trp			
9-NH	-	8.22 (1H, d, 8.5)	-	8.52 (1H, d, 7.4)	9-NH
9	52.7	4.70 (1H, ddd, m)	53.4	4.52 (1H, m)	9
10	28.0	2.89 (1H, m)	26.4	2.82 (1H, dd, 14.7, 4),	10
		3.01 (1H, dd, 14.0, 5.5)		3.36 (1H, dd, 14.7, 4)	
11	109.5	-	110.2	-	11
12	127.1	-	126.8	-	12
13	118.2	7.66 (1H, d, 7.9)	117.9	7.51 (1H, d, 7.9)	13
14	117.9	6.95 (1H, ddd, 7.9, 7.8, 1.1)	118.1	6.96 (1H, ddd, 7.9, 7.9, 1.0)	14
15	120.5	7.02 (1H, ddd, 7.9, 7.8, 1.1)	120.7	7.04 (1H, ddd, 8.0, 7.9, 1.0)	15
16	110.9	7.28 (1H, dd, 7.9, 1.0)	111.1	7.30 (1H, dd, 8.0, 1.0)	16
17	136.0	-	136.1	-	17
18-NH	-	10.77 (1H, d, 2.0)	-	10.80 (1H, d. 2.0)	18-NH
18	124.1	7.15 (1H, d, 2.0)	123.6	7.15 (1H, d, 2.0)	18
19	170.8	-	170.1	-	19
		4 D-Leu			
20-NH	-	8.14 (1H, d, 8.7)		7.78 (1H, d, 9.4)	20-NH
20	50.7	4.46 (1H, ddm)	52.2	4.41 (1H, m)	20
21	41.3	1.32 (1H, m), 1.40 (1H, m)	41.1	1.30 (1H, m), 1.37 (1H, m)	21
22	24.1	1.28 (1H, m)	23.9	1.24 (1H, m)	22
23, 24	19.1, 19.3	0.84 (3H, m), 0.87 (3H, m)	20.8*, 21.6*	0.79 (3H, m), 0.77 (3H, m)	23, 24
25	171.6	-	171.4	-	25
		5 L-Val			
26-NH	-	7.99 (1H, d, 9.2)	-	7.69 (1H, d, 9.3)	26-NH
26	56.9	4.39 (1H, m)	57.4	4.24 (1H, dd, 9.2, 9.2)	26
27	31.2	1.96 (1H, m)	29.7	1.89 (1H, m)	27
28, 29	19.1, 17.9	0.80 (3H, m), 0.83 (3H, m)	19.1, 19.3	0.85 (3H, m)*, 0.84 (3H, m)*	28, 29
30	170.2	-	171.0	-	30
		6 D-Val			
31-NH	-	7.77 (1H, d, 8.7)	-	8.02 (1H, d, 7.8)	31-NH
31	56.5	4.50 (1H, dd, 8.8, 4.6)	59.1	4.04 (1H, dd, 7.8, 7.8)	31
32	31.9	1.97 (1H, m)	29.0	1.98 (1H, m)	32
33, 34	17.4, 19.1	0.83 (3H, d, 6.5), 0.88 (3H, d, 6.5)	18.3, 19.1	0.88 (3H, m), 0.84 (3H, m)	33, 34
35	170.4	-	171.4	-	35
		7 L-Val-Thiazolidine			
36-NH	-	7.74 (1H, d, 9.2)	-	7.43 (1H, d, 9.3)	36-NH
36	57.2	3.70 (1H, m)	54.4	4.04 (1H, dm, 9.3)	36
37	29.2	1.99 (1H, m)	32.5	1.55 (1H, m)	37
38, 39	15.2,22.3	0.75 (3H, d, 6.9), 0.79 (3H, d, 6.9)	19.8,19.7	0.86 (3H, d, 6.7), 0.92 (3H, d, 6.7)	38, 39
40	72.0	4.60 (1H, dd, 10.6, 8.8)	72.1	4.73 (1H, dd, 13.1, 2.0)	40

Extended Data Table 2 | Primers used in this study.

Primer	Primer sequence 5'-3'	Gene annotation in *S. lugdunensis* N920143	Application for
Tn917 up	ATAGGCCTTGAAACATTGGTTTAGTGGG	---	Sequencing of transposon insertion site
Tn917 down	CCCATAGATAAGAAATACACCTGCAATAACC	---	Sequencing of transposon insertion site
SlPr1-up	TACGGTACCCGCTTAACAAGATGACTAGC	SLUG_RS03935	Replacement of *lugR* by *xylAP* promoter and *xylR* regulator gene
SlPr1-down	TCTTTATGGTACCTATTACATCTCTAAAG	SLUG_ RS03935	Replacement of *lugR* by *xylAP* promoter and *xylR* regulator gene
SlPr2-up	ATTTGTATTGATATCATAAAAAATGTCCG	SLUG_ RS03935	Replacement of *lugR* by *xylAP* promoter and *xylR* regulator gene
SlPr2-down	GTTAGATCTAAAGGAGGTCAATCAGATGG	SLUG_ RS03935	Replacement of *lugR* by *xylAP* promoter and *xylR* regulator gene
lugD upstream-SacI	TAGGAGCTCGCTTAATGAATTC	SLUG_RS03965	*S. lugdunensis* Δ*lugD*
lugD upstream-Acc65I	ATAGGTACCCTCCTTCTAGCTAAGC	SLUG_RS03965	*S. lugdunensis* Δ*lugD*
lugD downstream-Acc65I	AGTGGTACCCTCTATTAACTGAAAGG	SLUG_RS03965	*S. lugdunensis* Δ*lugD*
lugD downstream-BglII	ATTAGATCTGAAGTTAAGCATCCGTC	SLUG_RS03965	*S. lugdunensis* Δ*lugD*
lugD comp. forw-PstI	ATACTGCAGGCTTAGCTAGAAGGAGAG	SLUG_RS03965	Complementation of *S. lugdunensis* Δ*lugD*
lugD comp. rev-Acc65I	AATGGTACCCATCAGCATTATAGTT	SLUG_RS03965	Complementation of *S. lugdunensis* Δ*lugD*

Chapter 3

Staphylococcus lugdunensis is shaping the human nasal microbiota by the antibiotic lugdunin

Claudia Sauer, Ralf Rosenstein, Bernhard Krismer, Andreas Peschel

University of Tübingen, Interfaculty Institute for Microbiology and Infection Medicine Tübingen, Infection Biology Unit, Auf der Morgenstelle 28, 72076 Tübingen, Germany

Chapter 3 - *Staphylococcus lugdunensis* is shaping the human nasal microbiota by the antibiotic lugdunin

Abstract

Nasal *S. aureus* carriage poses a risk for invasive infections. A natural opponent from the same habitat, *S. lugdunensis*, can significantly reduce *S. aureus* colonization in the nose by producing a non-ribosomally synthesized peptide antibiotic, called lugdunin. A study with 270 healthy volunteers showed that *S. lugdunensis* carriage is associated with a 5.2-fold reduction of *S. aureus* colonization. In addition, a long-term survey of *S. lugdunensis* carriers indicated that nasal *S. lugdunensis* colonization seems to be mainly transient, but permanent colonization is also possible.

A metagenomic analysis of persistent *S. lugdunensis* carriers revealed that there are two types of metagenomic profiles at genus level, which correlate to the community state types (CST) defined by Liu *et al*.[1]. On the one hand a **CS-type**, which is characterized by the dominance of the genera *Corynebacterium* and *Staphylococcus* and on the other hand a **DC-type**, which is distinguished by *Dolosigranulum* and *Corynebacterium* as prevailing members.

Application of shotgun genome sequencing enabled us to determine the nasal microbiome at the species level at high-resolution. Especially, the CS-type showed an influence of *S. lugdunensis* carriage on the microbiome composition.

Chapter 3 - *Staphylococcus lugdunensis* is shaping the human nasal microbiota by the antibiotic lugdunin

Introduction

The nose is the preferred habitat of *Staphylococcus aureus*. About 20% of the population are permanently colonized with *S. aureus* in the nose, another 20% are defined as non-carriers and the remaining 60% of the population are considered as intermittent carriers[2]. Nasal colonization by *S. aureus* is usually symptomless, but it can facilitate infections of the skin and soft tissue and also lead to life-threatening invasive infections[3]. *S. aureus* carriage poses a risk of infection, which can be reduced by topical treatment with mupirocin[4]. The antibiotic mupirocin can be regarded as the first-line therapy in the decolonization of *S. aureus* in the nose[5], but resistance rates against mupirocin are on the rise. In general, the frequency of antibiotic resistances has increased in the recent decades. Methicillin-resistant *S. aureus* strains (MRSA) emerged at high numbers that are always resistant to the entire class of ß-lactam antibiotics, and also multidrug resistant *S. aureus* strains arised, which are resistant to several antibiotics[6-8]. Therefore, new antibiotics are needed for decolonization and treatment of *S. aureus* infections.

In search of new antibiotics, a nasal *Staphylococcus lugdunensis* strain (IVK28) was recently discovered that produces a novel antibiotic termed lugdunin. Lugdunin is a cyclic, thiazolidine containing peptide antibiotic with bactericidal activity against *S. aureus* and other Gram-positive bacteria like *Streptococcus pneumoniae*, *Listeria monocytogenes* and *Enterococcus faecalis*/*faecium*. It is synthesized by chromosomally encoded, non-ribosomal peptide synthetases. A human study with high-risk patients revealed that *S. lugdunensis* colonization of the nose is associated with a significantly reduced risk of *S. aureus* carriage[9].

S. lugdunensis is part of the natural human skin flora and is mainly localized in the pelvic and perineum regions, the axillae and in the nailbed of the first toe[10,11]. Even though the nose is not the preferred habitat of *S. lugdunensis*, the carriage rate is approximately 9%[9,10]. However, there are no data describing the longitudinal presence of *S. lugdunensis* in the nose of healthy people over a certain period.

Besides staphylococci, corynebacteria, propionibacteria and *Moraxella* are the most common members of the nasal microbiome[12]. Liu *et al.* investigated the nasal microbiota of twin pairs by 16S rRNA profiling. They identified seven community state types (CST) which are characterized by a “uniquely high prevalence and proportional abundance of specific nasal bacteria”. *S. aureus* dominates CST1, and *Enterobacteriaceae* are major colonizers in CST2. *S. epidermidis* defined CST3 and *Propionibacterium* is the

dominating genus of CST4. *Corynebacterium* spp. are most prevalent in CST5 and CST6 is defined by the occurrence of *Moraxella* spp., whereas CST7 is dominated by *Dolosigranulum pigrum*[1].

In 2012, the human skin microbiome has been analysed by the Human Microbiome Project Consortium by 16S rRNA profiling and whole genome shotgun sequencing. Within this project the anterior nares were also examined[12].

Since the bacterial density in the nose is rather low, only small amounts of DNA can be isolated and used for amplicon sequencing. That is the reason why until now metagenome analyses of the human nose microbiomes only rarely can identify bacteria below the genus level. Our group was one of the first to perform a taxonomic determination of the nasal microbiome up to the species level by whole genome shotgun sequencing. The specific aim of the study was to investigate if nasal colonization by *S. lugdunensis* has a shaping effect on the microbiome composition. Furthermore, we want to investigate if *S. lugdunensis* can influence the nasal colonization of *S. aureus* in healthy volunteers and we also wanted to examine if the results of the study with high-risk patients can be confirmed[9]. In addition, a long-term study was performed in order to investigate the temporal stability of the microbiome and the putative persistence of *S. lugdunensis*. Finally, the data of the metagenome analysis were compared with those of a culture-based analysis.

It is important to understand how members of the nasal microbiome influence each other. Especially the interaction of *S. lugdunensis* with *S. aureus* might help to develop new *S. aureus* elimination strategies.

Material & Methods

Colonization study

Swabbing, cultivation and phenotypic identification

Nasal swabs from 270 healthy volunteers of the University of Tübingen were collected by swabbing both nares with cotton swabs and suspending them in 1ml phosphate buffered saline (PBS). Various dilutions of each sample were plated on complex medium agar (basic medium, BM)[13], blood agar and selective *S. lugdunensis* medium agar (SSL)[14] for phenotypic identification of *S. lugdunensis*, *S. aureus* and other staphylococcal species. The plates were incubated for 24-48 h at 37°C under aerobic and anaerobic conditions, respectively. The bacterial identity was determined or confirmed by matrix-assisted laser desorption/ionization-time-of-flight mass spectrometry (mass spectrometer: AXIMA Assurance, Shimadzu Europa GmbH, Duisburg, database: SARAMIS with 23.980 spectra and 3.380 superspectra, BioMérieux, Nürtingen).

Bioactivity and sensitivity test

The antimicrobial activity of the collected nasal *S. lugdunensis* strains against *S. aureus* USA300 LAC was investigated by analysis of the inhibition zone in an agar diffusion assay. Therefore, *S. aureus* USA300 LAC was resuspended in PBS and streaked out equably on BM agar plates with a cotton swab. The *S. lugdunensis* test strains were spotted on the resulting bacterial lawn and the plates were incubated for 24-48 h at 37 °C. The uncharacterized *S. aureus* strains of the co-colonized volunteers were tested for their sensitivity against the lugdunin producing strain *S. lugdunensis* IVK28[9] in the same way.

Statistical analysis

Statistical analysis of the nasal colonization study was performed with binomial distributions by using GraphPad Prism (trials per experiment: 270, probability of success in each trial: 0.018459 (colonization frequencies: *S. aureus* 29.3%; *S. lugdunensis*: 6.3%)). *P* values of ≤0.05 were considered as significant.

Metagenome sequencing of nasal microbiome samples

Swabbing

Nasal microbiome samples were taken from individuals by swabbing both nares successively with one nylon-flocked E-Swab (ThermoFisher Scientific) and suspending them in 1ml Amies transport medium. Two replicate swabs were consecutively taken per volunteer.

Preparation of DNA

For degradation of contaminating host DNA and subsequent preparation of bacterial DNA, the suspended samples were mixed with AHL-buffer and treated with the QIAamp DNA Microbiome Kit (Qiagen) according to the manufacturer's instructions. Finally, DNA was eluted from the spin columns in 50 µl AVE-buffer. DNA concentration was determined with Qubit 3.0 (Thermo Fisher Scientific) using High Sensitivity (HS) reagents for low DNA concentrations. 2.5 µl of the preparation was used for whole genome amplification with REPLI-g Single Cell Kit (Qiagen). Subsequently, the amplified DNA was purified with Genomic DNA Clean & Concentrator (Zymo Research) and the final DNA concentration was determined with Qubit 3.0.

Sequencing

About 10 µg of the purified DNA was used for Next Generation Sequencing by GATC (Konstanz, Germany). In brief, libraries of fragments of ca. 400 bases were prepared and submitted to Illumina paired-end sequencing with read lengths of 150 bases. After quality-filtering, an average of 30 million read pairs was obtained per sample and provided as compressed fastq.gz file (separate files for each end of the sequenced inserts).

Bioinformatics

The sequence reads from each file were mapped against the NCBI non-redundant protein database (downloaded in August 2017) by using the optimized BLASTX algorithm of DIAMOND[15]. For the subsequent functional and taxonomic analysis with MEGAN6[16], the DIAMOND alignment files were "meganized" by combining the paired-end sequences for each sample and providing them with functional annotations.

Taxonomic binning, functional analysis and statistical analyses were performed by using the corresponding functions of MEGAN6. For the comparison of the metagenomes on a

selected taxonomy rank (genus or species), pairwise distances were calculated based on ecological distance according to Hellinger[17].

Assembly of metagenome sequencing reads

To exploit the genetic information obtained with the metagenome sequence reads we attempted to assemble the species-specific reads into larger contiguous sequences. For this, we used the MetaSpades tool, which is implemented in the SPADES assembler[18,19]. For species-specific read-assemblies, we first used MEGAN6 to extract the reads assigned to the species of interest as a Fasta file. Then we used MetaSpades to assemble these reads into contigs. In order to determine the coverage of the genome of the selected species, we used Mauve to align and re-arrange the contigs by comparing them with a reference genome.

Results

It has been shown recently, that there is a negative correlation between nasal colonization with *S. lugdunensis* and *S. aureus*. A study with high-risk patients demonstrated that *S. lugdunensis* strongly reduces the risk of nasal colonization by *S. aureus*[9]. Therefore, the current study intended to investigate whether this finding can be confirmed for healthy volunteers. Therefore, nasal swabs from 270 healthy volunteers were investigated whether the presence of *S. lugdunensis* can prevent co-colonization by *S. aureus* in the human nose. For this purpose, we examined the colonization rates of both species by culture tests, which were selective for staphylococci.

Culture-based results

About two third of the volunteers were female (63.7%) and the average age of all participants was 26.7 years (18-65 years). The determined colonization rates were 6.3% for *S. lugdunensis* and 29.3% for *S. aureus*, which corresponds to already published data[9,10,20]. Males were 4-fold more frequently colonized by *S. lugdunensis* than females. Altogether, 17 *S. lugdunensis* carriers could be identified, five of which were women and twelve men (Tab.1). Thus, the gender distribution of *S. lugdunensis* carriers resulted in an altered *S. lugdunensis* colonization rate for women (2.9%) and men (12.25%).

Table 1: Gender distribution of *S. lugdunensis* carrier in the first culture-based analysis (cult-I)

Gender	Carrier type	Number of persons	*S. lugdunensis* carriage (%)
Women	*S. lugdunensis* carrier	5	2.9
	Co-Carrier	0	
	S. aureus carrier	49	
	Total	172	
Men	*S. lugdunensis* carrier	11	12.25
	Co-Carrier	1	
	S. aureus carrier	30	
	Total	98	

Besides *S. lugdunensis* and *S. aureus,* other staphylococci could be identified. The most prevalent nasal species was *S. epidermidis* (87.4%) but also other coagulase-negative staphylococci (CoNS) such as *S. warneri* (4.4%) and *S. capitis* (9.4%) could be isolated.

Interestingly, only one of the 270 examined people was colonized simultaneously with *S. lugdunensis* and *S. aureus* in the nose. Thus, the percentage of *S. aureus* colonization in healthy *S. lugdunensis*-positive carriers is 5.2-fold lower than in *S. lugdunensis*-negative individuals (Fig. 1), confirming that colonization with *S. lugdunensis* significantly reduces the risk of *S. aureus* colonization.

a

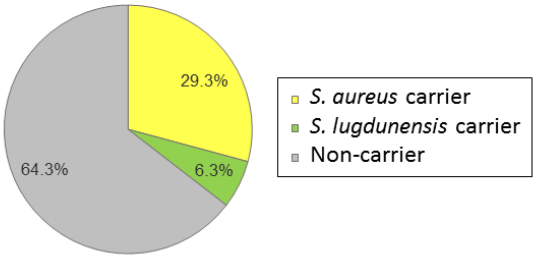

b

	S. lugdunensis-positive	*S. lugdunensis*-negative	Total
S. aureus-positive	1	78	79
S. aureus-negative	16	175	191
Total	17	253	270
S. aureus carriage (%)	5.9*	30.8*	29.3

*P=0.033

Figure 1 *S. lugdunensis* interferes with *S. aureus* nasal carriage in humans. Screening of 270 healthy volunteers. **a**, Colonization rates of *S. aureus* and S. *lugdunensis* in the human nose **b**, *S. aureus* and *S. lugdunensis* distribution in healthy volunteers

Long-term examination of *S. lugdunensis* carriers

After confirmation of the impact of *S. lugdunensis* colonization on the presence of *S. aureus* the question arose if *S. lugdunensis* carriage is transient or also permanent as described for *S. aureus*. For this purpose, 12 of the primary *S. lugdunensis* carriers (Cult-1) were screened again after seven months (Cult-2). A third screening was performed after another 11 months with eight of the original carriers and five months later these individuals were screened again for a fourth time (Cult-3 and Cult-4). Unfortunately, due to change of residence not all primary *S. lugdunensis* carriers could participate in all four screenings. A control group with 13 randomly selected *S. lugdunensis* non-carriers was defined in addition to the group of *S. lugdunensis* carriers. Altogether, the colonization with *S. lugdunensis* was investigated over a period of 23 months. The first and the last screening were performed in winter and the second and third screening in summer.

Analysis over a nearly two-year period identified three different types of colonization by *S. lugdunensis*. On the one hand, there are in fact individuals who are permanently colonized by *S. lugdunensis* and on the other hand, there are individuals who can be considered as intermittent carriers, or who belong to the group of non-carriers (Fig. 2).

Three individuals were colonized only with *S. lugdunensis* during the entire period and S. *aureus* was never detectable, defining these volunteers as persistent *S. lugdunensis* carriers (SS, PC, RS). However, the sequence type of these strains should be specified by MLST to confirm colonization by a single strain.

Subject (PL) can be regarded as an intermittent carrier because this person was always a *S. lugdunensis* carrier except for analysis Cult-2. In the control group two participants can also be considered as intermittent carriers (NS, AS). Both were tested positive for *S. lugdunensis* only at the second screening. However, in three participants (AP, AB, AE) *S. lugdunensis* could only be detected in Cult-1 or in Cult-2. Antibiotic treatment between the second and third swabbing might explain the loss of *S. lugdunensis* carriage in individual AP. Subject (YH) was only colonized in Cult-1 with *S. lugdunensis*, whereas participant (MB) was colonized with *S. lugdunensis* in Cult-1 and Cult-2. Unfortunately, both volunteers could not participate in the following study.

As mentioned before, only one person was co-colonized with both species at the beginning of the study (MA). However, at the second screening neither *S. aureus* nor *S. lugdunensis* could be detected on culture basis in this person. Instead, another *S. lugdunensis* carrier became a co-carrier (MI) and in the third and fourth screening, another *S. lugdunensis* carrier became a co-carrier (TS). There was also fluctuation in the control group where two non-carriers evolved to intermittent co-carriers (DS, OH). Interestingly, most of the *S. lugdunensis* strains isolated from co-carriers showed no lugdunin production under assay conditions. Only in Cult-1, a single person (MA) had a producer strain and nevertheless was co-colonized with *S. aureus*. Moreover, all tested *S. aureus* strains isolated from co-colonized individuals were sensitive to lugdunin (Fig. 2).

Since the carrier states refer exclusively to *S. lugdunensis* colonization (intermittent or persistent colonization), the volunteers DS, OH and TS were classified in the separate group of co-carriers, which is characterized by the simultaneous presence of *S. lugdunensis* as well as *S. aureus*.

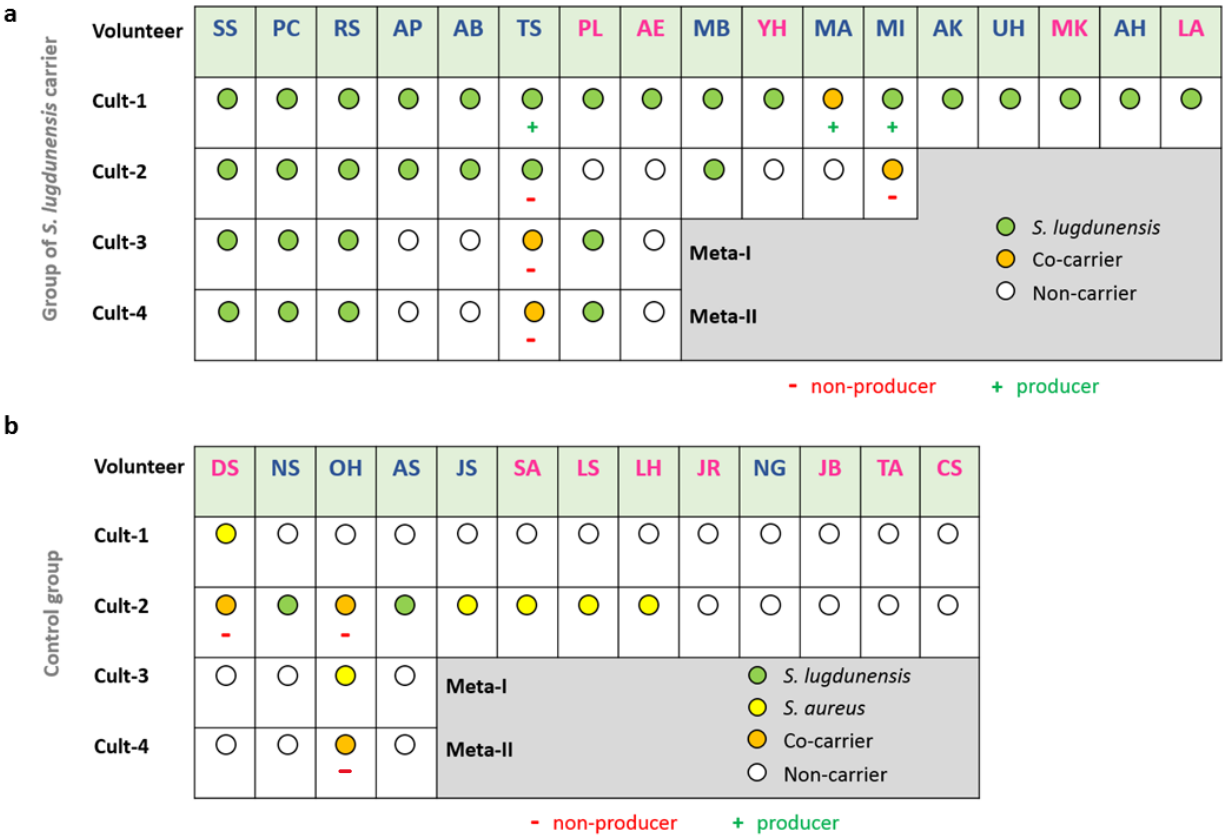

Figure 2 Carrier states of the healthy volunteers tested at four time points by culture-dependent assays (Cult-1 to Cult-4). Determination of the colonization with *S. lugdunensis* and *S. aureus* and their persistence in the human nose. The *S. lugdunensis* strains of co-carriers were also tested for the production of the antimicrobial lugdunin (**+** Lugdunin producer, **-** Lugdunin non-producer). Parallel to Cult-3 and Cult-4 a metagenome analysis was performed. Volunteers in pink are women and in blue are men **a,** Group of 17 *S. lugdunensis* carriers after the first nasal screening (primary carriers) **b,** Control group of 13 initial, randomly selected *S. lugdunensis* non-carriers.

Comparison of taxonomic profiles from the consecutive screenings

This longitudinal study confirmed the assumption that *S. lugdunensis* has a strong capacity to prevent human nasal colonization by *S. aureus* in healthy volunteers. *S. lugdunensis* clearly influenced the colonization rate of *S. aureus* as analysed by culture-based detection. Another aspect was to investigate the expected microbiome shaping effect by *S. lugdunensis*. Specifically, the metagenomes of *S. lugdunensis* carriers were examined and the results were compared with the culture-based analyses. To investigate the influence of *S. lugdunensis* on the nasal microbiota, metagenomic analyses (Meta-I and Meta-II) were performed in parallel to the culture-based assays Cult-3 and Cult-4.

The metagenomes of eight initial carriers and four participants of the control group, who were carriers at Cult-2, were examined.

To evaluate the method, we tested a mock community of different bacterial species and analyzed it by our metagenome sequencing protocol. The mock community had been prepared with equal optical densities of the bacteria added and we observed all of them in the metagenome profiles but with various percentages (data not shown). Since it is known that also 16S amplicon sequencing leads to biases [21,22], we were not concerned by this result.

Recently, the various human nasal microbiomes have been classified into seven distinct community state types (CSTs)[1]. Likewise, we observed two distinct types of metagenomic profiles at the genus level for the three persistent *S. lugdunensis* carriers (SS, PC, RS). In two of them (SS, PC) the microbiomes are dominated by the genera *Corynebacterium* and *Staphylococcus* (= **CS-type**) while the metagenome of RS is distinguished by *Dolosigranulum* and *Corynebacterium* as major members (= **DC-type**). Notably, in the CS-type microbiomes the relative abundance of *Corynebacterium* and *Staphylococcus* inverted from Meta-I to Meta-II (predominance of *Corynebacterium* in Meta-I, prevalence of *Staphylococcus* in Meta-II). On the other hand, the composition of the DC-type microbiome remained remarkably stable over time (Fig. 3). The remaining volunteers showed variable carrier states during the preceding and accompanying culture-dependent screenings (Fig. 2). Nevertheless, some of them showed taxonomic profiles that resembled those of the persistent carriers (Fig. 3). Generally, it is conspicuous that the microbiomes of *S. lugdunensis* carriers exhibit a lower diversity in their microbiomes compared to non-carriers.

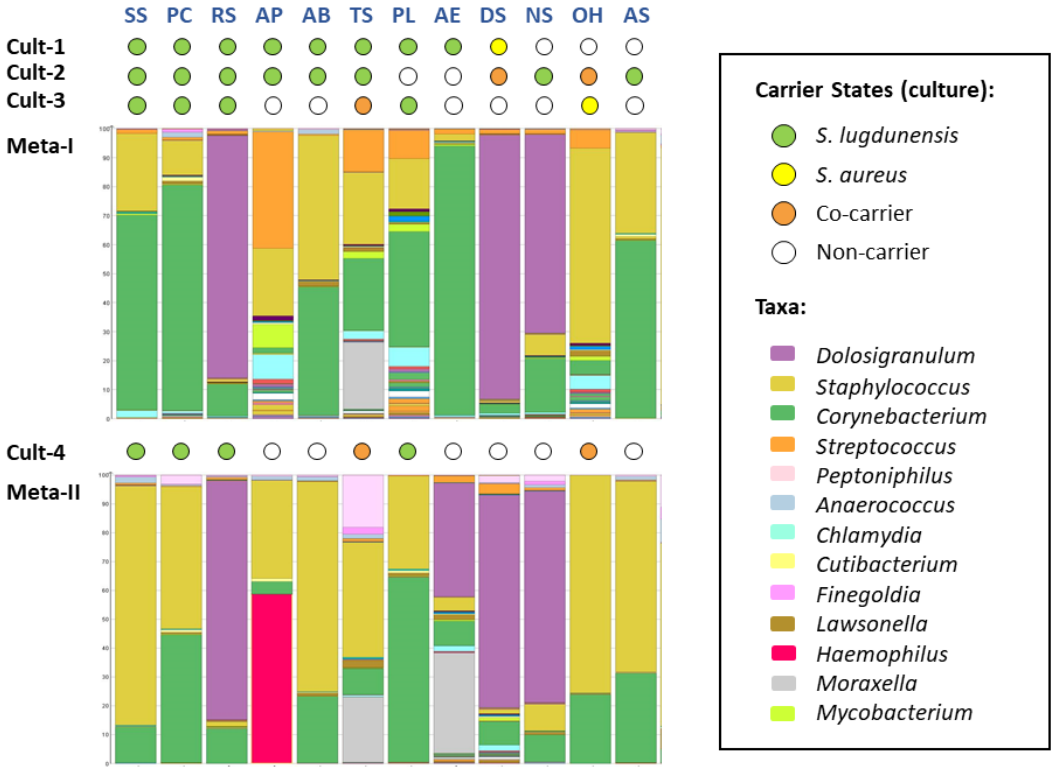

Figure 3 Metagenomic profiles at the genus level. Relative proportions of bacterial genera present in the nasal microbiomes of the volunteers SS to AS. The corresponding metagenome analyses were done in parallel with the culture-based assays Cult-3 and Cult-4. The carrier states as determined by the culture-based assays are indicated by coloured circles.

In order to analyse the taxonomic profiles with regard to similarity, a "phylogenetic network computation[17]" based on the genus level composition was performed. Strikingly, most of the microbiomes cluster around one of the profile types found for the persistent carriers (Fig. 4). The cluster representing the DC-type microbiomes forms a compact group of six samples whereas the larger CS-type cluster is subdivided into two groups with six samples each. While the whole cluster is generally characterized by *Corynebacterium* and *Staphylococcus* as predominant genera, the two subclusters reflect the change in the relative proportions of these genera in the taxonomic profiles that occurred between Meta-I and Meta–II (Fig. 4).

Besides the microbiomes that group with the CS- and DC-clusters, six of the taxonomic profiles show more diverse compositions and locate at outlying positions in the network. Notably, the compositions of two of the taxonomic profiles changed completely between both screenings (AP and AE: Meta-I to Meta-II, Fig. 4). Three of the outlying

microbiomes (OH, PL, TS) represent samples from the first metagenome screening (Meta-I) and turned into CS-type metagenomes in Meta-II (Fig. 4). On the other hand, one microbiome developed from a CS-type to an outlier (AE).

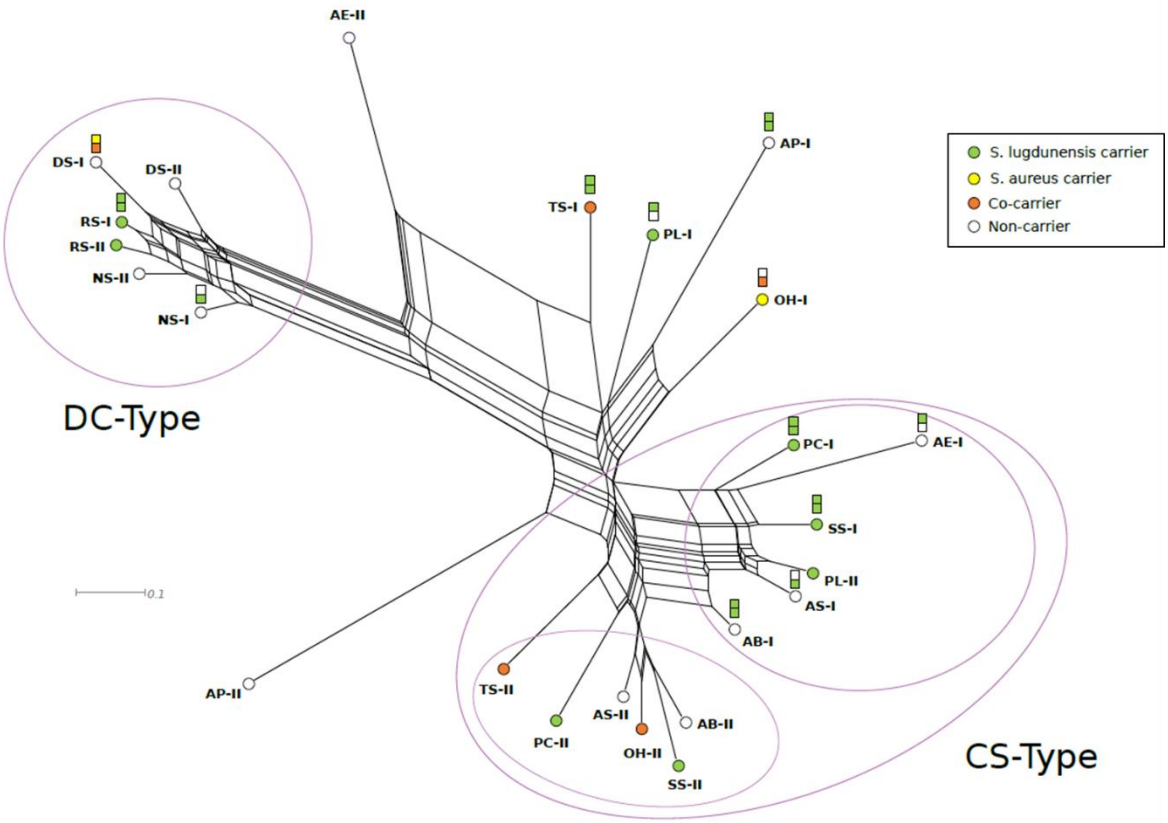

Figure 4 Phylogenetic network comparison of the microbiomes at genus level. Pairwise distances were calculated based on ecological distance according to Hellinger[17]. The culture-based carrier state preceding (squares) and accompanying (circles) the metagenome assays are indicated by corresponding colours (see legend). The microbiomes clustering with the CS-type are subdivided into two subclusters representing the inversed ratios of *Corynebacterium* and *Staphylococcus* in Meta-II as compared to Meta-I.

Indications for an influence of *S. lugdunensis* on the microbiome compositions

The fact that two of the persistent *S. lugdunensis* carriers reveal similar taxonomic profiles of the CS-type suggested that colonization with *S. lugdunensis* could have an impact on the taxonomic profile. This assumption was supported by similar compositions of the other microbiomes from the non-persistent carriers that cluster in the CS-group (Fig. 4).

According to the culture-based assays, their similarity with the CS-type microbiomes could not be explained by the presence of *S. lugdunensis*. In contrast to this, most of the corresponding metagenome data revealed *S. lugdunensis* reads. Therefore, an influence of *S. lugdunensis* on the microbiome composition remains plausible (Fig. 5).

Another strong indication for a microbiome forming effect of *S. lugdunensis* is provided by the changes in the taxonomic profile of sample PL during the consecutive screenings: the respective volunteer had been initially tested as *S. lugdunensis* carrier (Cult-1) who then turned into a non-carrier (Cult-2) and finally became a carrier again (Cult-3 and Cult-4, Fig. 2). The intermittent non-carrier state could account for the more diverse composition in the first metagenome assay resulting in an outlying position in the phylogenetic network (PL, Meta-I). In the second metagenome analysis however, the taxonomic profile (PL, Meta-II) clustered next to the microbiomes of the CS type indicating a microbiome shaping effect by the enduring influence of colonization with *S. lugdunensis* (Fig. 4).

While the indicators for a correlation between *S. lugdunensis* and the CS-type microbiome composition are quite convincing, the observation of a DC-type microbiome in only one of the persistent *S. lugdunensis* carriers makes the assumption of a putative shaping effect by *S. lugdunensis* for this microbiome type more daring. Furthermore, the microbiomes that cluster together with the RS sample were tested negative for *S. lugdunensis* not only in the culture-dependent tests but also in the metagenomic shotgun sequencing. Thus, a shaping effect of *S. lugdunensis* on the DC-like microbiome could only be explained by a previous colonization with *S. lugdunensis*, either as an exclusive carriage (NS, Cult-2) or as co-carriage with *S. aureus* (DS, Cult-2). The conspicuous stability of the DC-type microbiome composition as demonstrated by the almost identical profiles of samples RS in Meta-I and Meta-II corroborates this idea of a “memory effect”.

Composition of the microbiomes at the species level

Since most of the analysed microbiomes showed similar compositions at the genus level, we wanted to see whether these similarities were also reflected by the species composition of the major genera, *Corynebacterium*, *Staphylococcus* and *Dolosigranulum*. This analysis was facilitated by the methodological advantage of metagenome shotgun sequencing which allowed for a high-resolution taxonomical binning of the sequence data.

Staphylococcus species in the microbiomes

S. lugdunensis reads were found in most of the microbiomes – at least at one time point– except AE, DS and NS. In volunteer AB (Meta-I and Meta-II), AS (Meta-I and Meta-II), AP (Meta-I) *S. lugdunensis* reads were also present, although in the culture-based screening no *S. lugdunensis* could be identified. In general, they contribute to only a minor part to the total amount of *Staphylococcus* reads (Fig. 5).

S. aureus reads were present in all microbiomes including those that were tested negative for *S. aureus* in the culture-based assays. Interestingly, the *S. aureus* proportions were constantly low throughout both metagenome assays in all CS-type microbiomes that revealed *S. lugdunensis* reads (SS, PC, AB, AS; Fig. 5). In two cases (TS, PL), the taxonomic profiles revealed rather high *S. aureus* proportions in the first round that were significantly reduced in the second metagenome analyses. It is noteworthy that both microbiomes initially were at an outlier position in the phylogenetic network and then developed into CS-type microbiomes (Fig. 4). In sample AE, we found the converse development from a CS-type profile to an outlier microbiome. This change was accompanied by a significant increase of *S. aureus* reads, but at both points in time no *S. lugdunensis* reads were detected. An exception in this context is represented by the microbiome of volunteer OH, which also revealed *S. lugdunensis* reads and eventually developed into a CS-type microbiome but constantly showed exorbitantly high numbers of *S. aureus* reads. Of the DC-type microbiomes, only RS revealed *S. lugdunensis* reads. Interestingly, the *S. aureus* proportion in this microbiome decreased between Meta-I and Meta-II while the *S. lugdunensis* proportion increased significantly to more than 30% of all *Staphylococcus* species (Fig. 5). The other DC-type microbiomes, DS and NS, revealed no *S. lugdunensis* reads and showed converse developments from Meta-I to Meta-II with respect to the *S. aureus* proportions.

In the majority of the samples, the dominant *Staphylococcus* species was *S. epidermidis*. In the cases mentioned above, where a reduction of the *S. aureus* proportions occurred between Meta-I and Meta-II, the *S. epidermidis* fraction increased correspondingly (except RS). Beside *S. epidermidis*, *S. aureus* and *S. lugdunensis*, also other *Staphylococcus* species were found in some of the studied microbiomes. Noticeable amounts of *S. sciuri* counts were detected in most of the samples in the first screening (SS, RS, AP, TS, PL, AE, DS, NS, OH) but disappeared in the follow-up samples except for AE and DS. In most of the microbiomes *S. capitis* was found as being present in at

least one of the longitudinal samples except for samples AE, DS, NS and OH. *S. saprophyticus* was found with significant read counts only in one microbiome (PC, Meta-II). For a complete overview of all *Staphylococcus* species found in the microbiomes see figure 5.

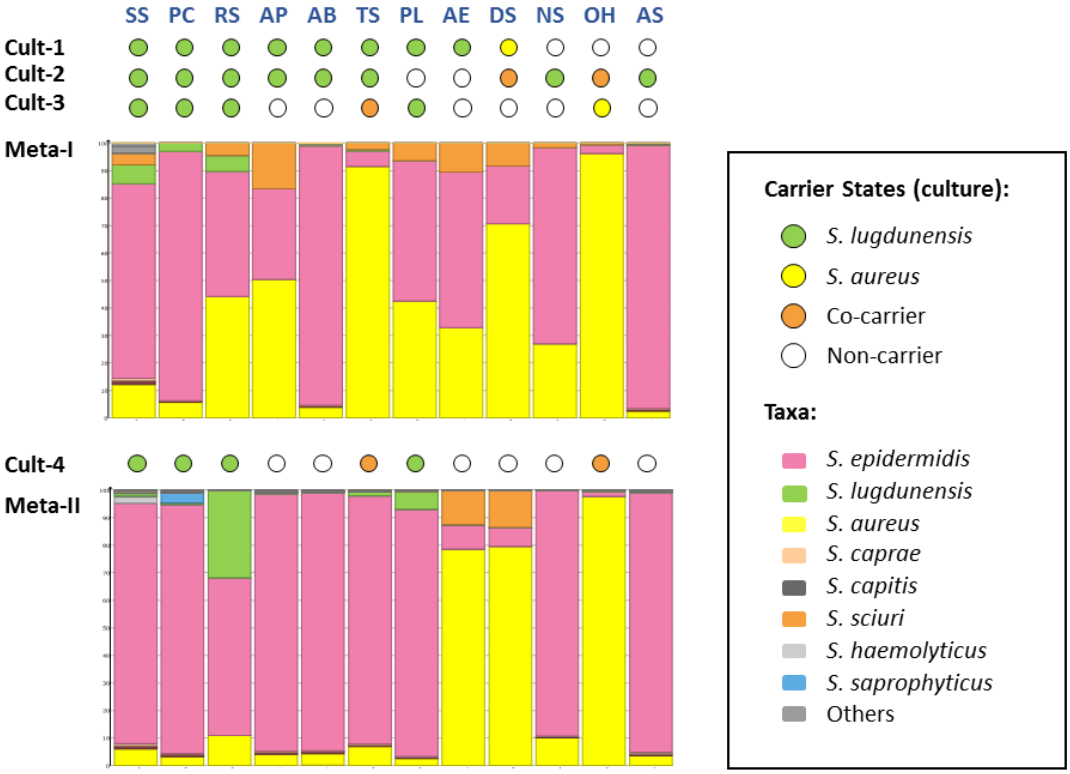

Figure 5 Metagenome compositions at *Staphylococcus* species level. Relative proportions of staphylococcal species present in the nasal microbiomes. The corresponding metagenome analyses were done in parallel with the culture-based assays Cult-3 and Cult-4. The carrier states as determined by the culture-based assays are indicated by coloured circles.

Corynebacterium species in the microbiomes

All analysed microbiomes contained a significant proportion of members of the genus *Corynebacterium*. When looking at the species level, it turned out that these proportions were composed of large variations of different species. Besides clearly assignable *Corynebacterium* species, a large proportion of the species were not exactly classifiable but only annotated as *Corynebacterium sp.* and differentiated by numbers according to the whole genome shotgun sequencing project they were derived of. Of the clearly

assignable species, the major representatives were *C. accolens*, *C. pseudogenitalium*, *C. pseudodiphteriticum*, *C. propinquum*, and *C. diphteriae*.

Interestingly, the two distinct microbiome types DC and CS that were detected by the metagenome analysis revealed different patterns of *Corynebacterium* species. While in the DC-type microbiomes *C. propinquum* and *C. pseudodiphteriticum* represent more than 50% of the *Corynebacterium* species, the CS-type microbiomes were dominated by *C. accolens* and *C. pseudogenitalium*.

Co-Occurrence Plots

Based on the similar compositions of most of the tested microbiomes at the genus level, we postulated that the observed comparable taxonomic profiles might be the result of an interaction of certain species in the microbiome. Given the similar taxonomic composition of most of the tested microbiomes, it could be assumed that observed microbiome shapes might be based on the co-occurrence of these species in the different microbiome types. In order to test this, we analysed the CS-type and DC-type microbiomes by co-occurrence plots with MEGAN 6. Thus, we were able to define “core microbiomes” comprising the species that are present in all tested microbiomes of the corresponding types. The members of the “core microbiomes” are listed in table 2. For the CS-type co-occurrence analysis, AE was omitted since it was the only CS-type microbiome that showed no *S. lugdunensis* reads. For the DC-types, of which only one microbiome revealed *S. lugdunensis* reads, all microbiomes were included. The lists are sorted by decreasing numbers of assigned reads. The applied threshold for the co-occurrence plots were 0.06% of all reads.

Table 2 Co-occurrence of species in different microbiome types. For the CS-type co-occurrence analysis, sample AE was omitted since it showed no *S. lugdunensis* reads. For the DC-type analysis, all microbiomes of this type were included, also those without *S. lugdunensis* reads. The lists are sorted by decreasing numbers of assigned reads. The applied threshold for the co-occurrence plots were 0.06% of all reads.

Co-occurrence in CS-type microbiomes	Co-occurrence in DC-type microbiomes
Staphylococcus epidermidis	*Dolosigranulum pigrum*
Staphylococcus aureus	*Corynebacterium propinquum*
Corynebacterium accolens	*Staphylococcus epidermidis*
Cutibacterium acnes	*Corynebacterium pseudodiphteriticum*
Corynebacterium pseudogenitalium	*Streptococcus pneumoniae*
Corynebacterium aurimucosum	*Staphylococcus aureus*
Corynebacterium diphteriae	*Alloiococcus otitis*
Corynebacterium striatum	*Alkalibacterium gilvum*
Staphylococcus lugdunensis	
Streptococcus pneumoniae	
Corynebacterium tuberculostearicum	

Discussion

This study was conducted to investigate if the presence of *S. lugdunensis* in the nose prohibits *S. aureus* colonization and if *S. lugdunensis* has an influence on the microbiome composition. Data of a culture-based assay of the nasal microbiota from different nasal cavity locations recently revealed individual host-specific microbiota compositions that were similar throughout the different nasal habitats tested per individual[23]. For this reason, nasal swabs from the anterior nares of healthy volunteers were taken and the bacterial composition was investigated.

Since the nose is a very nutrient-poor habitat, nasal bacteria have developed different mechanisms to get an advantage in the competition for nutrients[13,24]. One defence mechanism of nasal staphylococci is the production of antimicrobial compounds[25]. Thus, *S. lugdunensis* can prevent *S. aureus* colonization in the nose by producing the peptide antibiotic lugdunin. Our new data with healthy people confirms our previous observations from the study with high-risk patients, since in both cases the presence of *S. lugdunensis* rather completely precludes *S. aureus* carriage. In both studies, only one person out of 17 was co-colonized with *S. aureus* and *S. lugdunensis*[9].

One reason for the rare cases of co-carriage might be an insufficient lugdunin concentration based on the geographical distribution of *S. lugdunensis* and *S. aureus* in the human nose, hence *S. aureus* cannot be totally eradicated in these subjects (Cult-1). Another explanation might be that most of the *S. lugdunensis* strains of the co-carriers from later time points are lugdunin non-producers (Cult-2 to Cult-4). Although these strains contain the operon, they are incapable to produce lugdunin.

Furthermore, our data are in agreement with the results of Bieber *et al.* who observed a particularly high prevalence of nasal *S. lugdunensis* in males[10]. A younger age is also positively associated with *S. lugdunensis* colonization[26], since the average age of the participants was 26.7 years. Presumably, the age of the high-risk patients is higher than the age of the healthy volunteers and yet the carriage rate for *S. lugdunensis* was 9.1% in the group of the high-risk patients[9].

Hitherto, there are no data about nasal *S. lugdunensis* carriage of healthy volunteers over an extended time period, since the nose is not the preferred habitat of *S. lugdunensis*. For that reason, we have screened *S. lugdunensis* carriers four times over a period of almost two years and examined them by culture-based assays for the presence of staphylococci.

According to other studies, the nasal colonization rate of *S. lugdunensis* is about 9%[9,10], thus being different from our study that revealed a colonization rate of 6.3%, which was lower than expected. Our results confirm the assumption that there are also different *S. lugdunensis* carrier types similar to *S. aureus* colonization. The majority of the 270 examined participants were *S. lugdunensis* non-carriers. Regarding only the eight primary *S. lugdunensis* carriers, who participated during the entire study period, a persistence rate of 50% was detected (one co-colonized with *S. aureus*), but since the number of *S. lugdunensis* carriers was very low, the persistence rate is very likely much lower. Nevertheless, our findings suggest that persistent colonization by *S. lugdunensis* is possible, although transient colonization is more likely.

The occurrence of *S. lugdunensis* is unexpectedly high in the control group in the second culture-based screening (Cult-2), since in the control group of 13 primarily non-carriers, two *S. lugdunensis* carriers and two co-carriers were detected. It seems that the results depend on the time of sampling because the data indicate that colonization with *S. lugdunensis* is often transient. Nevertheless, these four participants were included in the subsequent metagenome analyses and examined for a third and fourth time.

Evaluation of the metagenome analysis method

The low bacterial count burden in human nostrils renders the microbiome analysis by metagenome shotgun sequencing a difficult approach. Therefore, the majority of microbiome data from human anterior nares are based on 16S rRNA amplicon sequencing. While this is an established and robust approach, its informative output is restricted as it exclusively yields taxonomic data, mainly on the genus level. As our goal was to resolve the nasal microbiome compositions of *S. lugdunensis* carriers as detailed as possible, we intended to use the metagenomics approach. By a prior amplification step, we were able to obtain sufficient amounts of DNA for the shotgun genome sequencing approach (see Materials and Methods). Since it could be assumed that this amplification step might lead to a distortion of the *in vivo* composition of the nasal microbiome, we wanted to estimate how reliable the obtained metagenome data was. On the one hand, we evaluated the method by testing a mock community composed of different bacterial species and analyzing it by our metagenome sequencing protocol. On the other hand, we checked the protocol for reproducibility by analyzing two replicas of each sample in parallel. In most instances, the replicas yielded very similar results. Furthermore, the obtained microbiome data of most of the volunteers were also

comparable between the two longitudinal samplings. Therefore, our method proved to be reliable and to give reproducible results.

The sample selection is biased towards *S. lugdunensis* carriers

Since we focused on volunteers that were at least once (co-)colonized with *S. lugdunensis* during the two-years sampling period, our cohort obviously was not representative for all nasal microbiome types. Liu *et al.* described seven different community state types (CST) they found by 16S rRNA sequencing in a representative cohort of 178 volunteers. While *S. aureus* defined its own CST (CST1), *S. lugdunensis* was only found in the two CSTs dominated by *Propionibacterium* spp. (CST4) and *Corynebacterium* spp. (CST5) respectively[1]. Most of the microbiomes we determined in our cohort were either dominated by the genera *Corynebacterium* and *Staphylococcus* (CS-type) or by *Dolosigranulum* and *Corynebacterium* (DC-type). Thus, they represented only three of the previously described seven CSTs with two of them being very similar to each other in differing only in the relative proportions of *Staphylococcus* and *Corynebacterium* (see next paragraph). This indicated that our selection of volunteers was most probably biased towards microbiome types that are associated with *S. lugdunensis*. Furthermore, this restriction to only a few of the possible microbiome types suggested that either *S. lugdunensis* could exert a microbiome shaping activity that resulted in a certain distinctive microbiome composition (as observed with the CS-type) or that *S. lugdunensis* might preferably colonize distinct “pre-formed” nasal microbiomes (as indicated by the three DC-type microbiome of which only one showed colonization with *S. lugdunensis*).

Concerning correlation of our metagenome data with CSTs defined by Liu *et al.*

The most prominent microbiome type in our cohort is dominated by the genera *Corynebacterium* and *Staphylococcus* (CS-type). The relative proportions of these two genera in the CS-types vary: in the first round of metagenome analyses (Meta-I) we observed a predominance of *Corynebacterium* in three CS-microbiomes (SS, PC and AE), almost equal proportions of both genera in one microbiome (AS) and a predominance of *Staphylococcus* in another sample (AB). In the second round of metagenome screenings (Meta-II) most CS-microbiomes are predominated by *Staphylococcus* (SS, PC, AB, TS, AS) while two (PC and PL) reveal almost equal proportions of *Corynebacterium* and *Staphylococcus*.

The seven “community state types” (CSTs) defined by Liu *et al.* are based on the significant proportional abundance and prevalence of specific indicator bacteria. Thus, one community state type is defined by the prevalence of corynebacteria (CST5) while another is defined by a significant proportion of *Staphylococcus epidermidis* (CST3)[1].

We observed varying relative proportions of corynebacteria and staphylococci in the CS-type microbiomes, either between different volunteers or even between the longitudinal samples of the same volunteer. Furthermore, in some CS samples no clear predominance of one of the two indicator taxa was observable. Thus, a clear and consistent assignment of the CS-type microbiomes to a CST was not always possible. The remaining microbiomes in our cohort were distinguished by a dominance of the genus *Dolosigranulum* and therefore could clearly be assigned to CST7. For a detailed comparison of the identified microbiome compositions and concordances with the CSTs as defined by Liu *et al.* see extended data table 1.

Microbiome shaping by *S. lugdunensis*

Of the two distinctive microbiome types we determined in the tested volunteers, the CS-type could in most cases be associated with the presence of *S. lugdunensis*. This suggests that *S. lugdunensis* might influence the composition of these microbiomes. Support for this assumption came from the fact that two of the persistent (either culture- and/or metagenome-positive for *S. lugdunensis* over the two-year sampling period) carriers also revealed this microbiome type. Volunteer (TS) was culture-tested as *S. lugdunensis* carrier in sampling rounds one and two and as a co-carrier in the remaining two rounds. Thus, he also carried *S. lugdunensis* over the complete sampling period. However, in the sampling round three (Cult-3) his metagenome profile did not cluster with the CS-type microbiomes (Fig. 4) while it showed this type again in the fourth round. This could be explained by the rather low absolute read number (about 20fold less than in the fourth round) for *S. lugdunensis* in the third round and a correspondingly low impact on the microbiome composition.

We found also discrepancies between the culture-based carrier-states and the metagenome data. Volunteer (AB) had been determined to be a culture-based non-carrier in rounds three and four but turned out to be a CS-type microbiome according to the corresponding metagenome analyses. This corresponded with *S. lugdunensis* reads present in the samples despite the aforementioned culture-based non-carrier state. The same discrepancy was found for volunteer (AS). Thus, it became obvious that a culture-

based carrier state does not correspond to the metagenome data and vice versa. A possible explanation could be a threshold of absolute read counts that have to be present for the culture outcome to be positive. This has been described for *S. aureus* nasal colonization[1]. However, our data base is not sufficient enough to confirm this also for *S. lugdunensis*. The most obvious clue for a microbiome shaping activity of *S. lugdunensis* was obtained from the development of volunteer PL's microbiome over time. According to the culture-based carrier state, it initially had been a *S. lugdunensis* carrier who became a non-carrier in the second round. The third round gave a culture-positive outcome, but the metagenome data showed no reads for *S. lugdunensis*. The corresponding microbiome composition at the genus level revealed weak similarity with the CS-type but located at an outlier position in the phylogenetic network (Fig. 4). In the fourth round, culture-based assay as well as metagenome data consistently showed a *S. lugdunensis* positive state and the taxonomic profile had turned into a CS-type microbiome. This fits well to the assumption that the return of *S. lugdunensis* had led to the observed microbiome type.

In conclusion, our data for the CS-type microbiomes quite clearly suggest an influence of the presence of *S. lugdunensis* on the microbiome composition. For the DC-type microbiomes of which only one revealed *S. lugdunensis* reads, a microbiome-shaping effect could not be deduced in a similar way. It could rather be assumed that the DC-type microbiome might be a "pre-existing" metagenome profile that could be exploited by *S. lugdunensis* for some reason.

Co-occurrence analyses

The fact that we found only two microbiome types in the *S. lugdunensis* carriers implied that the co-occurring bacterial species in these microbiomes might have a supporting effect on the colonization by *S. lugdunensis*. By co-occurrence analyses, we have identified the core microbiomes of the two detected microbiome type, which represent bacterial species present in all microbiomes of a type. The core microbiome members will represent promising candidates for being supporting microbiome partners of *S. lugdunensis*.

On one hand, metagenome sequencing reads can be used for taxonomic analysis and on the other hand, to exploit the genetic information obtained with the metagenome sequence reads. Hereby, metabolic pathways can be identified that are relevant for the microbiome composition and might explain why certain genera coexist or do not coexist

in the human nose. Promising candidates in this context could be genes related to vitamin biosynthesis[27], PKS/NRPS systems[9,28] or siderophores[29].

It is necessary to understand the interaction among the nasal members in order to achieve new prospects for *S. aureus* decolonization, since invasive infections are often caused by the same clonal *S. aureus* strain, which is also located in the nose[30]. To minimize the risk of invasive *S. aureus* infections, it must be eliminated from the nose. Application of *S. lugdunensis* and its subsequent production of the peptide antibiotic lugdunin might be a new strategy to prevent *S. aureus* colonization.

References

1 Liu, C. M. *et al.* Staphylococcus aureus and the ecology of the nasal microbiome. *Sci Adv* **1**, e1400216, doi:10.1126/sciadv.1400216 (2015).

2 Kluytmans, J., van Belkum, A. & Verbrugh, H. Nasal carriage of Staphylococcus aureus: epidemiology, underlying mechanisms, and associated risks. *Clin Microbiol Rev* **10**, 505-520 (1997).

3 Lowy, F. D. Staphylococcus aureus infections. *N Engl J Med* **339**, 520-532, doi:10.1056/NEJM199808203390806 (1998).

4 Bode, L. G. *et al.* Preventing surgical-site infections in nasal carriers of Staphylococcus aureus. *N Engl J Med* **362**, 9-17, doi:362/1/9 10.1056/NEJMoa0808939 (2010).

5 Septimus, E. J. & Schweizer, M. L. Decolonization in Prevention of Health Care-Associated Infections. *Clin Microbiol Rev* **29**, 201-222, doi:10.1128/cmr.00049-15 (2016).

6 Poovelikunnel, T., Gethin, G. & Humphreys, H. Mupirocin resistance: clinical implications and potential alternatives for the eradication of MRSA. *J Antimicrob Chemother* **70**, 2681-2692, doi:10.1093/jac/dkv169 (2015).

7 Otto, M. MRSA virulence and spread. *Cell Microbiol* **14**, 1513-1521, doi:10.1111/j.1462-5822.2012.01832.x (2012).

8 DeLeo, F. R., Otto, M., Kreiswirth, B. N. & Chambers, H. F. Community-associated meticillin-resistant Staphylococcus aureus. *Lancet* **375**, 1557-1568, doi:10.1016/S0140-6736(09)61999-1 (2010).

9 Zipperer, A. *et al.* Human commensals producing a novel antibiotic impair pathogen colonization. *Nature* **535**, 511-516, doi:10.1038/nature18634 (2016).

10 Bieber, L. & Kahlmeter, G. Staphylococcus lugdunensis in several niches of the normal skin flora. *Clin Microbiol Infect* **16**, 385-388, doi:10.1111/j.1469-0691.2009.02813.x (2010).

11 Becker, K., Heilmann, C. & Peters, G. Coagulase-negative staphylococci. *Clin Microbiol Rev* **27**, 870-926, doi:10.1128/CMR.00109-13 (2014).

12 Human Microbiome Project, C. Structure, function and diversity of the healthy human microbiome. *Nature* **486**, 207-214, doi:10.1038/nature11234 (2012).

13 Krismer, B. *et al.* Nutrient limitation governs Staphylococcus aureus metabolism and niche adaptation in the human nose. *PLoS Pathog* **10**, e1003862, doi:10.1371/journal.ppat.1003862 (2014).

14 Ho, P. L. *et al.* Novel selective medium for isolation of Staphylococcus lugdunensis from wound specimens. *J Clin Microbiol* **52**, 2633-2636, doi:10.1128/JCM.00706-14 (2014).

15 Buchfink, B., Xie, C. & Huson, D. H. Fast and sensitive protein alignment using DIAMOND. *Nat Methods* **12**, 59-60, doi:10.1038/nmeth.3176 (2015).

16 Huson, D. H. *et al.* MEGAN Community Edition - Interactive Exploration and Analysis of Large-Scale Microbiome Sequencing Data. *PLoS Comput Biol* **12**, e1004957, doi:10.1371/journal.pcbi.1004957 (2016).

17 Mitra, S., Gilbert, J. A., Field, D. & Huson, D. H. Comparison of multiple metagenomes using phylogenetic networks based on ecological indices. *ISME J* **4**, 1236-1242, doi:10.1038/ismej.2010.51 (2010).

18 Bankevich, A. *et al.* SPAdes: a new genome assembly algorithm and its applications to single-cell sequencing. *J Comput Biol* **19**, 455-477, doi:10.1089/cmb.2012.0021 (2012).

19 Nurk, S., Meleshko, D., Korobeynikov, A. & Pevzner, P. A. metaSPAdes: a new versatile metagenomic assembler. *Genome Res* **27**, 824-834, doi:10.1101/gr.213959.116 (2017).

20 Wertheim, H. F. *et al.* The role of nasal carriage in Staphylococcus aureus infections. *Lancet Infect Dis* **5**, 751-762, doi:10.1016/S1473-3099(05)70295-4 (2005).

21 Ranjan, R., Rani, A., Metwally, A., McGee, H. S. & Perkins, D. L. Analysis of the microbiome: Advantages of whole genome shotgun versus 16S amplicon sequencing. *Biochem Biophys Res Commun* **469**, 967-977, doi:10.1016/j.bbrc.2015.12.083 (2016).

22 Sharpton, T. J. An introduction to the analysis of shotgun metagenomic data. *Front Plant Sci* **5**, 209, doi:10.3389/fpls.2014.00209 (2014).

23 Kaspar, U. *et al.* The culturome of the human nose habitats reveals individual bacterial fingerprint patterns. *Environ Microbiol* **18**, 2130-2142, doi:10.1111/1462-2920.12891 (2016).

24 Brugger, S. D., Bomar, L. & Lemon, K. P. Commensal-Pathogen Interactions along the Human Nasal Passages. *PLoS Pathog* **12**, e1005633, doi:10.1371/journal.ppat.1005633 (2016).

25 Janek, D., Zipperer, A., Kulik, A., Krismer, B. & Peschel, A. High Frequency and Diversity of Antimicrobial Activities Produced by Nasal Staphylococcus Strains against Bacterial Competitors. *PLoS Pathog* **12**, e1005812, doi:10.1371/journal.ppat.1005812 (2016).

26 Ho, P. L. *et al.* Carriage niches and molecular epidemiology of Staphylococcus lugdunensis and methicillin-resistant S. lugdunensis among patients undergoing long-term renal replacement therapy. *Diagn Microbiol Infect Dis* **81**, 141-144, doi:10.1016/j.diagmicrobio.2014.10.004 (2015).

27 Bosi, E. *et al.* Comparative genome-scale modelling of Staphylococcus aureus strains identifies strain-specific metabolic capabilities linked to pathogenicity. *P Natl Acad Sci USA* **113**, E3801-E3809, doi:10.1073/pnas.1523199113 (2016).

28 Ling, L. L. *et al.* A new antibiotic kills pathogens without detectable resistance. *Nature* **517**, 455-+, doi:10.1038/nature14098 (2015).

29 Stubbendieck, R. M. *et al.* Competition among Nasal Bacteria Suggests a Role for Siderophore-Mediated Interactions in Shaping the Human Nasal Microbiota. *Appl Environ Microbiol* **85**, doi:10.1128/AEM.02406-18 (2019).

30 von Eiff, C., Becker, K., Machka, K., Stammer, H. & Peters, G. Nasal carriage as a source of Staphylococcus aureus bacteremia. Study Group. *N Engl J Med* **344**, 11-16, doi:10.1056/NEJM200101043440102 (2001).

Extended data

Extended data table 1: Assignment of the microbiome composition to CSTs defined by Liu *et al.*[1]

Sample	Meta-Round	Relative abundance of CST indicator taxa				Type*	CST***	Slu abundance	Culture
		Corynebacterium	*S. epidermidis*	*S. aureus*	*Dolosigranulum*				
SS	I	43,2	21,6	3,7	0,0	CS	5	2,11	Slu
	II	10,8	69,3	4,7	0,0	CS	3	0,77	Slu
PC	I	59,0	14,3	0,9	0,0	CS	5	0,48	Slu
	II	32,4	36,5	1,3	0,4	CS	?	0,44	Slu
RS	I	3,2	0,2	0,2	93,6	DC	7	0,03	Slu
	II	3,5	0,3	0,1	94,1	DC	7	0,19	Slu
AP	I	0,0	5,0	7,6	0,0	outlier	?	0,00	non
	II	6,5	32,0	1,4	0,0	outlier	?	0,07	non
AB	I	29,5	51,4	2,1	0,0	CS	3	0,12	non
	II	15,2	71,5	3,2	0,0	CS	3	0,20	non
TS	I	5,5	1,6	27,0	0,0	outlier	?	0,19	Co
	II	5,4	26,5	2,0	0,2	CS	3	0,39	Co
PL	I	16,3	7,3	6,1	0,0	outlier	?	0,00	Slu
	II	32,3	46,7	1,3	0,0	CS	?**	3,37	Slu
AE	I	81,4	2,0	1,1	0,0	CS	5	0,00	non
	II	2,4	1,4	1,2	48,6	outlier	7	0,00	non
DS	I	0,9	0,1	0,3	95,1	DC	7	0,00	non
	II	2,5	0,1	1,2	82,3	DC	7	0,00	non
NS	I	9,5	2,2	0,8	82,3	DC	7	0,00	non
	II	5,0	3,1	0,4	85,9	DC	7	0,00	non
OH	I	0,3	0,5	91,4	0,0	outlier	1	0,04	Sau
	II	16,6	1,3	67,6	0,2	CS	1	0,27	Co
AS	I	47,2	44,6	1,2	0,0	CS	?	0,08	non
	II	18,7	73,2	2,8	0,0	CS	3	0,11	non

Slu = S. lugdunensis carrier
non = Non-carrier
Co = S. aureus/S. lugdunensis Co-carrier
Sau = S. aureus carrier

* Clustering in phylogenetic network
** See replica values
*** According to Liu et al.

Chapter 4 - General discussion

Staphylococcus aureus is a human pathogen that can cause a variety of infections. One fifth of the human population is permanently colonized by *S. aureus* in the nose, whereas another 20% are never colonized. The remaining population can be considered as intermittent carriers[1]. Resistance against *S. aureus* has increased dramatically in recent years, making the search for new antibiotics more important than ever. Human associated bacteria represent a new source of antimicrobial compounds.

During a nasal screening of bacterial isolates, the peptide antibiotic lugdunin was found in the search for new antibiotics. Lugdunin is non-ribosomally produced by *S. lugdunensis,* which had not yet been described as an antibiotic producer[2]. The nose is not the preferred habitat of *S. lugdunensis*, but rather the pelvic and perineum regions, the axillae, the groins and the lower extremities[3]. Lugdunin shows potent antimicrobial activity against *S. aureus* as well as other Gram-positive bacteria. Lugdunin forms a new class of thiazolidine-containing cyclic peptide antibiotics[2]. Moreover, lugdunin acts bactericidal by disrupting the proton gradient in *S. aureus*, whereupon the membrane potential in the cell dissipates[4].

Janek *et al*. could recently show that nasal staphylococci often produce antimicrobial substances. It has been demonstrated that 84% of the examined nasal staphylococci were characterized by the production of antimicrobial substances. Besides the lugdunin producing strain *S. lugdunensis* IVK28 another strain, *S. epidermidis* IVK83, was found in this screening with a broad activity spectrum against *S. aureus* as well as *Micrococcus luteus*, *Propionibacterium acnes*, *Dolosigranulum pigrum*, *Moraxella catarrhalis* and *Streptococcus pyogenes*[5].

However, also many previously reported antimicrobial molecules are produced by *S. epidermidis*, which all belong to the bacteriocin group of lantibiotics. They include epidermin, Pep5, epilancin K7 and 15X, epicidin 280 [6-10]. These ribosomally, synthesized antimicrobial peptides are often produced by *Staphylococcus* strains and they are characterized by the presence of the thioether amino acids lanthionine and/or methyllanthionine[11]. In addition, further lantibiotics have been described for *S. hominis* (nukacin, Sh-lantibiotic-α and -β), for *S. gallinarum* (gallidermin) as well as for *S. aureus* (staphylococcin C55)[12-15].

It has been shown previously that the production of the two lantibiotics epidermin and gallidermin represents a burden for the producer strains[16]. On the one hand, the bacterial growth is affected by the production of the antibiotics and on the other hand, the membrane integrity is impaired by the accumulation of the antimicrobial peptides.

However, the production of antibiotics also represents a major advantage in competition with other bacteria[16].

Since *S. lugdunensis* was identified during a nasal screening for new antimicrobial compounds, we performed a colonization study of the human nose to elucidate the influence of *S. lugdunensis* on the nasal microbiome. A study by Wos-Oxley *et al*. revealed that there were no significant differences between bacterial fingerprints at four different anatomical areas of the nose[17]. For this reason, nasal swabs of the anterior nares were taken for the colonization study from high-risk patients as well as from healthy persons.

As one of the first groups, we performed a metagenome analysis of the nose, which elucidated the nasal microbiome composition to the species level by whole genome shotgun sequencing. In contrast, Liu *et al.* were able to define seven different community state types (CSTs) by investigating the nasal microbiota of twin pairs by 16S rRNA profiling. CSTs are characterized by a "uniquely high prevalence and proportional abundance of specific nasal bacteria". Bacterial densities are mainly dependent on the sex of the host irrespective of the nasal CST[18]. Thus, men have a higher nasal bacterial density than women. In addition, some taxa have been identified, which predict presence/absence of *S. aureus* with a good probability. The firmicute *Dolosigranulum* was found to be the most informative predictor of *S. aureus* presence/absence while other species predict absolute abundance of *S. aureus*. Likewise, threshold effects for *P. granulosum* (negatively correlated) and *S. epidermidis* (positively correlated) were derived[18].

A further study focusing on the culture-based determination of the nasal microbiome revealed that the cultivable core microbiome can be categorized by seven species[19]. Most prevalent were *S. epidermidis* and *Cutibacterium acnes* (formerly *Propionibacterium acnes*) (each 97.1%), *Corynebacterium accolens* and *C. tuberculostearicum* (each 64.7%), *Cutibacterium avidum* (formerly *Propionibacterium avidum*) (58.8%) and *P. granulosum* (50%). Highest variability within a genus was found for *Corynebacterium* with 23 different species[19]. Corynebacteria can be regarded as part of the normal skin and nose flora and are predominant in moist regions[20].

Our metagenomic analysis of persistent *S. lugdunensis* carriers indicated that there were two types of metagenomic profiles at genus level. On the one hand a **CS-type**, which is dominated by the genera *Corynebacterium* and *Staphylococcus* and on the other hand a **DC-type**, which is distinguished by *Dolosigranulum* and *Corynebacterium* as major

members. Both types of metagenomic profiles showed also a significant proportion of members of the genus *Corynebacterium*. More precisely, in the CS-type *C. accolens* and *C. pseudogenitalium* are the dominant species, whereas in the DC-type *C. propinquum* and *C. pseudodiphteriticum* are predominant.

Corynebacteria are often part of the natural nasal microbiota and, depending on the species, are associated with a higher or lower abundance of *S. aureus*. Recently it could be shown that *C. accolens* positively correlates with *S. aureus*[21], presumably it secrets a lipase, which can convert human nasal triacylglycerol into free fatty acids and glycerol. These free fatty acids have a strong bactericidal effect against *Streptococcus pneumoniae*. Hence, *C. accolens* may influence the nasal *S. aureus* carrier status through reduction of the competition among other nasal bacterial members[22,23].

In contrast to *C. accolens*, C. *pseudodiphteriticum* is negatively correlated with *S. aureus*[21]. C. *pseudodiphteriticum* is able to eliminate *S. aureus* from the human nose by contact-independent mechanisms. A transposon mutant library showed that *S. aureus* strains in which *agrC* was inactivated are more resistant to C. *pseudodiphteriticum*-mediated bactericidal activity. *AgrC* encodes a sensor kinase of the Agr quorum sensing system, which controls the expression of many virulence factors in *S. aureus*. A deletion of the *psm* genes, which are effectors of the Agr quorum sensing system, also results in resistance to C. *pseudodiphteriticum*-mediated bactericidal activity. The exact role of the PSMs in this scenario is still unclear, but it is assumed that *C. pseudodiphtheriticum* can specifically influence the activity of the PSMs or their transporter (PMT). This mechanism induces changes in the cell surface morphology of *S. aureus*, which presumably result in cell lysis[23].

Wos-Oxley *et al*. have shown in a 16s rRNA analysis of the anterior nares that *D. pigrum* is frequently present. Therefore, they have regarded *D. pigrum* as part of the nasal core community[24]. In our metagenome analysis of the nose, three out of 12 participants were predominantly colonized by this species. Liu *et al*. revealed that one of the seven nasal CST is dominated by *Dolosigranulum* spp. (CST7)[18]. Thus, our results confirm that *D. pigrum* can colonize the nose dominantly.

The nose is a very nutrient-poor and iron-limited habitat[25]. Since *S. lugdunensis* seems to mainly co-occur with specific *Corynebacterium* species, it is conceivable that *S. lugdunensis* may benefit from these other nasal members. Especially siderophores or vitamins produced by other bacteria may be used by *S. lugdunensis*. It is conceivable that *S. lugdunensis* is also auxotrophic for vitamins similar to *S. aureus*, because it has

already been shown that *S. aureus* is auxotrophic for niacin (vitamin B3) and thiamin (vitamin B1)[26]. Moreover, *S. lugdunensis* can neither produce staphyloferrin A nor staphyloferrin B, which is in contrast to *S. aureus* [27]. Stubbendieck *et al*. were able to show that the genome of *C. propinquum* contains an increased number of genes for iron acquisition as well as a biosynthetic gene cluster to produce siderophores compared to a comparative genomics approach. Thus, *C. propinquum* has an inhibitory effect on some coagulase-negative staphylococci by the sequestration of iron through the production of the siderophore dehydroxynocardamine[28]. It is conceivable that *S. lugdunensis* might be able to use these siderophores to obtain available iron. These might be possible reasons why *S. lugdunensis* often occurs with corynebacteria in the human nares.

In 2016, Oh *et al.* presented a metagenome analysis of the human skin focused on temporal stability of the microbiome. 12 healthy individuals were sampled across 17 skin sites at three points in time, but no nasal samples were taken. They revealed that microbiome composition at high-diversity sites such as the feet or moist areas was likely to be less stable than at low-diversity sites[29]. In the Human Microbiome Project, the microbiomes of 242 adults was analyzed by 16S rRNA profiling and whole genome shotgun sequencing. It could be demonstrated that the skin, airways and urogenital tracts have a lower microbial diversity than the oral or gut microbiota[30]. A further systematic analysis of these data showed that small-molecule biosynthetic gene clusters (BGCs) are widely distributed in human associated bacteria. Corynebacteria, for example, are associated with a relatively high number of BGCs[31]. BGCs produce small molecules with often unclear functions, but with the potential of shaping the human microbiota. For example, the widespread skin commensal *Propioniobacterium acnes* harbors a BGC, which produces a new thiopeptide antibiotic (cutimycin) that is active against *S. aureus*[32].

It is important to understand how bacterial competitors influence each other. This knowledge of species interaction can be used to change the natural microbial composition by eliminating *S. aureus* from the human nose, which minimizes the risk of *S. aureus* infections. Thus, the application of lugdunin or lugdunin-producing *S. lugdunensis* strains as well as of yet unknown competitors represent a new strategy for *S. aureus* decolonization. In general, human-associated bacteria represent a new source of bioactive compounds and it can be assumed that these agents are well adapted to the human organism. In addition, these substances are presumably also effective against certain human bacteria. Therefore, human-associated bacteria have a great potential for

the search for novel antimicrobial compounds and should be placed in the focus of the current research.

References

1 Kluytmans, J., van Belkum, A. & Verbrugh, H. Nasal carriage of Staphylococcus aureus: epidemiology, underlying mechanisms, and associated risks. *Clin Microbiol Rev* **10**, 505-520 (1997).

2 Zipperer, A. *et al.* Human commensals producing a novel antibiotic impair pathogen colonization. *Nature* **535**, 511-516, doi:10.1038/nature18634 (2016).

3 Becker, K., Heilmann, C. & Peters, G. Coagulase-negative staphylococci. *Clin Microbiol Rev* **27**, 870-926, doi:10.1128/CMR.00109-13 (2014).

4 Grond, S. C. *et al.* Synthetic Lugdunin Analogues Reveal Essential Structural Motifs for Antimicrobial Action and Proton Translocation Capability. *Angew Chem Int Ed Engl*, doi:10.1002/anie.201901589 (2019).

5 Janek, D., Zipperer, A., Kulik, A., Krismer, B. & Peschel, A. High Frequency and Diversity of Antimicrobial Activities Produced by Nasal Staphylococcus Strains against Bacterial Competitors. *PLoS Pathog* **12**, e1005812, doi:10.1371/journal.ppat.1005812 (2016).

6 Allgaier, H., Jung, G., Werner, R. G., Schneider, U. & Zahner, H. Epidermin: sequencing of a heterodetic tetracyclic 21-peptide amide antibiotic. *Eur J Biochem* **160**, 9-22 (1986).

7 Kaletta, C. *et al.* Pep5, a new lantibiotic: structural gene isolation and prepeptide sequence. *Arch Microbiol* **152**, 16-19 (1989).

8 van de Kamp, M. *et al.* Elucidation of the primary structure of the lantibiotic epilancin K7 from Staphylococcus epidermidis K7. Cloning and characterisation of the epilancin-K7-encoding gene and NMR analysis of mature epilancin K7. *Eur J Biochem* **230**, 587-600 (1995).

9 Ekkelenkamp, M. B. *et al.* Isolation and structural characterization of epilancin 15X, a novel lantibiotic from a clinical strain of Staphylococcus epidermidis. *FEBS Lett* **579**, 1917-1922, doi:10.1016/j.febslet.2005.01.083 (2005).

10 Heidrich, C. *et al.* Isolation, characterization, and heterologous expression of the novel lantibiotic epicidin 280 and analysis of its biosynthetic gene cluster. *Appl Environ Microbiol* **64**, 3140-3146 (1998).

11 Bierbaum, G. & Sahl, H. G. Lantibiotics: mode of action, biosynthesis and bioengineering. *Curr Pharm Biotechnol* **10**, 2-18 (2009).

12 Wilaipun, P., Zendo, T., Okuda, K., Nakayama, J. & Sonomoto, K. Identification of the nukacin KQU-131, a new type-A(II) lantibiotic produced by Staphylococcus hominis KQU-131 isolated from Thai fermented fish product (Pla-ra). *Biosci Biotechnol Biochem* **72**, 2232-2235, doi:10.1271/bbb.80239 (2008).

13 Nakatsuji, T. *et al.* Antimicrobials from human skin commensal bacteria protect against Staphylococcus aureus and are deficient in atopic dermatitis. *Sci Transl Med* **9**, doi:10.1126/scitranslmed.aah4680 (2017).

14 Navaratna, M. A., Sahl, H. G. & Tagg, J. R. Two-component anti-Staphylococcus aureus lantibiotic activity produced by Staphylococcus aureus C55. *Appl Environ Microbiol* **64**, 4803-4808 (1998).

15 Kellner, R. *et al.* Gallidermin - a New Lanthionine-Containing Polypeptide Antibiotic. *Eur J Biochem* **177**, 53-59, doi:DOI 10.1111/j.1432-1033.1988.tb14344.x (1988).

16 Ebner, P. *et al.* Lantibiotic production is a burden for the producing staphylococci. *Sci Rep* **8**, 7471, doi:10.1038/s41598-018-25935-2 (2018).

17 Wos-Oxley, M. L. *et al.* Exploring the bacterial assemblages along the human nasal passage. *Environ Microbiol* **18**, 2259-2271, doi:10.1111/1462-2920.13378 (2016).

18 Liu, C. M. *et al.* Staphylococcus aureus and the ecology of the nasal microbiome. *Sci Adv* **1**, e1400216, doi:10.1126/sciadv.1400216 (2015).

19 Kaspar, U. *et al.* The culturome of the human nose habitats reveals individual bacterial fingerprint patterns. *Environ Microbiol* **18**, 2130-2142, doi:10.1111/1462-2920.12891 (2016).

20 Grice, E. A. & Segre, J. A. The skin microbiome. *Nat Rev Microbiol* **9**, 244-253, doi:10.1038/nrmicro2537 (2011).

21 Yan, M. *et al.* Nasal microenvironments and interspecific interactions influence nasal microbiota complexity and S. aureus carriage. *Cell Host Microbe* **14**, 631-640, doi:10.1016/j.chom.2013.11.005 (2013).

22 Bomar, L., Brugger, S. D., Yost, B. H., Davies, S. S. & Lemon, K. P. Corynebacterium accolens Releases Antipneumococcal Free Fatty Acids from Human Nostril and Skin Surface Triacylglycerols. *Mbio* **7**, e01725-01715, doi:10.1128/mBio.01725-15 (2016).

23 Hardy, B. L. *et al.* Corynebacterium pseudodiphtheriticum Exploits Staphylococcus aureus Virulence Components in a Novel Polymicrobial Defense Strategy. *Mbio* **10**, doi:10.1128/mBio.02491-18 (2019).

24 Wos-Oxley, M. L. *et al.* A poke into the diversity and associations within human anterior nare microbial communities. *ISME J* **4**, 839-851, doi:ismej201015 [pii] 10.1038/ismej.2010.15 (2010).

25 Krismer, B. *et al.* Nutrient limitation governs Staphylococcus aureus metabolism and niche adaptation in the human nose. *PLoS Pathog* **10**, e1003862, doi:10.1371/journal.ppat.1003862 (2014).

26 Bosi, E. *et al.* Comparative genome-scale modelling of Staphylococcus aureus strains identifies strain-specific metabolic capabilities linked to pathogenicity. *P Natl Acad Sci USA* **113**, E3801-E3809, doi:10.1073/pnas.1523199113 (2016).

27 Brozyna, J. R., Sheldon, J. R. & Heinrichs, D. E. Growth promotion of the opportunistic human pathogen, Staphylococcus lugdunensis, by heme, hemoglobin, and coculture with Staphylococcus aureus. *Microbiologyopen* **3**, 182-195, doi:10.1002/mbo3.162 (2014).

28 Stubbendieck, R. M. *et al.* Competition among Nasal Bacteria Suggests a Role for Siderophore-Mediated Interactions in Shaping the Human Nasal Microbiota. *Appl Environ Microb* **85**, doi:UNSP e02406-18 10.1128/AEM.02406-18 (2019).

29 Oh, J. *et al.* Temporal Stability of the Human Skin Microbiome. *Cell* **165**, 854-866, doi:10.1016/j.cell.2016.04.008 (2016).

30 Human Microbiome Project, C. Structure, function and diversity of the healthy human microbiome. *Nature* **486**, 207-214, doi:10.1038/nature11234 (2012).

31 Donia, M. S. *et al.* A systematic analysis of biosynthetic gene clusters in the human microbiome reveals a common family of antibiotics. *Cell* **158**, 1402-1414, doi:10.1016/j.cell.2014.08.032 (2014).

32 Jan Claesen, J. B. S., Stephany Flores Ramos, Kenji L Kurita, Allyson L Byrd, Alexander A Aksenov, Alexey V Melnik, Weng R Wong, Shuo Wang, Ryan D Hernandez, Mohamed S Donia, Pieter C Dorrestein, Heidi H Kong, Julia A Segre, Roger G Linington, Michael A Fischbach, Katherine P Lemon. Cutibacterium acnes antibiotic production shapes niche competition in the human skin microbiome. *bioRxiv*, doi:https://doi.org/10.1101/594010 (2019).

Appendix

The regulation of the antibiotic lugdunin in *Staphylococcus lugdunensis*

Introduction

In search of new antimicrobial agents, a nasal *Staphylococcus lugdunensis* strain was found, which can significantly influence the colonization of *S. aureus* in the human nose by producing an antimicrobial substance. This novel antibiotic, called lugdunin, is active against *S. aureus* and other Gram-positive bacteria. Thereby, lugdunin is synthesized by non-ribosomal peptide synthetases (NRPS), which are chromosomally encoded. The lugdunin gene cluster shows a typical multi-modular structure and has typical NRPS elements (*lugA*-*lugD*) as well as genes which are required for the synthesis and the transport of lugdunin[1] (Fig. 1).

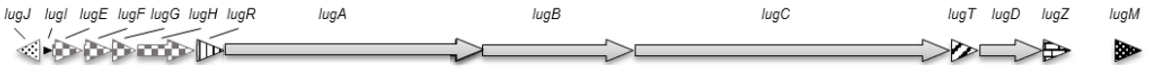

Fig. 6: Lugdunin gene cluster. The 30kbp lugdunin operon consists of the putative regulator gene *lug*R which is in front of the four NRPS modules (*lugA*-*lugD*), the putative ABC transporter genes (*lugE*-*lugH*), a putative type-II thioesterase (*lugT*), a 4'-phosphopantetheinyl transferase (*lugZ*) and also a putative monooxygenase (*lugM*). The function of the genes *lugJ* and *lugI* are still unknown[1].

So far, little is known about the regulation of the lugdunin synthesis. As recently demonstrated, the production of antimicrobials represents a burden for staphylococci[2]. For this reason, their expression is often regulated. Since the nose is a very nutrient-poor and iron-limited habitat, the production of antimicrobial compounds seems to be beneficial in the rivalry against other nasal competitors[3,4]. Hitherto, it has been shown that lugdunin production can be induced by physical interaction with *S. aureus* as well as iron limitation[1].

Based on this data, I deliberately focused on the regulation of the lugdunin operon. For my investigations, I generated three different promotor plasmid constructs. Since the regulator *lugR* is directly in front of the NRPS genes *lugA*-*lugD*, three different promotor fragment lengths were selected, because the actual promoter region is not defined: A short fragment, including only the non-coding region between *lugR* and *lugA*, and a medium and a long fragment (Fig. 2), spanning two varying sequence lengths upstream of *lugR*. Furthermore, two reporter systems were chosen based on the expression of a superfolder green fluorescent protein (sfGFP) and the beta-galactosidase from

Staphylococcus carnosus (LacH). Based on these constructs the question was investigated, how the lugdunin operon is regulated. For this purpose, experiments were done under iron limited conditions as well as with physical interaction of *S. aureus.* The intention was to characterize the inducing factor and to elucidate the regulatory circuits.

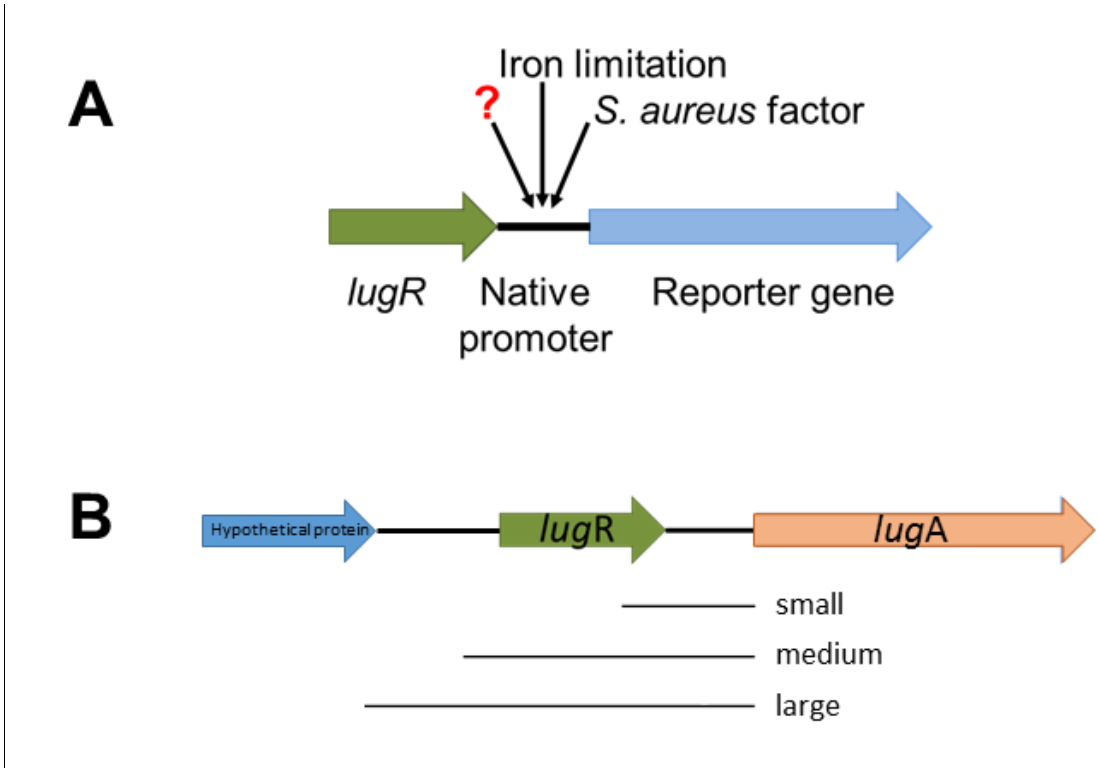

Fig. 7: Approach of the promotor study. A The principle of this assay is to clone the native promotor sequence of the lugdunin operon in front of a reporter system (GFP and β-gal) to examine under which conditions protein expression can be detected and to determine the inducing factor. **B** The promoter constructs were generated with three different promoter fragment lengths, since the actual promoter sequence is still unknown. Thus, a short fragment was amplified by Klenow reaction and a medium as well as a long fragment were amplified by PCR.

Material & Methods

Generation of *S. lugdunensis* GFP reporter strains

The plasmids pCX-sfGFP[5] and pRB473 were isolated from overnight cultures of *S. aureus* Sa113 pCX-sfGFP and *E. coli* SURE pRB473. After digestion with the enzymes PstI and BamHI, the *gfp*-containing fragment was ligated into the digested pRB473 vector and transferred to *E. coli* DC10B resulting in pRB473-sfGFP. For the construction of the *S. lugdunensis* GFP reporter strains, three different hypothetical promotor fragments were generated. For the short promotor fragment primers GFP-upstream-XhoI and Frag.-short downstream-BamHI were mixed in equimolar amounts and denatured at 96°C for 3 min. After cooling to room temperature, Klenow enzyme and dNTPs were added and incubated for 30 min at 30°C. Finally, the short promotor fragment was purified by ethanol precipitation. The medium and long promotor fragments were amplified by PCR with the primer pairs GFP-upstream-XhoI/ Frag.-medium downstream-BamHI and GFP-upstream-XhoI/Frag.-long-downstream-BamHI, respectively (Tab. 1). Subsequently, all promotor fragments were digested with the enzymes BamHI and XhoI and ligated into the equally digested plasmid pRB473-sfGFP. The resulting plasmids were first transferred to *E. coli* DC10B and afterwards to *S. aureus* PS187ΔhsdR ΔsauUSI by electroporation. Finally, these plasmids were transduced into *S. lugdunensis* IVK28 wild type via the bacteriophage Φ187[6]. In this way, also a control strain *S. lugdunensis* pRB473-sfGFP was generated, which had no promotor region (Fig. 3).

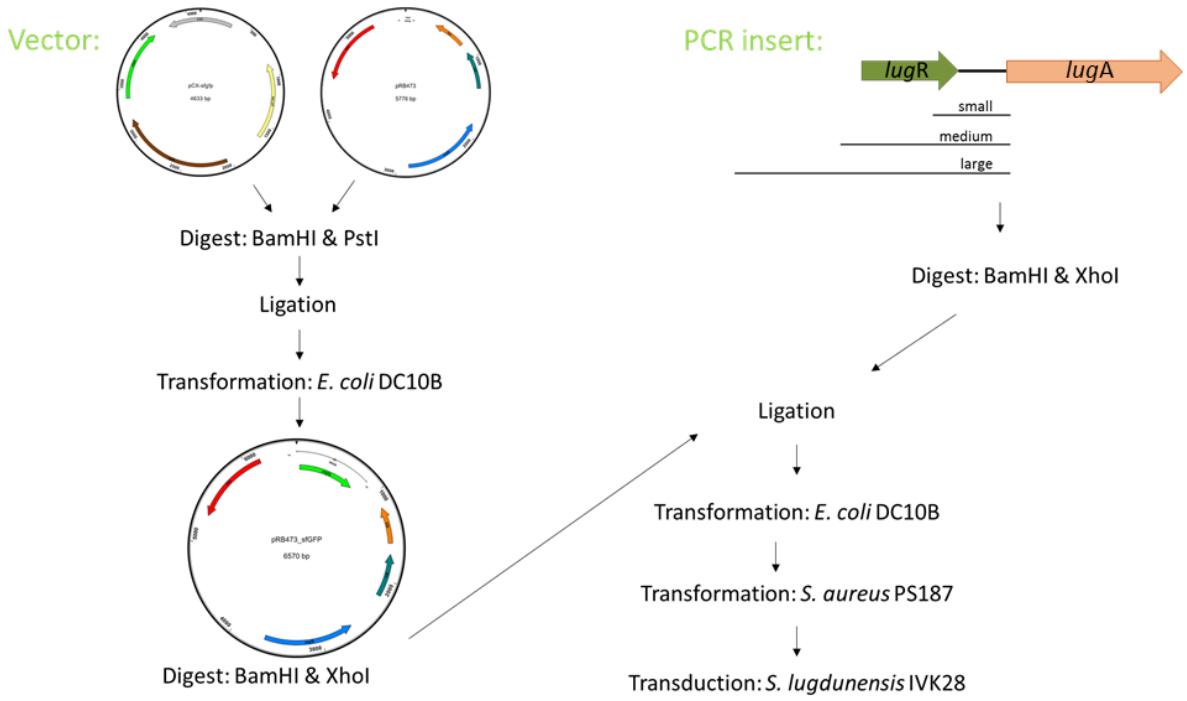

Fig. 8: Generation of *S. lugdunensis* GFP reporter strains.

Table 3: Primers used in this study

Name	Sequence	Tm°C
GFP-upstream-XhoI	TCC ATC TCG AGA ACC TCC TTT AAC TAA AAC TTA TTC AAA AATCC	69
Frag.-short downstream-BamHI	TCG AGG ATC CAA TTG ACA TAA CCG TTG ATA GGA TTT TTG AAT AAG	72
Frag.-medium downstream-BamHI	AAA ATA TTC GGA TCC TAT AGT TGA CAT ATT AAT T	57
Frag.-long-downstream-BamHI	CTT TAT TGG ATC CTT TTA TAG AAA TGG CAG	58
LacH-upstream-BglII	GAA CAG ATC TTA ACT AAA ACT TAT TCA AAA ATC CTA TC	59
LacH-new-upstream-SacI	AGA TGA AGA GCT CAC ACG TAA ACG CAT CCG	67
LacH-new-downstream	GGC GCA TTT GTT TGG GAA TGG TGT	66

Generation of *S. lugdunensis* LacH reporter strains

The plasmids pPT1-lacH and pRB473 were isolated from an overnight culture of *S. carnosus* pPT1-lacH[7] and *E. coli sure* pRB473. After digestion with the enzymes SacI and BamHI, the LacH fragment was ligated into pRB473 and the construct transferred to *E. coli* DC10B. For the construction of the *S. lugdunensis* LacH reporter strains, the same three hypothetical promotor fragments were generated as described for the GFP reporter system, except that the primer pairs contained a BglII restriction site instead of XhoI. For the short promotor fragment primers LacH-upstream-BglII/Frag.-short-downstream-BamHI were mixed in equimolar amounts and denatured at 96°C for 3 min. After cooling to room temperature, Klenow enzyme and dNTPs were added and incubated for 30 min at 30°C. Afterwards, the short promotor fragment was purified by ethanol precipitation. The medium and long promotor fragments were amplified by PCR with the LacH-upstream-BglII/Frag.-medium-downstream-BamHI and LacH-upstream-BglII/Frag.-long-downstream-BamHI primers, respectively (Tab.1). Subsequently, all promotor fragments were digested with the enzymes BamHI and BglII and ligated with the plasmid pRB473-LacH, which was previously linearized with BamHI and treated with alkaline phosphatase to inhibit religation. The respective plasmids were transferred first to *E. coli* DC10B by transformation. However, it turned out that the LacH fragment was

about 300 bp shorter than the reference genome. Therefore, the missing segment of LacH was amplified again by PCR with the primer pair LacH-new-upstream-SacI/LacH-new-downstream from the DNA of *S. carnosus* TM300. After digestion with the enzymes SacI and HpaI, the PCR product was ligated into the three different, identically digested promotor plasmids. After transformation of *E. coli* DC10B with these plasmids and the confirmation of correctness, they were subsequently transferred to *S. aureus* PS187ΔhsdR ΔsauUSI by electroporation. Finally, these plasmids were transduced into *S. lugdunensis* IVK28 wild type via the bacteriophage Φ187[6]. In this way, also a control strain *S. lugdunensis* pRB473-LacH was generated (Fig. 4).

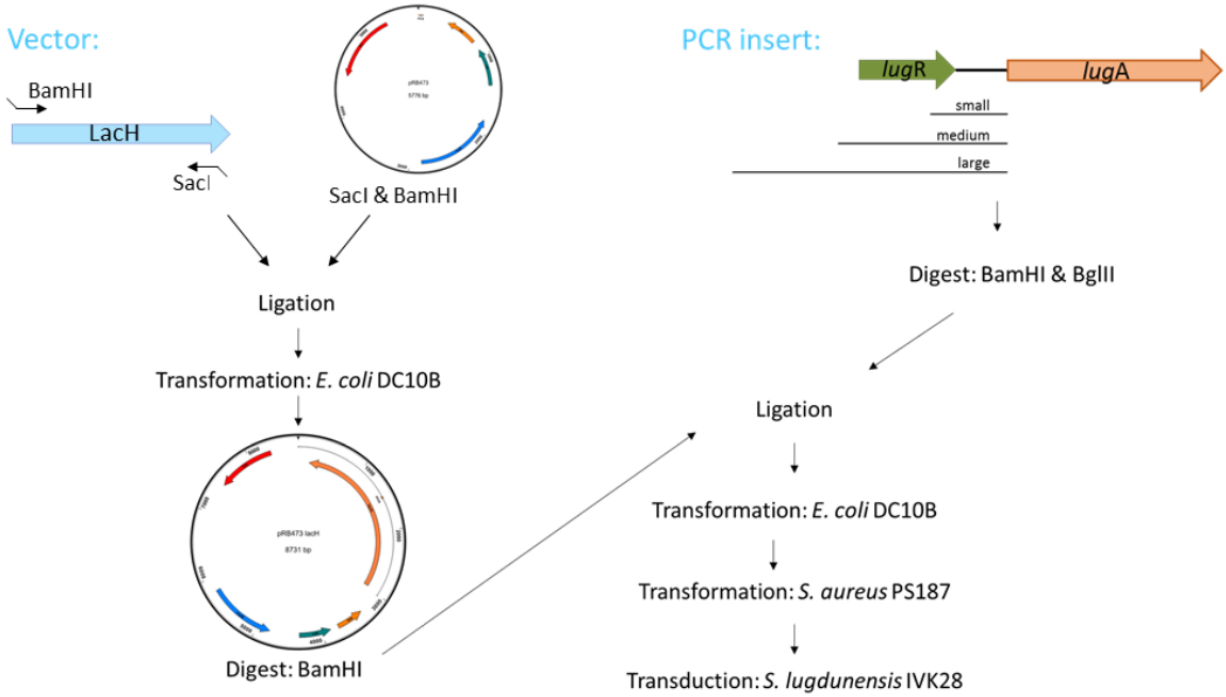

Fig. 9: Generation of *S. lugdunensis* LacH reporter strains (simplified).

Workflow sample preparation and GFP measurement

The experimental procedure was as follows (Fig. 5): *S. aureus* USA300 LAC wild type was incubated in basic medium (BM) overnight (9 h) at 37°C on the shaker at 160 rpm. After filtration of the culture, the cell pellet was discarded, and the supernatant was sterile filtered (= **spent medium**) and poured with varying degrees of BM agar to spent medium agar plates. The respective *S. lugdunensis* GFP reporter strains were adjusted with PBS to OD_{600}=1 and in each case 20 µl were pipetted on the spent medium agar plates and on BM plates as a control. After Incubation over night at 37°C, the grown *S. lugdunensis* spots were scraped off and resuspended in PBS. After adjustment to

OD_{600}=1, 100 µl of the bacterial suspension as well as 100 µl PBS as blank were pipetted as triplicates into a 96-well plate. Afterwards, the GFP signal was measured at gain 2000.

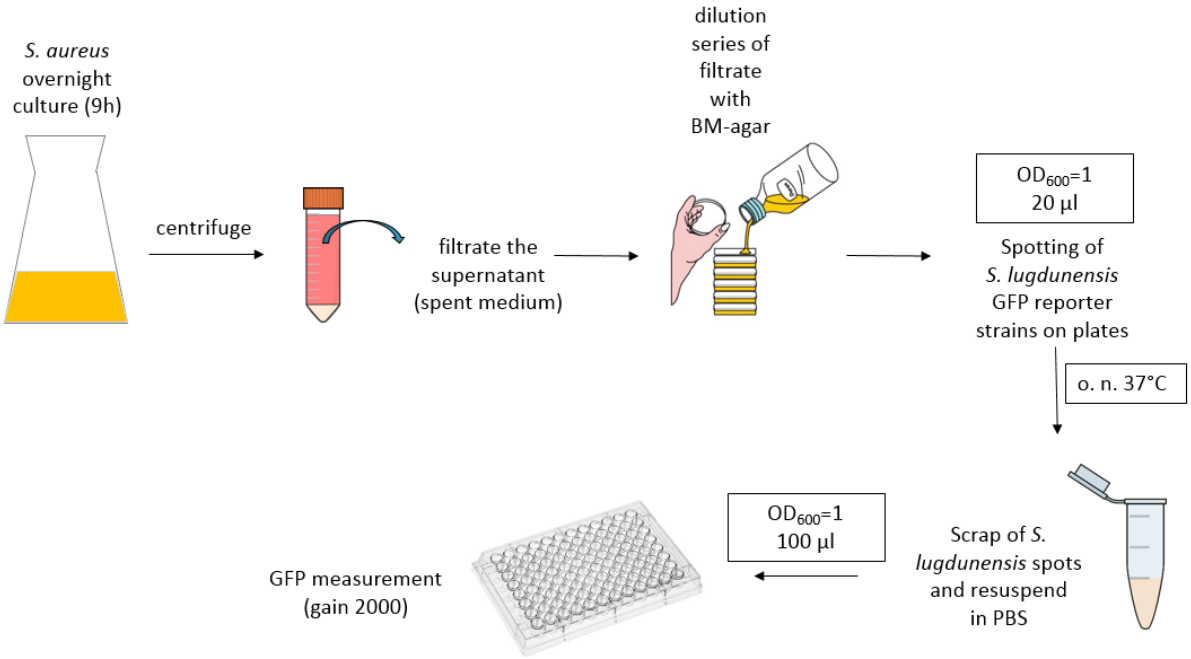

Fig. 10: Workflow sample preparation and GFP measurement.

Different spent media from *S. aureus* transposon mutants of the Nebraska library were examined for their inducing abilities of the GFP plasmid. The various *S. aureus* mutants, which were used for the assay, are listed in Table 2.

Table 4: *S. aureus* USA300 JE2 transposon mutants of the Nebraska library[8]

Strain Name	Gene Name	Gene Description
NE 1566	sirC	iron compound ABC transporter permease SirC
NE 1767	sirA	iron compound ABC transporter iron compound – binding protein SirA
NE 675	sirB	iron compound ABC transporter, permease protein SirB
NE 665		transcriptional regulator, Fur family
NE 1742	hemA	glutamyl-tRNA reductase
NE 1845	hemB	delta-aminolevulinic acid dehydratase
NE 1172		iron/heme permease

NE 1468	fhuG	ferrichrome transport permease protein fhuG
NE 1881	fhuB	ferrichrome transport permease fhuB
NE 406	fhuA	ferrichrome transport ATP-binding protein fhuA
NE 1031	sbnC	IucC family siderophore biosynthesis protein
NE 200		iron compound ABC transporter, permease protein
NE 869		iron compound ABC transporter permease
NE 400		iron compound ABC transporter, iron compound-binding protein
NE 379		conserved hypothetical protein
NE 158		conserved hypothetical protein
NE 548		putative transporter
NE 745		conserved hypothetical protein
NE 99		conserved hypothetical protein
NE 1198		pyridoxal-phosphate dependent enzyme superfamily protein
NE 1626		ornithine cyclodeaminase
NE 749		putative drug transporter
NE 185		siderophore biosynthesis protein, IucA/IucC family
NE 214		siderophore biosynthesis protein, IucC family
NE 922		HPCH/HPAI aldolase family protein
NE 232		pyridoxal-dependent decarboxylase
NE 990		hypothetical protein
NE 1489		ABC transporter ATP-binding protein
NE 521		ABC transporter, permease protein
NE 1089		response regulator protein
NE 820		sensor histidine kinase

Quantitative real-time PCR:

The approach was as described by Simon Heilbronner[9]. However, deviating from this approach the RT-PCR cycler Step One Plus (Applied Biosystems) with the associated Design & Analysis software was used. Another deviation was that the RT-qPCR was not made with chromosomal DNA but with RNA. Therefore, RNA was isolated from *S. lugdunensis* IVK 28 after incubation at 37°C for nine hours on 30% spent medium plates

or BM plates. For this, cells were scraped off from the outer part of the spots, resuspended in trizole and disrupted with glass beads. RNA was purified from the lysate with the Zymo Direct-zol™ RNA MiniPrep Plus Kit. RNA was transcribed into cDNA using the Power SYBR® Green RNA-to-CT™ 1-Step Kit and used for RT-qPCR. Primers, which were used for these experiments, are summarized in Table 3.

Table 5: qRT-PCR Primer

Name	Sequence	Tm°C
lugC_forward	CAC ACA GCG TTT CAA CTA ATG	57
lugC_reverse	TGA CTG CTT GCC TAA ACT G	55
gyrB_forward	CTT GAA GCG GTT CGA AAA AG	56
gyrB_reverse	CAC GGC CAT TAT CCG TTA CT	58

Results & Discussion

Hitherto, it is not known how the lugdunin synthesis is regulated. However, iron limitation and direct cell-cell contact of *S. lugdunensis* with *S. aureus* led to the production of lugdunin. A promoter study was intended to investigate under which conditions the production of lugdunin can be induced.

Since the exact promoter sequence of the lugdunin operon is not known, three potential promoter regions were selected. The intergenic region between the 3'-end of *lugR* and the start codon of *lugA* was defined as the short promoter fragment and the region 98 bp upstream of *lugR* to the start codon of *lug*A was determined as the medium fragment. Since the intergenic region between the 3'-end of *lugH* and the start codon of *lugR* is very large and thus may have an influence on the promoter activity, a long promoter fragment spanning this entire region was additionally selected. Moreover, two different reporter systems (GFP/ LacH) were chosen to visualize the respective promoter activity.

LacH is a gene from the lactose operon of *Staphylococcus carnosus* encoding the enzyme ß-galactosidase, which is able to hydrolyze lactose into glucose and galactose[7,10]. Furthermore, ß-galactosidase is able to convert colorless X-Gal into a blue dye, why it is often used for molecular biological analyses for blue-white selection[10]. Genomic data showed that *S. lugdunensis* encodes no ß-galactosidase but a phospho-ß-galactosidase making LacH from *S. carnosus* suitable for the promotor study.

First experiments with the three *S. lugdunensis*-pRB473 LacH reporter strains showed that only a weak blue staining on BM-X-gal plates could be observed in the *S. lugdunensis* LacH reporter strain with the long promotor construct under iron limited conditions and in direct cell-contact with *S. aureus*, respectively. Due to this low enzymatic activity further experiments were only performed with the *S. lugdunensis* GFP reporter strains.

The green fluorescent protein is a protein from the jellyfish *Aequorea victoria* that emits green fluorescence when excited with blue/ultraviolet light. Thus, it can be used as a reporter for the gene expression[11]. The superfolder GFP (sfGFP) used for this experiment is an optimised variant of GFP[12].

In this way, the inducing capability of spent medium on the GFP expression can be investigated. In this proceeding, spent medium is defined as culture supernatant of *S. aureus*, which has grown nine hours in basic medium (BM). Characteristic for spent medium is that on the one hand nutrients were consumed and on the other hand that

there are components of *S. aureus* in this medium. However, BM shows strong intrinsic fluorescence, for which reason the promoter activity cannot be measured in real time in liquid culture. Hence, the promoter activity of the various *S. lugdunensis* GFP reporter strains was measured after growth on spent medium agar plates. Besides, an enhanced effect could be observed on spent medium agar plates compared to spent medium liquid culture. Experiments with *S. aureus* tryptic soy broth (TSB) spent medium showed no GFP activation neither in liquid culture nor on agar plates. Therefore, the following experiments have been made with BM spent medium of *S. aureus* USA300.

After growing the *S. lugdunensis* reporter strains on spent medium agar plates a GFP signal was detectable in two of the three constructs. This suggests that the promoter can be activated in principle. Thereby, the GFP signal of the plasmid of the long promotor fragment was stronger than the signal of the medium fragment, whereas the plasmid with the short promotor fragment showed no expression. Presumably, this construct was too short and the typical promotor elements such as the -10 element and the -35 element are missing. Therefore, it seems that the sequence region between the genes *lugR* and *lugA* is not a promoter sequence. Hence, the following experiments were done solely with the plasmids with the medium/long construct as well as with the control construct.

The strongest activation could be observed on BM plates with a fraction of 20% *S. aureus* spent medium. On these plates, the GFP expression increased 3-4-fold in comparison to BM control plates. Nevertheless, higher concentrations of spent medium led to a reduction of the GFP signal. That is the reason why mainly 20% spent medium plates were used in the following experiments (Fig. 6).

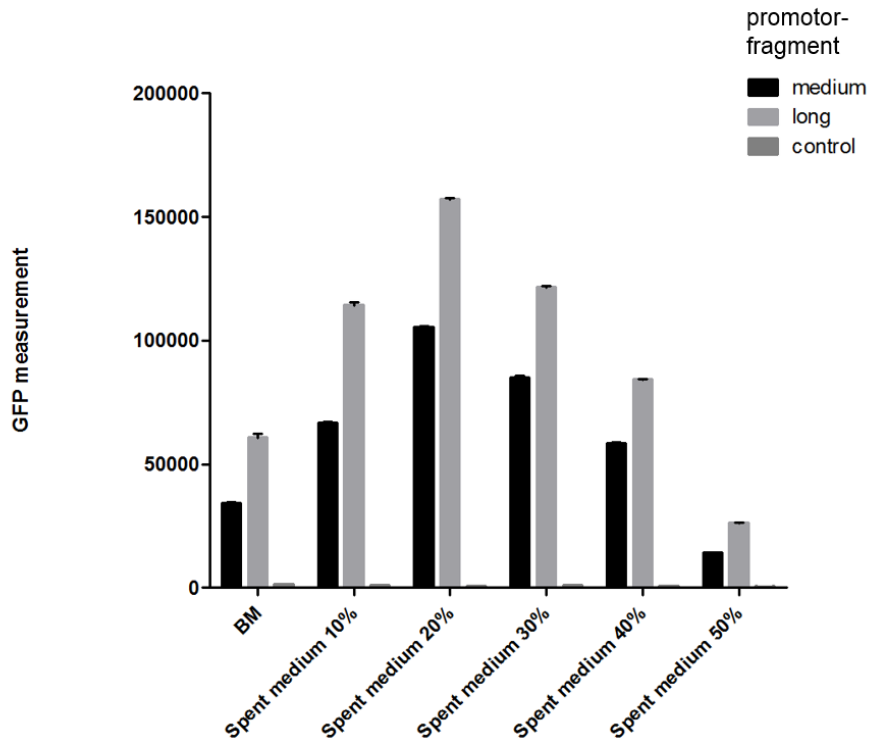

Fig. 11: GFP measurement of *S. lugdunensis* GFP reporter strains after growing on BM agar plates with different concentrations of spent medium.

Furthermore, a certain time dependence regarding the incubation time of *S. aureus* in BM could be noticed. Spent medium from *S. aureus* led to the strongest induction of GFP expression after 9 hours of growth in BM. Moreover, an incubation time of *S. lugdunensis*-pRB473-GFP-medium on these spent medium plates was strongest after growing 20 hours at 37°C.

One of the first experiments was to determine if bacteria besides *S. aureus* are able to activate the lugdunin promoter. Therefore, spent media from different bacterial strains were tested for their inducing effect on the GFP plasmid. Interestingly, other bacteria are also able to induce GFP expression, but the strongest GFP signal could be noticed with Gram-positive bacteria. The highest expression levels could be achieved with *Listeria monocytogenes* and *Streptococcus pyogenes*, but *Staphylococcus warneri* und *Bacillus subtilis* are also able to activate the promotor. By contrast, spent medium of Gram-negative bacteria like *Escherichia coli*, *Klebsiella pneumoniae* or *Moraxella catarrhalis* did not lead to an increased GFP expression compared to lysogeny *broth* (LB) medium. Therefore, the activating factor does not seem to be a *S. aureus* specific factor, but a Gram-positive specific factor. It is known, that physical interactions with *S. aureus* leads

to the production of lugdunin[1]. Therefore, further experiments were made with various *S. aureus* strains and *S. aureus* spent medium, respectively.

The accessory gene regulator (*agr*) is a global regulator in staphylococci and is part of a quorum sensing system in *S. aureus*. It is responsible for the expression of several virulence (e.g. toxins) and colonisation factors[13]. Hence, our first assumption was that the *agr* system of *S. aureus* is responsible for lugdunin expression by production of auto inducing peptides (AIPs). For this reason, spent medium agar plates of *S. aureus* USA 300 LAC wild type as well as *S. aureus* USA 300Δ*agr* mutant were prepared and investigated for their different abilities to activate the GFP promoter. However, spent medium of the *S. aureus* wild type as well as the *S. aureus* USA 300Δ*agr* mutant can induce the GFP plasmid, but the repressing effect at higher concentrations of spent medium was stronger with the spent medium of the *agr*-mutant (Fig. 7). Nevertheless, these experiments revealed no correlation between the *agr* system and the lugdunin expression. Therefore, the hypothesis cannot be confirmed and was no longer pursued.

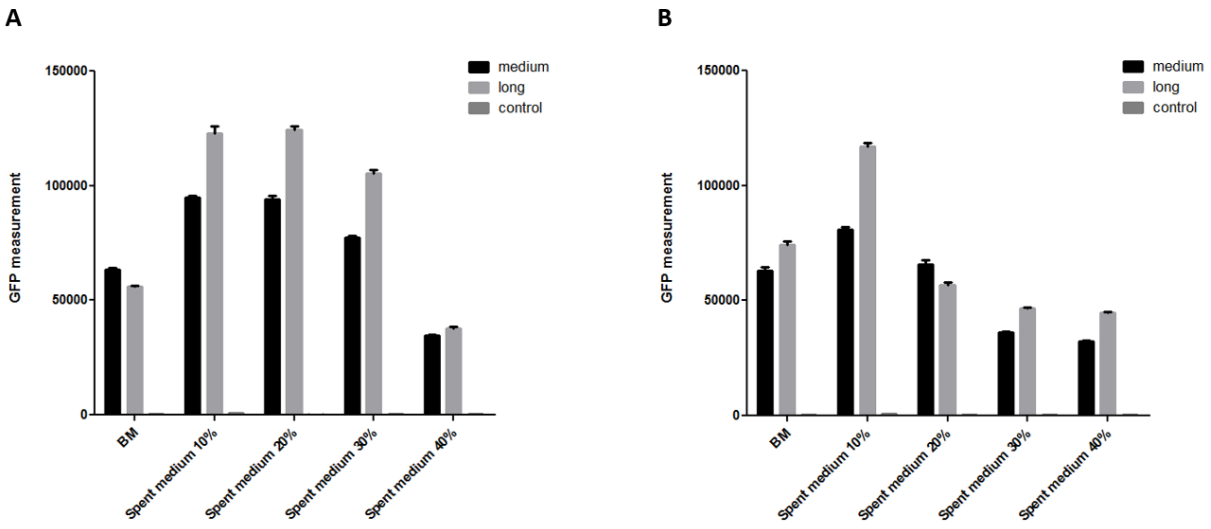

Fig. 12: GFP measurement of *S. lugdunensis* GFP reporter strains after growth on BM agar plates with various spent media. A Spent medium of *S. aureus* USA300 **B** Spent medium of *S. aureus* USA300Δ*agr*.

Various staphylococci were transformed with the GFP plasmid and afterwards it has been investigated if GFP expression can be measured beside *S. lugdunensis* also in

other staphylococci. However, *S. aureus* spent medium did not induce GFP expression in *S. epidermidis* 1457, *S. aureus* USA300, *S. aureus* 113, or *S. aureus* RN4220.

To test if lugdunin expression is ascribed to a secreted *S. aureus* factor or to *S. aureus* cell fragments, the assay was done with heat inactivated spent medium or heat inactivated *S. aureus* cells. For this purpose, *S. aureus* spent medium and *S. aureus* cells grown in the same volume were heat inactivated at 95°C for one hour. It could be shown, that heat inactivated spent media plates were still able to induce the GFP promoter. Although the induction with heat inactivated spent medium plates was slightly lower than with normal spent medium plates, a duplication of the GFP signal compared to control BM plates could be measured. In addition, the strongest GFP signal was gained with 10% spent medium plates. The next step was to investigate if co-cultivation of *S. lugdunensis* reporter strains with heat-inactivated *S. aureus* cells in liquid culture causes GFP induction. It revealed that the incubation with heat-inactivated *S. aureus* cells did not lead to GFP induction indicating that a secreted factor provokes GFP expression. The absence of the gene *tag*O is associated with a loss of wall teichoic acid (WTA) in the corresponding *S. aureus* mutant[14]. Likewise, the deletion of phosphatidylglycerol-prolipoprotein-diacylglyceryl transferase (*lgt*) leads to a lack of lipoproteins in the *S. aureus*Δ*lgt* mutant[15]. Therefore, the experiments were also performed with spent medium of *S. aureus* USA300Δ*tag*O and *S. aureus* USA300Δ*lgt* to investigate if an altered cell surface can induce GFP expression. However, there was no altered GFP expression between the wild type and the mutants. Consequently, neither wall teichoic acids nor lipoproteins are responsible for the lugdunin induction.

The next step was to examine if osmolar stress induces GFP expression. For this purpose, various concentrations of NaCl as well as sucrose were added to BM agar plates to investigate if these additives are able to induce the GFP plasmid. By adding NaCl to BM plates, no increased GFP signal was measurable. Instead, increasing concentrations of NaCl (0.5-5%) led to a reduction, because the measured GFP signal decreased with increasing NaCl concentrations. There was a similar effect with sucrose, because addition of 0.5-5% sucrose did not support increased GFP induction. On the contrary, even a concentration of 0.5% sucrose led to a quenching of the GFP signal. In addition, oxidative stress did not lead to an enhanced induction, which was shown by adding different H_2O_2 concentrations to BM agar plates.

Since on the protein level only a threefold to fourfold increase in the GFP expression was observed, a real-time qPCR was performed to investigate if there is a stronger

upregulation on the transcription level. For this reason, *S. lugdunensis* IVK28 wild type was grown on 30% spent medium plates as well as on BM plates for nine hours and afterwards the lugdunin expression was observed via RT-qPCR. A detectable effect was measured, because the *lugC* activity was 2.6 times higher when grown on spent medium compared to fresh BM.

To narrow the search for the inducing factor, further experiments were made. On the one hand spent medium was treated with trypsin and proteinase K to examine if there are differences between treated and untreated spent medium regarding their inducing capability. However, both spent media showed the same effect, because the inducing effect persists despite protease treatment. Nevertheless, in the treated spent medium putatively repressing proteins are degraded, because with increasing amounts of treated spent medium in the agar plates, the repressive effect of the untreated spent medium could no longer be observed. However, by the protease treatment it could be shown that the inducing factor is evidently not a protein.

On the other hand, further experiments have been made to clarify if the lugdunin regulation is iron dependent, since iron limited conditions are known to induce lugdunin expression and the nasal habitat is low in nutrients and iron as well[1,3]. However, iron is essential for many cellular processes. *S. aureus* has developed a possibility to get extracellular iron through the production of siderophores. Staphyloferrin A and staphyloferrin B are two structurally characterized siderophores of *S. aureus*[16]. Due to their high affinity to iron, they are responsible for the ferric uptake in staphylococci[17]. Staphyloferrin A is synthesized by the *sfnABCD* operon and the HtsABC transporter is responsible for the uptake of staphyloferrin A, whereas staphyloferrin B is encoded by the *sbnABCDEFGHI* operon and the SirABC transporter is responsible for the uptake[16,18]. The required energy for the transport of staphyloferrin A or staphyloferrin B through the membrane is provided by the ferric hydroxymate uptake operon *fhuCBG*, which encodes the putative ATPase *fhuC*[17].

Besides siderophore iron uptake, there is also a siderophore independent iron uptake system. The iron regulated surface determinant (*isd*) consists of five operons and is responsible for the uptake of heme. Heme is a complex of an iron ion and a tetrapyrrole ring. The Isd proteins can bind hemoglobin and remove the cofactor heme. Subsequently, heme is transported through the cell wall into the cytoplasm, where free iron is released[17,19].

At the beginning, different iron sources were added to BM or it was treated with different chelators to investigate if this effects the GFP induction. However, neither the supplementation of various iron sources (ferric chloride, iron citrate) nor the treatment with various iron chelators (EDDHA, bipyridine, deferoxamine) had a strong effect, because the expression remained unchanged or slightly decreased. However, the low reduction of the GFP signal by EDDHA and deferoxamine suggested a correlation between iron and lugdunin induction and since the presence of *S. aureus* affects the availability of free iron for *S. lugdunensis*, the inducing effect of the spent medium of various *S. aureus* iron uptake or siderophore biosynthesis mutants from the Nebraska transposon mutant library were tested[8]. The various *S. aureus* mutants, which were used for the assay, are listed in Table 2. All but one tested iron mutants showed no altered expression compared to the wild type strain *S. aureus* USA300JE2.

Only the spent medium of the strain *S. aureus* NE1172, which is characterized by a deletion of the iron/heme permease *isdF*, showed an increased GFP expression under normal growth conditions compared to the spent medium of the wild type. Moreover, under iron-limited conditions the spent medium of this mutant showed a reduced GFP expression compared to the wildtype.

IsdF is an ABC permease, which is responsible for the transport of heme across the membrane[17]. Hence, further experiments were done to investigate if heme can activate the promotor. Therefore, BM agar plates supplemented with heme or BM agar plates previously treated with EDDHA and supplemented with heme were tested for their inducibility. Thereby the GFP expression of *S. lugdunensis*-pRB473-GFP-long was measured after growth on these plates. It could be shown that the addition of heme led to an increased GFP signal. This signal was enhanced again under iron limitation (Fig. 8).

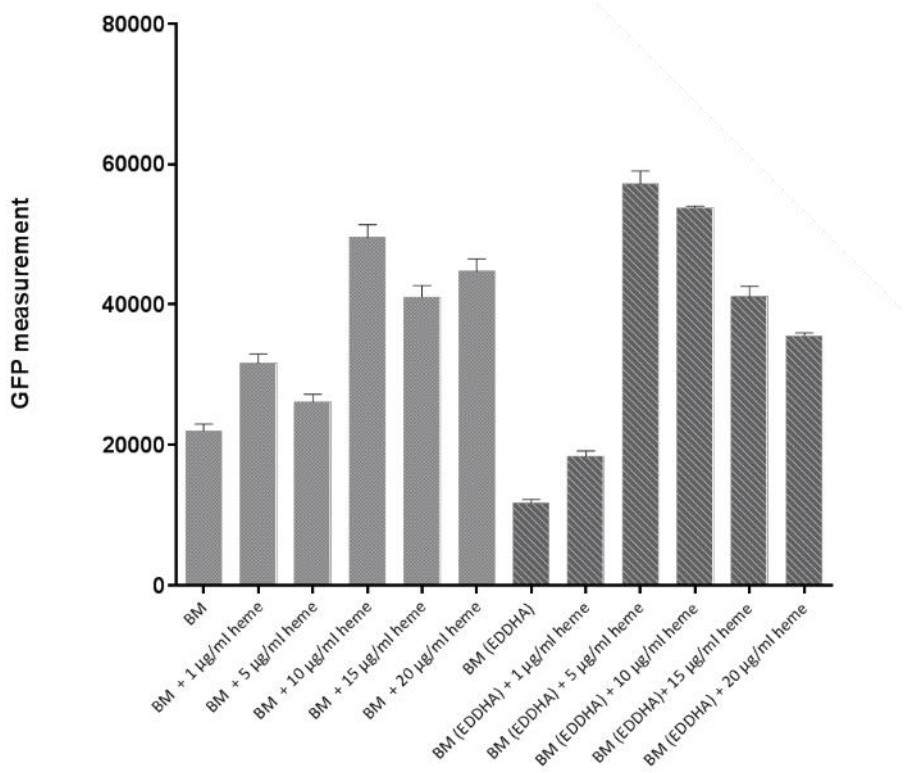

Fig. 13: Addition of heme. GFP measurement of *S. lugdunensis*-pRB473-GFP-long after growing on BM agar plates with various concentrations of heme (light grey) or on BM agar plates, which were treated with EDDHA and supplemented with heme afterwards (dark grey).

The next step was to investigate if the activating factor can be isolated from spent medium by solvent extraction. For this purpose, *S. aureus* spent medium was extracted with butanol, chloroform and ethyl acetate. However, GFP activity was only observed with the aqueous phase and not with the extracted sample.

Therefore, further experiments were made with water, in which a dilution effect could be observed. By adding different volumes of water to BM agar plates (0-50%) instead of spent medium, the measured GFP signal was enhanced with increasing water content. Hence, the highest GFP signal was measured with BM plates containing 35% additional water volume (Fig. 9).

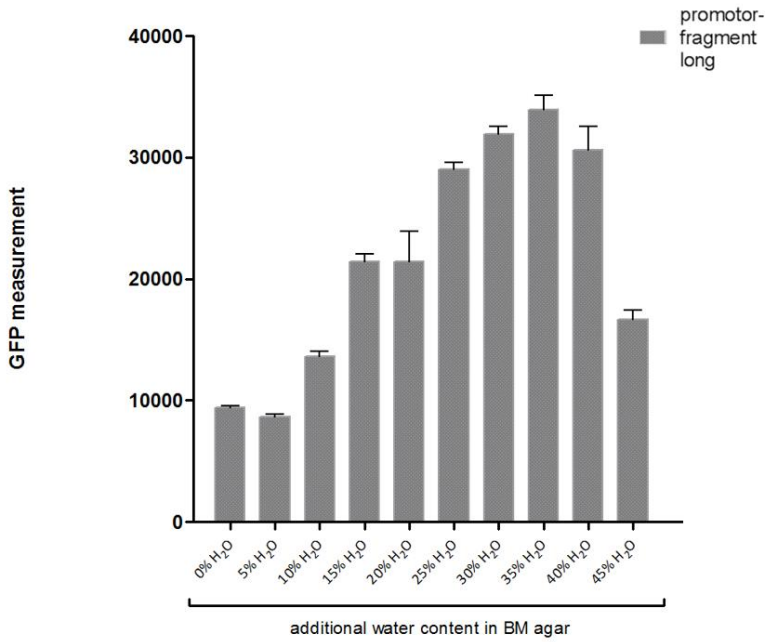

Fig. 14: Dilution effect. GFP measurement of *S. lugdunensis* pRB473-GFP-long after growth on BM agar plates with different volumes of additional water.

This dilution effect has shown that the experimental setup is problematic and can be influenced by too many factors. Hereby, it could not be ruled out that also artifacts have been measured. Although *S. aureus* spent medium has an inducing effect, a dilution of the medium showed similar results. In this way, it was no longer possible to clearly distinguish what induced the measured GFP activity. In addition, it was also problematic that the measured values varied considerably. The GFP signal of the non-induced sample (BM) was between 10,000 and 50,000 despite the same experimental procedure and reader settings. For this reason, a useful analysis was very difficult, and a continuation of the project would have been promising only with much more effort. For this reason, the project was discontinued.

References

1 Zipperer, A. *et al.* Human commensals producing a novel antibiotic impair pathogen colonization. *Nature* **535**, 511-516, doi:10.1038/nature18634 (2016).

2 Ebner, P. *et al.* Lantibiotic production is a burden for the producing staphylococci. *Sci Rep* **8**, 7471, doi:10.1038/s41598-018-25935-2 (2018).

3 Krismer, B. *et al.* Nutrient limitation governs Staphylococcus aureus metabolism and niche adaptation in the human nose. *PLoS Pathog* **10**, e1003862, doi:10.1371/journal.ppat.1003862 (2014).

4 Krismer, B., Weidenmaier, C., Zipperer, A. & Peschel, A. The commensal lifestyle of Staphylococcus aureus and its interactions with the nasal microbiota. *Nat Rev Microbiol* **15**, 675-687, doi:10.1038/nrmicro.2017.104 (2017).

5 Yu, W. & Gotz, F. Cell wall antibiotics provoke accumulation of anchored mCherry in the cross wall of Staphylococcus aureus. *Plos One* **7**, e30076, doi:10.1371/journal.pone.0030076 (2012).

6 Winstel, V., Kuhner, P., Krismer, B., Peschel, A. & Rohde, H. Transfer of plasmid DNA to clinical coagulase-negative staphylococcal pathogens by using a unique bacteriophage. *Appl Environ Microbiol* **81**, 2481-2488, doi:10.1128/AEM.04190-14 (2015).

7 Kamps, A. Molekularbiologische Studien zur Regulation der dissilatorischen Nitrat- und Nitritreduktion bei *Staphylococcus carnosus*. *Cuvillier Verlag Göttingen* (2002).

8 Fey, P. D. *et al.* A Genetic Resource for Rapid and Comprehensive Phenotype Screening of Nonessential Staphylococcus aureus Genes. *Mbio* **4**, doi:ARTN e00537-1210.1128/mBio.00537-12 (2013).

9 Heilbronner, S. *et al.* Competing for Iron: Duplication and Amplification of the isd Locus in Staphylococcus lugdunensis HKU09-01 Provides a Competitive Advantage to Overcome Nutritional Limitation. *PLoS Genet* **12**, e1006246, doi:10.1371/journal.pgen.1006246 (2016).

10 Juers, D. H., Matthews, B. W. & Huber, R. E. LacZ beta-galactosidase: structure and function of an enzyme of historical and molecular biological importance. *Protein Sci* **21**, 1792-1807, doi:10.1002/pro.2165 (2012).

11 Tsien, R. Y. The green fluorescent protein. *Annu Rev Biochem* **67**, 509-544, doi:10.1146/annurev.biochem.67.1.509 (1998).

12 Pedelacq, J. D., Cabantous, S., Tran, T., Terwilliger, T. C. & Waldo, G. S. Engineering and characterization of a superfolder green fluorescent protein. *Nat Biotechnol* **24**, 79-88, doi:10.1038/nbt1172 (2006).

13 Otto, K. Y. L. a. M. Quorum-sensing regulation in staphylococci—an overview. *Frontiers in Microbiology* **6**, doi:ttps://doi.org/10.3389/fmicb.2015.01174 (2015).

14 Weidenmaier, C. *et al.* Role of teichoic acids in Staphylococcus aureus nasal colonization, a major risk factor in nosocomial infections. *Nat Med* **10**, 243-245, doi:10.1038/nm991 (2004).

15 Stoll, H., Dengjel, J., Nerz, C. & Gotz, F. Staphylococcus aureus deficient in lipidation of prelipoproteins is attenuated in growth and immune activation. *Infect Immun* **73**, 2411-2423, doi:10.1128/Iai.73.4.2411-2423.2005 (2005).

16 Beasley, F. C. & Heinrichs, D. E. Siderophore-mediated iron acquisition in the staphylococci. *J Inorg Biochem* **104**, 282-288, doi:10.1016/j.jinorgbio.2009.09.011 (2010).

17 Hammer, N. D. & Skaar, E. P. Molecular mechanisms of Staphylococcus aureus iron acquisition. *Annu Rev Microbiol* **65**, 129-147, doi:10.1146/annurev-micro-090110-102851 (2011).

18 Sheldon, J. R. & Heinrichs, D. E. The iron-regulated staphylococcal lipoproteins. *Front Cell Infect Mi* **2**, doi:UNSP 4110.3389/fcimb.2012.00041 (2012).

19 Stauff, D. L. & Skaar, E. P. The heme sensor system of Staphylococcus aureus. *Contrib Microbiol* **16**, 120-135, doi:10.1159/000219376 (2009).

Contributions to publications

Chapter 1 – Staphylococcus aureus colonization of the human nose and interaction with other microbiome members

I wrote the review with assistance of Bernhard Krismer and Andreas Peschel.

Chapter 2 – Human commensals producing a novel antibiotic impair pathogen colonization

I designed the human nasal colonization study of high-risk patients and analyzed the data.

Publications

Zipperer, A., Konnerth, MC & **Laux, C.** *et al.* Human commensals producing a novel antibiotic impair pathogen colonization. *Nature* 535, 511-516 (2016).

Laux, C., Peschel, A. & Krismer, B. Staphylococcus aureus Colonization of the Human Nose and Interaction with other Microbiome Members. *Microbiol Spectr* 7, doi: 10.1128/microbiolspec.GPP3-0029-2018 (2019).